

A NUMERICAL STUDY OF THE PERFORMANCE OF TUNED LIQUID DAMPERS

A NUMERICAL STUDY OF THE PERFORMANCE OF TUNED LIQUID DAMPERS

By

HASSAN MORSY, B.Sc.

A Thesis

Submitted to the School of Graduate Studies

In Partial Fulfillment of the Requirements

For The Degree

Master of Applied Science

McMaster University

©Copyright Hassan Morsy, January 2010

MASTER OF APPLIED SCIENCE (2009)
(Mechanical Engineering)

McMaster University
Hamilton, Ontario

TITLE: A Numerical Study of The Performance of Tuned Liquid Dampers

AUTHOR: Hassan Morsy, B.Sc. (Ain Shams University, Cairo, Egypt)

SUPERVISOR: Dr. Mohamed .S. Hamed

NUMER OF PAGES: 112, xvii

Abstract

Using an integrated Tuned Liquid Damper (TLD)-Structure in-house developed numerical algorithm that has been validated against recent rigorous experimental tests, the TLD performance was analyzed when coupled with a vibrating Single Degree of Freedom (SDOF) body representing a civil structure. The numerical algorithm solves the full two dimensional Navier-Stokes equations with no linearization assumptions. It uses the Volume of Fluid method to reconstruct the free surface, and the Partial Cell Treatment method to model the effect of any obstructions. This study investigated the structure response when coupled to a TLD with and without a screen under harmonic excitations. Structure sway was found to decrease by 71% in the case of a TLD without a screen, and 80% in the case of a TLD with one screen. The best screen configuration was then determined for the TLD-Structure coupling under non-harmonic excitations, taking minimal structure sway and acceleration as the deciding criteria. Eighteen different cases considering different screen locations and solidities were investigated, and the case with one screen placed in the middle with a solidity of 0.4 proved to be the best.

The study also investigated the effect of fluid height on structure sway under a wide range of excitation amplitudes. Harmonic Excitations with amplitudes up to 3% of the tank length and fluid heights up to 40% of tank length were considered. The results showed better structure response with lower fluid heights in the case of low to moderate excitation amplitudes. With high excitation amplitudes, the results confirmed an opposite trend where higher fluid heights resulted in better structure response.

The numerical code was then modified to model a Sloped Bottom (SB) TLD using the Partial Cell Treatment method. The numerical model for the SB TLD has been validated against experimental data to ensure accuracy. Numerous cases have been considered to investigate structure response under the new configuration, and to analyze how a SB TLD compares to a standard TLD. The results showed an increased damping ratio and better structure response for SB TLDs, and a significant softening spring behaviour that is important upon excitation cessation.

Acknowledgements

I would like first to convey my utmost appreciation for my supervisor Dr. Mohamed Hamed for his continued support and understanding. There were times during the past couple of years when one felt he had reached dead ends, and if it wasn't for Dr. Hamed's willingness to listen, advise, and guide in solving problems, my graduate experience would never have been the same. I also want to express my gratitude for Dr. Hamed for the numerous occasions when he extended his understanding and help even when I had personal problems.

I would like to thank Mr. Morteza Marivani, the author of the numerical algorithm that was used in this study, and a fellow Ph.D. student in our TPL research group. If it wasn't for his mentoring and help in understanding the code, I honestly do not believe I could have completed this Masters the way I did. He communicated all his accumulated knowledge in the TLD area graciously, and humbly listened to my opinion when I voiced it.

I am grateful to all my friends and staff of the Mechanical Engineering Department for their support and encouragement. I specially thank Mr. Sherif Abdo, Mr. Hossam Sadek, Mr. Ahmed Omar, and Mr. Mohamed Abo Gabal, all Ph.D. students in the department. It was just amazing how every one of them was willing to put so much of his own time to solve any problem I encountered during the course of my work.

Last but never least, my family is just simply my life. This thesis is dedicated to my wife, my mother, and my father. I simply cannot do without them, and their influence on my life is immeasurable.

Table of Contents

1	CHAPTER 1: INTRODUCTION AND LITERATURE REVIEW	1
1.1	Introduction.....	1
1.1.1	Dampers Introduction	1
1.1.2	Tuned Mass Dampers	3
1.1.2.1	Undamped Tuned Mass Dampers	3
1.1.2.2	Damped Tuned Mass Dampers	5
1.1.2.3	Structural Implementations	7
1.1.3	Tuned Liquid Dampers	8
1.1.3.1	Introduction.....	8
1.1.3.2	Structural Implementations	11
1.1.4	TLD Design Parameters	12
1.2	Literature Review.....	19
1.2.1	Nature of Excitation Considered in Literature.....	19
1.2.2	TLD Additional Damping Techniques	19
1.2.2.1	Screens	19
1.2.2.2	Sloped Bottom TLDs	22
1.2.3	Evolution of Numerical Work	23
1.2.3.1	Models based on the Potential Flow Theory	23
1.2.3.2	Models based on the Shallow Water Wave Theory	24
1.2.3.3	Models based on the Equivalent TMD Method	25
1.2.3.4	Non-linear Models	28
1.3	Research Scope and Objectives.....	29
1.4	Organization Of Thesis	30
2	CHAPTER TWO: MATHEMATICAL FORMULATION AND NUMERICAL MODEL	31
2.1	Introduction.....	31
2.2	Geometry of Submerged Slat Screens.....	32
2.3	Flow Governing Equations and Boundary Conditions.....	33
2.4	Partial Cell Treatment Method.....	36
2.4.1	Screens.....	36
2.4.2	Sloped Bottom TLDs.....	37
2.5	Treatment of Free Surface.....	39

2.6	Motion of Structure	41
2.7	Flow Chart of the Algorithm	43
2.8	Grid Dependence.....	45
2.9	Model Validation	46
2.9.1	TLD-Structure System with One Screen and without Screens Exposed to Harmonic Excitation. ..	46
2.9.2	TLD-Structure System With Two Screens Exposed to Non-Harmonic Time Varying Excitation..	49
2.9.3	Frequency Domain Comparison with Equivalent TMD and Shallow Wave Numerical Methods...	52
2.9.4	Sloped Bottom TLD.	55
3	CHAPTER THREE: INVESTIGATION OF THE EFFECT OF SCREEN SOLIDITY ON STRUCTURE RESPONSE UNDER HARMONIC EXCITATION	58
3.1	Introduction	58
3.2	TLD and Structure Geometry.....	58
3.3	Harmonic Excitation Used	59
3.4	Structure Displacement and Acceleration	59
3.5	Analysis of Results.....	63
4	CHAPTER FOUR: INVESTIGATION OF THE EFFECT OF SCREEN CONFIGURATION ON THE RESPONSE OF STRUCTURE UNDER A NON-HARMONIC TIME VARYING EXCITATION	64
4.1	Introduction.....	64
4.2	Non-harmonic Excitation Definition.....	64
4.3	Different Screen Configurations Tested.....	66
4.4	Analysis and Selection Criteria.....	66
4.5	Conclusions.....	75
5	CHAPTER FIVE: TLD FLUID HEIGHT EFFECT ON STRUCTURE RESPONSE.	77

5.1	Introduction.....	77
5.2	Description of Parameters Involved.....	78
5.3	Test Cases	81
5.4	Results and Analysis	82
5.5	Analysis.....	86
6	CHAPTER SIX: SLOPED BOTTOM TLD.....	88
6.1	Introduction.....	88
6.2	Performance and Significance of Sloped Bottom TLDs	94
7	CHAPTER SEVEN: COMMENTS ON TLD PERFORMANCE CRITERIA.....	102
8	CHAPTER EIGHT: SUMMARY AND CONCLUSIONS.....	105
8.1	Summary of Rectangular TLD Investigation	105
8.2	Sloped Bottom TLD Importance.....	107
8.3	Recommendations and Future Work.....	107

List of Tables

Table 1.1 Structural protective systems [Soong and Dargush,1997].....	2
Table 1.2 Test cases reported in Tait (2004).....	21
Table 2.1 Grid dependency analysis for TLD without screens.....	45
Table 2.2 Grid dependency analysis for TLD with one screen.....	46
Table 2.3 SDOF structure properties	50
Table 3.1 Results of maximum structure deflection at solidities 0.4, 0.5, and 0.6	63
Table 4.1 Test cases conducted under non-harmonic excitation	66
Table 4.2 Results of structure response under non-harmonic excitation	70
Table 4.3 Maximum velocity at the screen for different test cases	74
Table 5.1 Test cases of different fluid height and corresponding natural frequency and structure properties.....	82

List of Figures

Figure 1.1 Schematic of undamped TMD [Hamelin, 2007]	4
Figure 1.2 Amplitude response vs excitation frequency in undamped TMD	5
Figure 1.3 Schematic of damped TMD [Hamelin, 2007]	6
Figure 1.4 Amplitude response vs excitation frequency of a Damped TMD	7
Figure 1.5 Taipei 101 bottom TMD schematic [Taipei 101 Official Website].	8
Figure 1.6 Taipei 101 top TMD [Taipei 101 Official Website].....	8
Figure 1.7 Schematic of a Tuned Liquid Damper.....	9
Figure 1.8 Schematic of TLD principles [Yamamoto and Kawahara, 1999]	10
Figure 1.9 TLD installed on the roof of One Rincon Hill Tower [Skyscraperpage.com].	11
Figure 1.10 Schematic of practical damped equivalent TMD [Hamelin, 2007].....	13
Figure 1.11 Displacement Vs. excitation frequency for a SDOF system (single vibrating mass)	15
Figure 1.12 Displacement Vs excitation frequency for a two degree of freedom system [Den Hartog, 1956]	15
Figure 1.13 Actual natural frequency of a TLD compared with the linear calculation [Tait, 2004]	18
Figure 1.14 Wave breaking illustration [Soong and Dargush (1997)].....	20
Figure 1.15 Schematic of the development of TMD equivalency method [Tait, 2004] ...	27
Figure 2.1 Schematic of TLD-Structure coupling used in this study.....	31
Figure 2.2 TLD fitted with one screen	32
Figure 2.3 Screen Solidity [Marivani, 2009]	33

Figure 2.4 Contour plot of the θ value for cases of TLDs with screens [Marivani, 2009]	37
Figure 2.5 Setting obstruction ratio to zero in areas representing the sloped bottom.....	38
Figure 2.6 An upclose view of the modelled sloped bottom	38
Figure 2.7 Volume fraction values around a free surface interface [Poo and Ashgriz (1990)].....	39
Figure 2.8 Donor acceptor diagram [Marivani, 2009].....	40
Figure 2.9 Free surface reconstruction [Marivani, 2009]	41
Figure 2.10 Free body diagram of structure properties shown with TLD [www.eng.nus.edu.sg].....	42
Figure 2.11 Flow Chart of Overall Solver [Marivani, 2009].....	43
Figure 2.12 Comparison between numerical and experimental data of Free Surface Deflection [Marivani, 2009]	48
Figure 2.13 Comparison between numerical and experimental data of Free Surface Deflection [Marivani, 2009]	48
Figure 2.14 TLD fitted with 2 screens [Tait, 2004].....	49
Figure 2.15 Schematic of the experimental test rig used by Tait (2005).....	50
Figure 2.16 Non-harmonic excitation force used in both experimental and numerical runs	51
Figure 2.17 Comparison between experimental data and numerical results of structure acceleration [Marivani, 2009].....	52
Figure 2.18 Energy absorption Vs normalized excitation frequency at $h/L=0.2$ [Tait et al, 2005]	53

Figure 2.19 Normalized excitation force Vs excitation frequency [Marivani & Hamed, 2009]	54
Figure 2.20 Schematic of the sloped bottom TLD [Olson and Reed, 2001].....	55
Figure 2.21 Comparison between numerical results, and experimental data of the frequency response of a sloped bottom TLD [Olson and Reed, 2001].....	56
Figure 2.22 Comparison between experimental data [Gardarsson et al, 2001], equivalent TMD numerical data [Olson and Reed, 2001] and present numerical results of sloshing force Vs excitation frequency	57
Figure 3.1 Temporal variation of structure deflection in cases without TLD, with TLD and no screen, and with TLD with one screen with $S= 0.4$	61
Figure 3.2 Temporal variation of structure deflection in cases without TLD and with TLD with one screen with $S=0.4$	61
Figure 3.3 Temporal variation of structure deflection in cases without TLD and with TLD with one screen with $S=0.5$	62
Figure 3.4 Temporal variation of structure deflection in cases without TLD and with TLD with one screen with $S=0.6$	62
Figure 4.1 Fast Fourier Transformation on the excitation signal shown in figure 2.16....	65
Figure 4.2, 4.3 Structure deflection and acceleration, case without screen	67
Figure 4.4, 4.5 Structure deflection and acceleration, case of one screen with $S=0.4$	67
Figure 4.6, 4.7 Structure deflection and acceleration, case of one screen with $S=0.5$	67
Figure 4.8, 4.9 Structure deflection and acceleration, case of one screen with $S=0.6$	68

Figure 4.10, 4.11 Structure deflection and acceleration at $x=0.1L$ and $0.9L$, case of two screens with $S=0.4$	68
Figure 4.12, 4.13 Structure deflection and acceleration at $x=0.2L$ and $0.8L$, case of two screens with $S=0.4$	68
Figure 4.14, 4.15 Structure deflection and acceleration at $x=0.25L$ and $0.75L$, case of two screens with $S=0.4$	69
Figure 4.16, 4.17 Structure deflection and acceleration at $x=0.4L$ and $0.6L$, case of two screens with $S=0.4$	69
Figure 4.18 Maximum structure acceleration and deflection for the case of no screen and one screen with different solidities	71
Figure 4.19 Maximum structure acceleration and deflection for the case of two screens at solidity 0.4 and different locations.....	71
Figure 4.20 Maximum structure acceleration and deflection for the case of two screens at solidity 0.5 and different locations.....	72
Figure 4.21 Maximum structure acceleration and deflection for the case of two screens at solidity 0.6 and different locations.....	72
Figure 5.1 TLD dimensions	78
Figure 5.2 Frequency sweep (sloshing force vs excitation frequency) for $h/L = 0.1$	80
Figure 5.3 Frequency sweep (sloshing force vs excitation frequency) for $h/L = 0.2$	80
Figure 5.4 Structure response Vs fluid height at $A/L=0.2\%$	83
Figure 5.5 Structure response Vs fluid height at $A/L=0.8\%$	84
Figure 5.6 Structure response Vs fluid height at $A/L=3\%$	84

Figure 5.7 Time Capture of Sloshing under $A/L = 0.2\%$ showing wave breaking.....	85
Figure 5.8 Generalized damping ratio Vs fluid height [Deng, 2007]	87
Figure 5.9 Actual sloshing mass and damping ratio Vs excitation amplitude [Tait, 2004]	88
Figure 6.1 Experimental apparatus used for sloped bottom TLD [Gardarsson et al, 2001]	89
Figure 6.2 Schematic of the sloped bottom TLD [Olson and Reed, 2001]	90
Figure 6.3 . Recirculation Zone forming at a rectangular TLD corner	91
Figure 6.4 Streamlines in the rectangular TLD at 3 time captures showing the recirculation zone.....	92
Figure 6.5 Streamlines in the sloped bottom TLD at 3 time captures showing no recirculation zone.....	93
Figure 6.6 Schematic of the braces fitted on the One Rincon Hill, [www.structuremag.com/images]	95
Figure 6.7 Sloped bottom TLD Geometry	96
Figure 6.8 a) Structure deflection with sloped bottom TLD b) Structure deflection with rectangular TLD without screen	97
Figure 6.9 Comparison of structure response in cases of sloped and rectangular TLD ...	98
Figure 6.10 Comparison of structure response in cases of sloped and rectangular TLD in case of non-harmonic excitation	98
Figure 6.11 Non-harmonic excitation generated to test TLD dampening behaviour	100

Figure 6.12 Dampening behaviour in terms of structure response in cases of sloped and rectangular TLDs	100
Figure 6.13 Dampening behaviour in terms of structure response in case of rectangular TLD with two screens.....	101
Figure 7.1 Comparison between structure responses in the case of one screen and two screens [Morteza, 2009].....	103
Figure 7.2 Comparison between sloshing forces in the case of one screen and two screens [Morteza, 2009].....	104

Nomenclature

A	Amplitude of external dynamic excitation, m
g_x	Horizontal acceleration, m/s^2
g_y	Gravitational acceleration, m/s^2
L	Length of tank, m
B	Tank Width, m
d	Tank height, m
h	Height of the initial flat free surface, m
p	Pressure, Pa
t	Time, s
u,v	Velocity component in the horizontal and vertical directions, respectively
x,y	Cartesian coordinates
F	Volume of fluid per unit volume of cell
F_e	External excitation force, N
D_s	The slat height, mm
S	Solidity ratio
P	Total momentum of fluid, $kg.m/s$
U_s	Velocity at screen, m/s
F_{TLD}	Sloshing force, N
f_{TLD}	Natural frequency of TLD, Hz
k_s	Spring stiffness of main structure, N/m

ρ	Density, kg/m ³
ν	Kinematics viscosity, m ² /s
μ	Mass ratio
τ	Shear stress, N/m ²
σ	Surface tension, N/m
θ	Partial flow flag
φ	Phase angle, degree
ω	Frequency of sloshing, rad/s
ζ	Damping ratio
β	Normalized Frequency Ratio, Ratio of excitation frequency and natural frequency
θ_i	Angle of sloped bottom, degree

1 Chapter 1: Introduction and Literature Review

1.1 Introduction

1.1.1 Dampers Introduction

It is quite reasonable to say that within the last 100 years, structural engineering has shifted its position on the levels and thresholds necessary for building codes. The building codes which were enforced in the early and mid twentieth century, dictated limitations of lateral force on structures, and were to provide what was quoted as “life safety”. This meant that if a structure met these codes, it would more than likely not collapse upon severe excitation such as earthquakes, and would thus save lives. This fact was put to the test with the earthquakes that struck between 1989 and 1999 (California in 1989 and 1994, Japan in 1995, Turkey in 1999, and Taiwan in 1999). The buildings that met the codes in these areas did stay up but suffered damages that were far greater than expected [Hanson and Soong (2001)]. In the early 1980s, research efforts in various parts of the world had suggested that increasing lateral force design levels is not enough, and it should be accompanied with auxiliary methods to maintain structural integrity. These studies were taken far more seriously after the mentioned events, and this marked a shift in how building codes were perceived and developed. During that time another shift happened with the trend of taller and leaner buildings, especially in densely populated areas. Wind forces were causing these buildings to sway considerably. In most, if not all, of the cases, the deflection was never a threat to the structural integrity, but more an extreme discomfort for residents of the top floors. Concerns were raised about structural acceleration and human perception of motion in tall buildings. Conferences and panels in

the civil structure community concluded that while the ability of the building design to withstand loads was important, there was a maximum threshold for structure acceleration after which occupants feel discomfort. Building codes were modified in the 1990s again to take into consideration this important habitability criterion.

As a result, there was significant focus on developing auxiliary damping systems for structures. The studies investigating these methods can be categorised into three main methodologies: Seismic isolation systems, passive energy dissipation systems, and active structural control systems (see Table 1.1). The main difference between passive and active methods is that the latter requires a power supply, and can vary some of the system damping characteristics depending on the nature of excitation. Naturally active methods are usually more efficient but are significantly more expensive.

Table 1.1 Structural protective systems [Soong and Dargush,1997]

<u>Seismic Isolation</u>	<u>Passive Energy Dissipation</u>	<u>Semi-active and Active Energy Dissipation</u>
Elastomeric Bearings	Metallic Dampers	Active Bracing Systems
	Friction Dampers	Active Mass Dampers
Lead Rubber Bearings	Viscoelastic Dampers	Variable Stiffness or Damping Systems
	Viscous Fluid Dampers	Smart Materials
Sliding Friction Pendulum	Tuned Mass Dampers	
	Tuned Liquid Dampers	

The research scope of this thesis focuses on Tuned Liquid Dampers (TLD), which are devices that fall under the category of Passive Energy dissipation. Prior to the discussion of TLDs and how they work, another well established passive energy dissipation device, which is the Tuned Mass Damper (TMD), will be discussed. This is because most of the basic principles and properties of TLDs are analogous to those of TMDs.

1.1.2 Tuned Mass Dampers

In its simplest form, a TMD consists of an auxiliary mass-spring or mass-spring-dashpot system anchored to the main structure, where its main task is to absorb some of the structural vibrational energy and counter effect of the excitation force.

1.1.2.1 Undamped Tuned Mass Dampers

Figure 1.1 shows a schematic representation of a structure of mass m_1 and stiffness k_1 acted upon by a harmonic excitation $F_0 \sin \Omega t$. The TMD is a comparatively small vibratory system of mass m_2 and stiffness k_2 attached to the main system mass m_1 . The local natural frequency $\sqrt{k_2/m_2}$ of the absorber is chosen to be equal to the natural frequency of the main system $\sqrt{k_1/m_1}$, hence the term “tuned”.

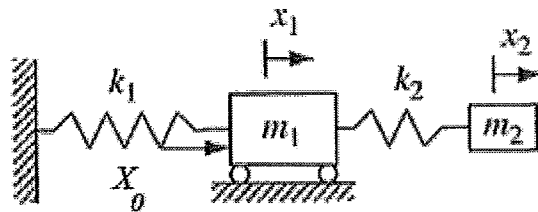


Figure 1.1 Schematic of undamped TMD [Hamelin, 2007]

Figure 1.2 shows the variation of the resultant amplitude response ratio, $\frac{X_1}{X_0}$, with frequency ratio, β , where X_1 is the amplitude of the effective main mass m_1 , X_0 is the amplitude of excitation imposed on the structure, and β is ratio of the excitation frequency and the natural frequency of m_1 or m_2 . Under the condition of $\beta = 1$ specifically, the main mass m_1 does not vibrate at all, and the absorber mass m_2 vibrates in such a way that its spring force is at all instants equal and opposite to the harmonic excitation. This means that the net force on m_1 is zero. On the other hand, resonance will occur at two different excitation frequencies ($\beta = 0.8$ and $\beta = 1.25$), which is expected for a two degree of freedom system.

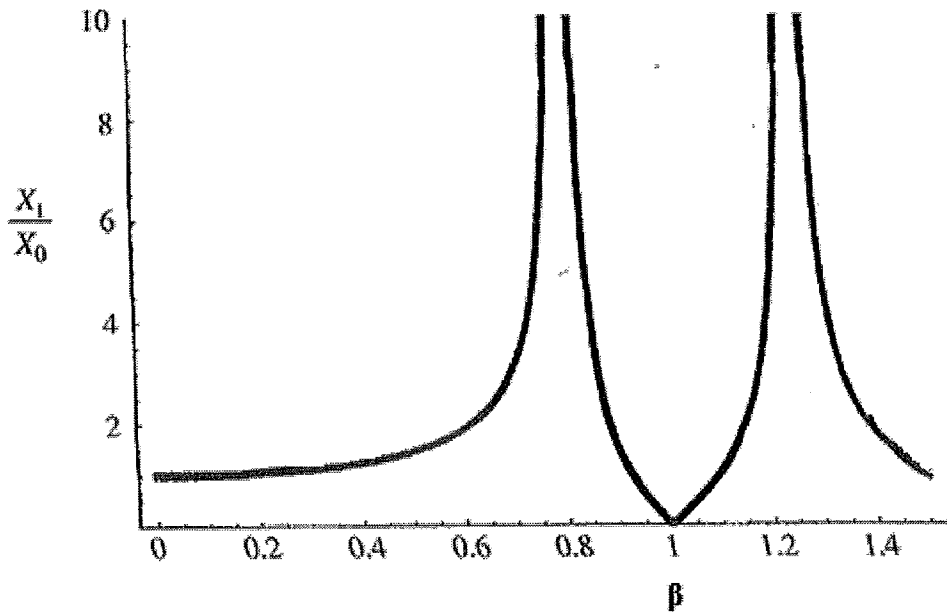


Figure 1.2 Amplitude response vs excitation frequency in undamped TMD

1.1.2.2 Damped Tuned Mass Dampers

Complete suppression of the main mass m_1 is possible with the latter system, nevertheless there is a need for a slightly more complicated auxiliary system to be used as a damper.

The reasons would be:

- First, the exciting frequency in actual engineering applications is never known before-hand. Thus tuning of the vibration absorber frequency to excitation frequency is practically impossible, and therefore a perfectly damped system is impossible.
- Second, at two external excitation frequencies the system resonates, which turns the situation of a standalone mass m_1 with one probability of resonating to a chaotic

situation of two probabilities of resonance, when this inefficient undamped vibration absorber is used.

Figure 1.3 shows a schematic of the alternative damped TMD.

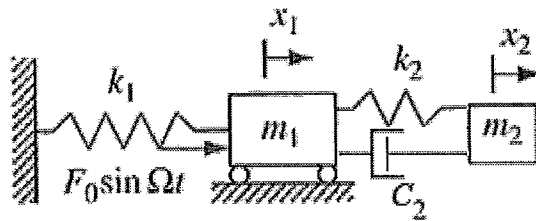


Figure 1.3 Schematic of damped TMD [Hamelin, 2007]

Figure 1.4 illustrates the resultant response of the main system mass with a typical damping ratio $\zeta=10\%$. One can immediately notice that the perfect damping of the main mass that happened using the undamped TMD at $\beta=1$ did not occur. However, the damped TMD controls the system vibration at any other excitation frequency (i.e. no more resonance). This type of TMD is the one actually used in practical civil applications.

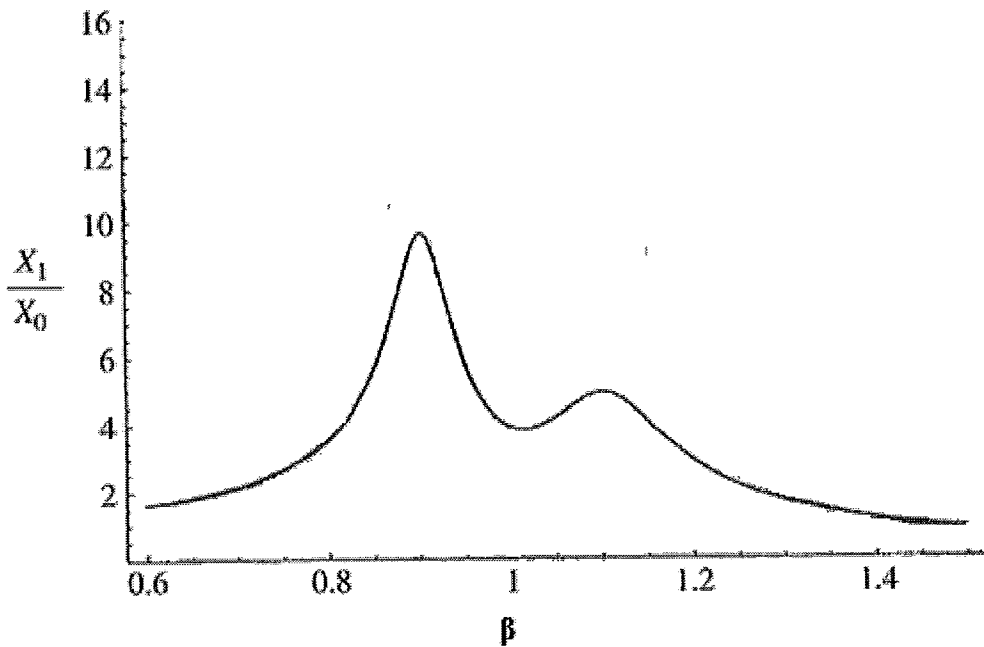


Figure 1.4 Amplitude response vs excitation frequency of a Damped TMD

1.1.2.3 Structural Implementations

The first TMD installed in a structure was in the Centerpoint Tower in Australia in 1987 [Soong and Dargush (1997)]. More recent TMDs were installed in the Taipei 101 building in Taiwan in 2004. The main TMD, shown in figure 1.5, weighs 660 metric Tons, and cost 4 million US dollars. Eight dampers beneath the pendulum shaped TMD provide the needed inherent damping, and limit the motion of the TMD to 1.5 metres. This should only happen in the most extreme weather; otherwise the sway is in the order of tens of centimetres. Two other relatively small TMDs (6 tons each) limit the motion of the top spire on the building, and are shown in figure 1.6.

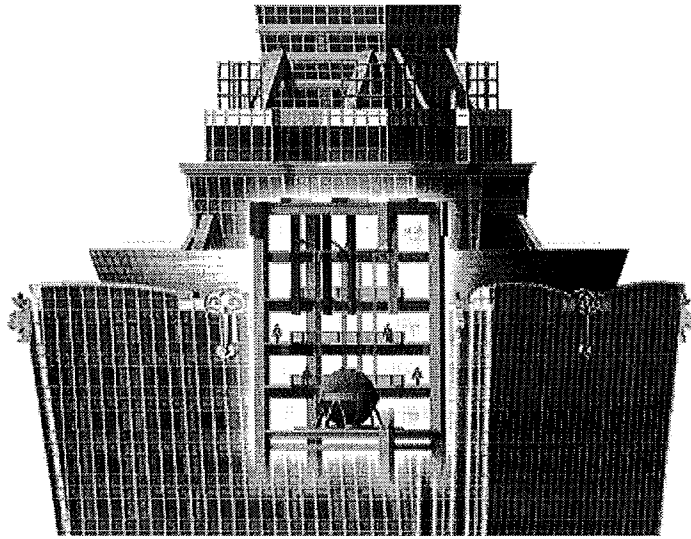


Figure 1.5 Taipei 101 bottom TMD schematic [Taipei 101 Official Website].

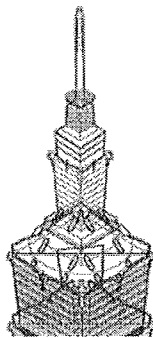


Figure 1.6 Taipei 101 top TMD [Taipei 101 Official Website].

1.1.3 Tuned Liquid Dampers

1.1.3.1 Introduction

Tuned Liquid Dampers (TLDs) are tanks partially filled with liquid that have increasingly being used as vibration dampers in numerous engineering applications. Figure 1.7 shows a schematic of a TLD with length L , and water height, h . Upon excitation, the water

inside the TLD sloshes creating a wave as shown by the figure, which in turn produces a force opposite to the excitation direction. Since the 1980s, TLDs have been coupled to structures to mitigate their sway, especially in taller leaner buildings. The attractiveness in using TLDs lies in their low cost and maintenance and simple design compared to other vibration dampers. Additionally, the necessity of installing fire water tanks in current building codes creates an opportunity for using the same tanks as TLDs by accurately tuning their design to meet both objectives. The TLD is designed to have the same natural frequency of the structure [Lamb (1932)], so that sloshing motion of fluid inside the TLD caused by the external excitation produces a sloshing force approximately anti-phase to the building motion (see Figure 1.8). This is similar to the operation of the TMD, which has lead many researchers to draw analogies and develop equivalent TMD systems to describe TLD behaviour. This analogy will be discussed in section 1.2.2 in detail.

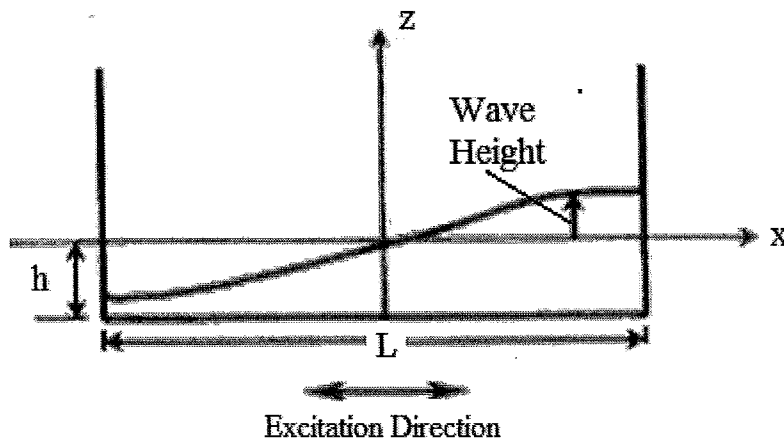


Figure 1.7 Schematic of a Tuned Liquid Damper

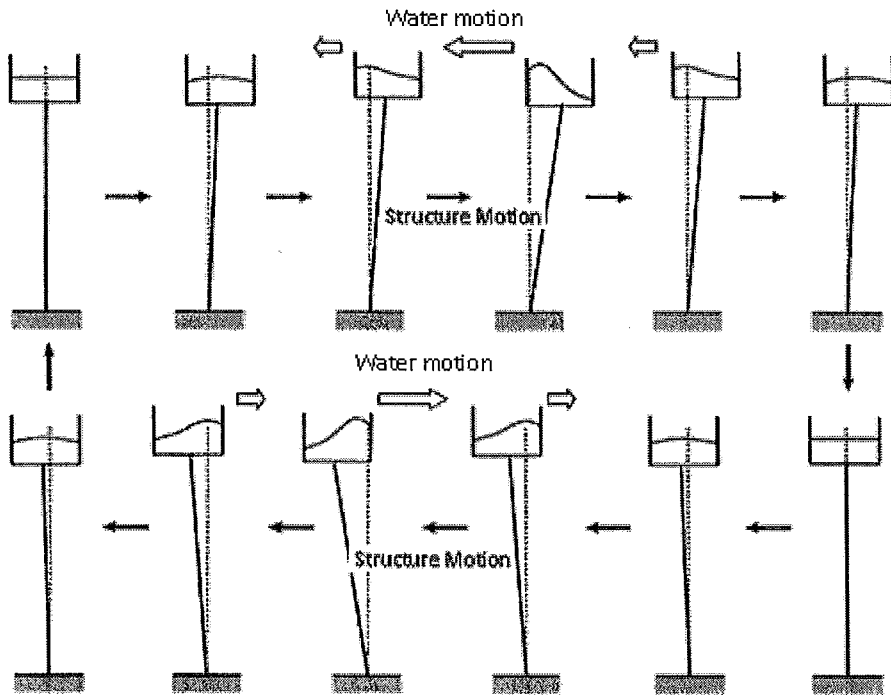


Figure 1.8 Schematic of TLD principles [Yamamoto and Kawahara, 1999]

The idea of using a liquid tank as a TLD was proposed almost 100 years ago by Frahm in 1909 [Den Hartog (1956)]. At that time the TLD was termed a “Dynamic Vibration Absorber”, and was primarily used for ship applications, specifically for reducing rolling in rough seas. It was also reportedly used in the 1960’s in space applications to reduce satellite oscillation [Bhuta and Koval (1966); Carrier and Miles (1960)]. The first attempt at coupling a TLD to civil engineering structures was carried out by Bauer (1984), and further investigated by Kareem and Sun (1987).

1.1.3.2 Structural Implementations

The very first commercial installation of a TLD was in Japan around the late 1980s. Since then, many existing buildings that suffered from vibrational problems had been outfitted with TLD systems, simply through modifying the existing water storage tanks that already existed for firefighting purposes. Because of limited space on building rooftops, the idea of using denser, more viscous fluids than water in TLDs has not found much appeal, as TLDs are usually used as water reservoirs for firefighting as well. Two recent examples of towers fitted with TLDs are the One King West Tower in Toronto, Canada, completed in 2005, and the One Rincon Hill Tower in San Francisco, U.S.A, completed in 2009. They both employ rectangular TLDs fitted with screens for increased damping. Figure 1.9 shows a computer generated image of the TLD in One Rincon Hill, and its location on top of the building.

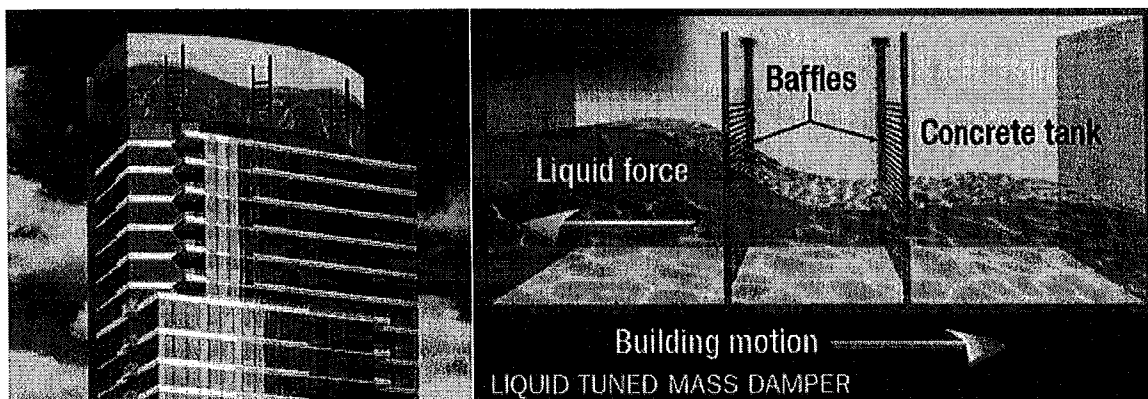


Figure 1.9 TLD installed on the roof of One Rincon Hill Tower [Skyscraperpage.com].

1.1.4 TLD Design Parameters

Mass Ratio

The mass ratio, μ , is simply defined as the ratio of the mass of the liquid inside the TLD to the mass of the structure. This would mean that:

$$\mu = \frac{m_2}{m_1} \quad (1.1)$$

where m_2 is the mass of the damper system, in this case the TLD, and the m_1 is the mass of the structure.

It has been indicated in literature that high mass ratios are desirable [Ju et al. (2004)]. A 200 to 300 metre tower would weigh between 50 to 150 thousand metric tons depending on its size. A TLD having a 1% mass ratio would have between 500 and 1500 metric tons of liquid. Considering the density of water and a standard water depth of 10 to 20% of tank length, one would need 500 to 1500 square metre of roof space for the TLDs. This is usually unattainable, thus mass ratios usually have practical limitations rather than an optimal targeted value. Even with TMDs that are made of dense metals, mass ratios are rarely above 1%. For example the TMD used in Taipei 101 has a mass ratio of 0.11 %.

It is also worth noting that not all the mass of liquid inside the TLD contributes fully to the sloshing force. Due to the formation of recirculation zones in the tank, a portion of the fluid does not give its momentum in the desired direction. In the 1950s, researchers using the potential flow theory [Graham and Rodriguez (1952)], attempted to

determine the effective liquid mass (m_{eff}) and the non-contributing mass (m_0). They proposed the following equation for m_{eff} :

$$m_{eff} = \frac{8 \tanh\left(\pi \frac{h}{L}\right)}{\pi^3 \left(\frac{h}{L}\right)} m_2 \quad (1.2)$$

where h is fluid depth inside the TLD, and L is TLD length in the direction of excitation. Figure 1.10 illustrates the split of m_2 into an inactive mass, m_0 , rigidly attached to the structure and not contributing to countering the excitation force, and an active mass, m_{eff} , that contributes to the sloshing force.

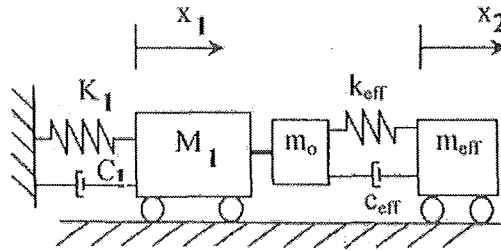


Figure 1.10 Schematic of practical damped equivalent TMD [Hamelin, 2007]

Damping Ratio

The damping ratio is defined by Chopra (2000) as:

$$\zeta = \frac{C}{C_{critical}} \quad (1.3)$$

where C is a measure of energy dissipation over a cycle of vibration, and $C_{critical}$ is the critical damping coefficient, defined as:

$$C_{critical} = 2 * m_2 * (2\pi f_{TLD}) \quad (1.4)$$

where f_{TLD} is the natural frequency of the TLD. Using linear wave theory Sun (1991) developed the following expressions for the damping ratio for TLDs:

$$\zeta = \frac{1}{2h} \sqrt{\frac{\nu}{\pi f}} \left(1 + \frac{h}{L}\right) \quad (1.5)$$

where ν is the kinematic viscosity of the liquid inside the TLD. One might assume that the larger the ζ value, the better the vibration absorber would perform. This is true in case of SDOF system as shown in figure 1.11. A TLD-structure system is a two degree of freedom system. The response would be similar to the response shown in figure 1.4 for a TMD-structure system. Den Hartog (1956) carried out an analysis of TMDs where he increased the inherent damping ratio of the TMD repeatedly and calculated the resultant displacement of the main mass over a frequency sweep, see figure 1.12: increasing the damping ratio from 0 to 0.32. As the damping ratio is increased till 0.1, the overall response of the main mass was improved. A further increase to 0.32 (very heavy damping) deteriorated the performance of the TMD and the main mass maximum displacement increased by 55%. This was because very heavy damping lead to an increase in the non-contributing mass (m_0) and a decrease in the effective mass (m_{eff}).

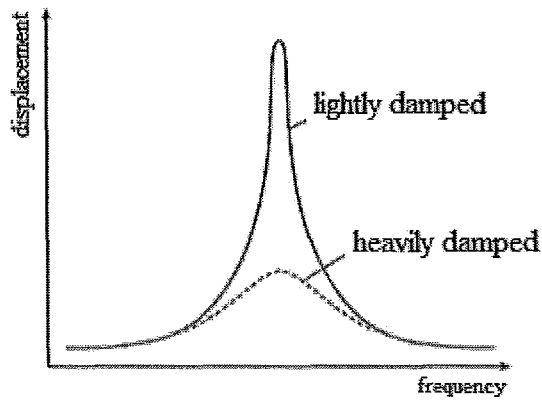


Figure 1.11 Displacement Vs. excitation frequency for a SDOF system (single vibrating mass)

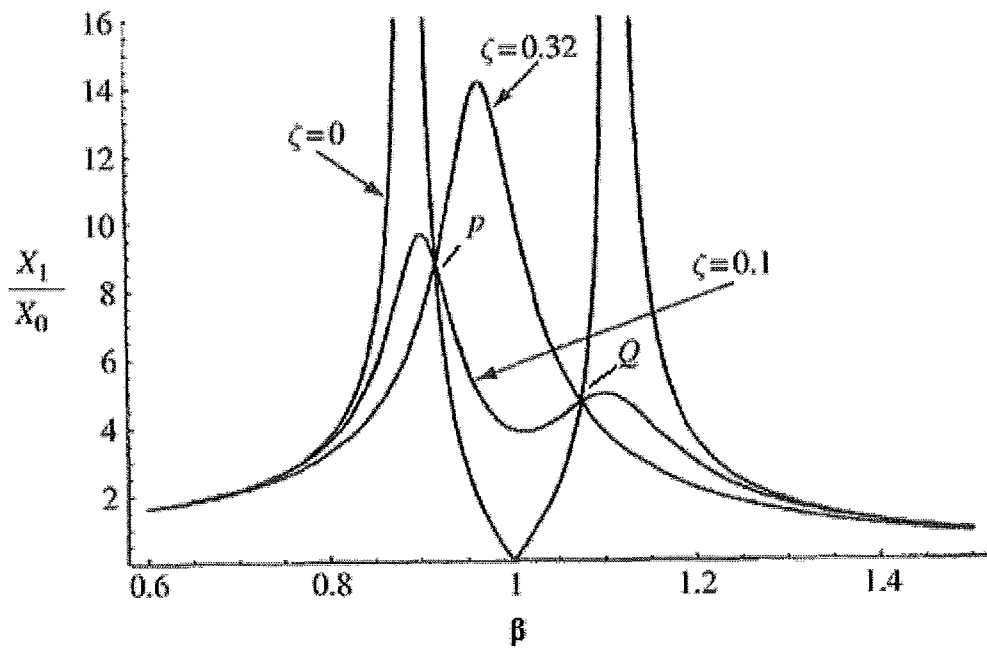


Figure 1.12 Displacement Vs excitation frequency for a two degree of freedom system [Den Hartog, 1956]

Points P and Q in figure 1.12, represent the two peaks that indicate the best structure response. The damping ratio that produced the response at those two points was calculated from the following equation:

$$\zeta_{opt} = \sqrt{\frac{3\mu}{8(1+\mu)}} \quad (1.6)$$

This equation has been used frequently in literature for estimating the optimal damping of a TLD, because of its close analogy with TMDs. In the study done by Den Hartog (1956), the main structural system was assumed to have no damping. In 1978 and 1982 Warburton experimentally and analytically estimated more accurate methods for calculating the optimum damping taking into account the following variables:

- Level of structure damping.
- Type of excitation: harmonic and random.
- Line of action of the external excitation: forces applied to the structure, as in the case of wind, or applied to the base, as in the case of earthquakes.

It was concluded that for mass ratios within the practical application, the optimal damping ratio is around 5%.

Tuning Ratio

The tuning ratio, Ω , is the ratio of the TLD natural frequency, f_{TLD} , and the natural frequency of the structure, f_1 , i.e.,

$$\Omega = \frac{f_{TLD}}{f_1} \quad (1.7)$$

f_{TLD} can be calculated by using the linear wave theory, Lamb (1932), from:

$$f_{TLD} = \frac{1}{2\pi} \sqrt{\frac{\pi g}{L} \tanh\left(\frac{\pi h}{L}\right)} \quad (1.8)$$

Initially, one would think that the optimal tuning ratio would be unity to ensure that the generated sloshing force inside the TLD would be anti-phase to the motion of the structure. However Den Hartog (1956) showed that the optimal value of Ω can be calculated from:

$$\Omega_{opt} = \frac{1}{1+\mu} \quad (1.9)$$

With mass ratios around 1 % the optimal value of Ω given by equation (1.9) would not deviate much from unity. The further detailed analysis carried out by Warburton (1982) also included determining the optimal Ω , and lead to the same conclusion.

Recent analysis carried out experimentally by Tait et al. (2004), and numerically by Marivani (2009), indicated that the more accurate method of determining f_{TLD} , is by performing an excitation frequency sweep and measuring the sloshing force generated by the TLD, or the free surface deflection. The point at which maximum response occurs corresponds to the actual natural frequency. Figure 1.13 shows a comparison between the numerical prediction of the sloshing force using a linear model (equivalent TMD) and experimental values. The linear model prediction of the natural frequency is equal to the

value calculated by equation 1.8, which is about 5% deviated from the actual natural frequency indicated by experimental testing.

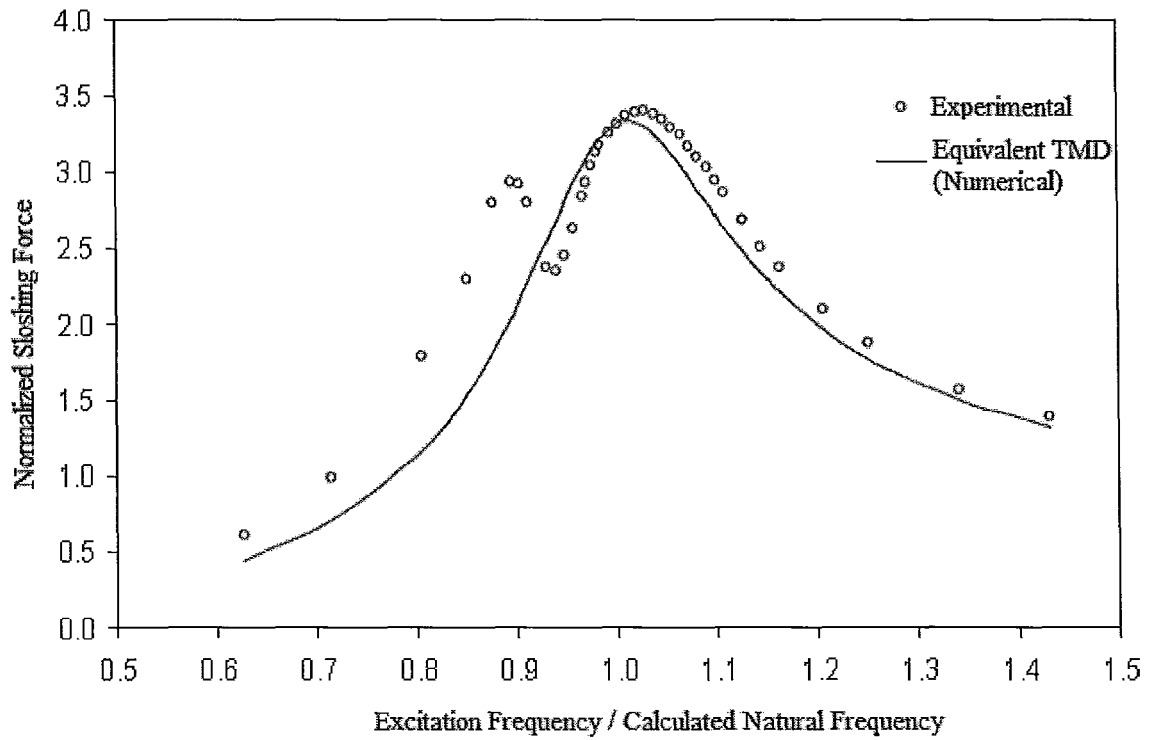


Figure 1.13 Actual natural frequency of a TLD compared with the linear calculation [Tait, 2004]

1.2 Literature Review

1.2.1 Nature of Excitation Considered in Literature

In most of the research carried out on liquid dampers, excitation force was considered to be only unidirectional. In experimental test setups, this is either created by a one dimensional shake table or a unilateral wave maker. When wind forces on high-rise towers are considered, the force is safely assumed to be harmonic in nature, with low to moderate amplitudes. This means an amplitude of less than 1% of the TLD length. If earthquake forces are considered, high amplitudes are used (greater than 2% of TLD length). Most of the studies that tested TLD damping effectiveness under earthquake forces used white noise excitation signals rather than harmonic.

1.2.2 TLD Additional Damping Techniques

1.2.2.1 Screens

TLDs can be classified into shallow water TLDs and deep water TLDs, based on the ratio of fluid depth to tank length. According to Dean and Dalrymple (1984), the limit for shallow water TLDs is a fluid depth around 10-12% of tank length. Damping in deep water TLDs is mainly due to fluid viscosity, which has been proven to be too low to be sufficiently effective [Sun (1991)]. Shallow water TLDs, on the other hand, have desirable high damping, due to the fact that they tend to experience wave breaking as shown in figure 1.14. Wave breaking results in damping ratios that can be an order of magnitude higher than damping ratios experienced in deep water TLDs. However, shallow water TLDs are not practical due to the extreme nonlinearity and unpredictable

nature of wave breaking. The limit on liquid depth in shallow water TLDs also leads to low water mass inside the tank. All studies have shown that TLD effectiveness is proportional to its mass ratio. Therefore, using shallow water TLDs means using a larger number of tanks to achieve the desired mass ratio, which is not always possible due to space limitations. Therefore there is a need to install additional damping devices inside deep water TLDs to increase their inherent damping. This would also result in maintaining desirable mass ratios, reducing nonlinearities, and enhancing performance predictability.

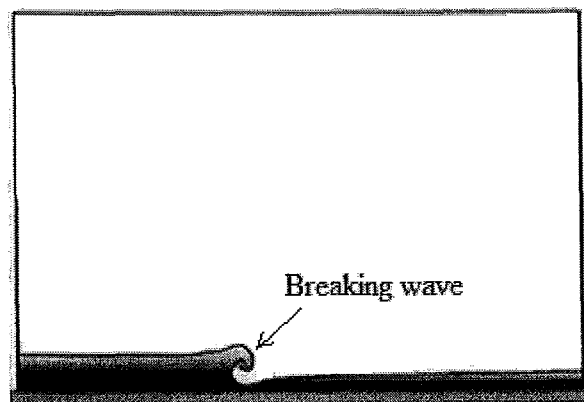


Figure 1.14 Wave breaking illustration [Soong and Dargush (1997)]

Attempts at adding damping devices to TLDs started in the 1950's and included adding ring baffles to the tank walls by Miles (1967), Bauer (1964), and Abramson (1967). A more recent approach is to use submerged nets or screens in the TLD, to induce energy dissipation due to fluid flow through the orifices [Kaneko and Ishikawa (1999); Tait et al. (2005)]. The main attractive feature of screens is the fact that the damping can be

easily adjusted by changing the screen solidity ratio (ratio of blocked area to open area in the screen). Hamelin (2007) conducted a rigorous experimental study to investigate the effect of screen geometry on TLD performance. The study considered harmonic amplitudes of 1-3% of TLD length, and a wide range of solidity ratios. Cassolato (2007) considered TLDs with moving screens that are hinged at one point and allowed to move with fluid sloshing within certain angles.

To the author’s best knowledge, the only prominent attempt to define the effect of number of screens and location within a TLD was carried out by Tait (2004). Only four basic test cases were considered (shown in Table 1.2). Screen locations were expressed as a ratio of the tank length, and measured from middle of the tank. In all cases, the screen solidity was kept constant at 0.42. Only harmonic excitation was considered in this study. The deciding criterion for the best arrangement was determined based on the amount of energy absorbed by the TLD. The case of three screens was found to be the best.

Table 1.2 Test cases reported in Tait (2004)

Test Case	Number Of Screens	Screen Location (% L)	Normalized Excitation Amplitudes (A/L)
A	2	+/- 10	0.003-0.041
B	2	+/- 20	0.005-0.021
C	2	+/- 25	0.010-0.021
D	3	+/- 25 & 0	0.010

1.2.2.2 Sloped Bottom TLDs

Mei (1983) studied ocean dynamics and noticed that the sloping beach is an effective energy and wave dissipater. It has become common knowledge in tsunami research that most of the wave energy is dramatically dissipated along the shores [Olson and Reed (2001)]. Recently, research has applied the same physical phenomenon in TLDs, and studied the effect of creating a sloped bottom towards the ends of a rectangular TLD. Gardarsson et al. (2001) experimentally studied the effect of a 30° sloped bottom at the two corners of the TLD, and empirically modified the linear equation used to estimate TLD natural frequency. Their results confirmed the high level of damping and the significant increase in the contributing sloshing mass a sloped bottom TLD has. There has been some numerical research efforts to simulate sloshing in sloped bottom TLDs using the equivalent TMD methods [Yu (1997), Olson and Reed (2001)]. Upon validation, some discrepancies aroused due to non-linearities not accurately accounted for. To the author's best knowledge, there have been no further numerical attempts to accurately model this type of TLDs and assess its full behaviour when coupled to structures.

XiaoHua et al. (2009) experimentally investigated the effect of a sloped bottom TLD on the response of a three storey structure. The study assessed the effect of various geometries of the sloped bottom (V-, W-, and Arc shaped), and concluded that the V-shaped bottoms are the most effective in structure vibration mitigation.

1.2.3 Evolution of Numerical Work

1.2.3.1 Models based on the Potential Flow Theory

When numerical studies of the performance of TLDs first started around the mid-twentieth century, the coupling of a TLD to a civil structure was not considered. The main use was for marine applications. Numerical investigations at the time considered only the simulation of fluid flow inside a TLD exposed to external harmonic forces. The potential flow theory was used in the early 1950s, and considered the flow to be irrotational and inviscid. This linearized form of the solution was only valid at small excitation amplitudes. It is not surprising to learn that many numerical investigations until early this century [Dutta and Laha (2000) and Frandsen (2005)] still used the same theories. This is because experimental research carried out in the 1980s and 1990s had coupled TLDs with structures and confirmed that while flow non-linearities have a profound effect on the observed TLD parameters when the TLD is studied alone, when coupled with a structure, the effect of these non-linearities did not greatly affect the predicted structure response within limited excitation amplitudes (less than 1% of tank length) [Fediw et al. (1995)]. Consequently research based on the potential flow theory did not cover any applications except the effect of wind on high-rise structures, as any other application involves amplitudes outside the range of validity of numerical models based on the potential flow theory.

1.2.3.2 Models based on the Shallow Water Wave Theory

The shallow water wave theory has also been widely used in developing numerical models for TLDs [Shimizu and Hayama (1987)]. Numerical models based on this theory solved the nonlinear Navier Stokes equations under the assumption of relatively low wave height compared to the mean depth of liquid layer. Dean and Dalrymple (1984) defined the limit for applying this theory to $h/L < 0.1$, however numerical investigations later verified that it could be used for h/L up to 0.2, with a noted deviation from experimental data up to 14% [Tait et al. (2004)]. This theory also limits the level of excitation amplitude that can be used. Amplitudes greater than 1.6% of the TLD length resulted in deviation from experimental data up to 20% [Tait (2004)]. A numerical model based on the shallow water wave theory was later developed by accounting for the effect of wave-breaking using a semi-empirical parameter added to the governing equations [Sun and Fujino (1994)]. Even with such development, the numerical models based on the shallow water wave theory are still limited to low fluid heights, and relatively low values of excitation amplitudes [Tait (2004)]. Reed et al. (1998) developed a numerical algorithm using the shallow wave theory and used it with large amplitude excitation (greater than 1% of tank length). Although results did not quite match experimental data, the trends were predicted adequately enough to justify the use of the shallow wave theory with some experimental add-on knowledge for adjustment of tuning. Banerji et al. (2000) employed the shallow wave theory to predict TLD-structure performance under random excitation, modelling an earthquake signal. Their study considered 12 different cases of structure properties with various natural frequencies and damping ratios. They found the

TLD to decrease structure sway between 3% and 39%. However Yalla and Kareem (2002) later published a study refuting results obtained by Banerji et al. (2000), and showing that, with non-harmonic excitation, utilising the shallow water theory without proper empirical add-ons results in consistent under estimation of the sloshing force due to improper prediction of sloshing/slamming characteristics of the wave motion.

The shallow water wave theory was also utilised as the numerical model by Tait et al. (2005) in the numerical and experimental study they conducted on rectangular TLDs under two-dimensional excitation. The experimental part of the study calculated the two dimensional sloshing force generated in the TLD under two-dimensional excitation (circular shake table motion). To numerically predict the two dimensional sloshing force generated in the TLD, they ran two separate sets of numerical runs. Each numerical run considered a TLD under unilateral excitation of amplitude equal to the component of the circular motion in the direction considered. The decoupled sloshing force was adequately predicted using this method but under the limitation of low amplitude of excitation and low fluid height.

1.2.3.3 Models based on the Equivalent TMD Method

Many TLD investigations have been carried out based on the equivalent TMD method by researchers in Civil engineering. As noted previously, in the 1980s, TLD studies became increasingly popular due to its many advantages. It was very convenient to use the analogy between TLDs and TMDs to build on previous extensive research on

TMDs. This approach went through a series of milestones of advancement listed below in chronological order and shown in figure 1.15:

- a. Kareem and Sun (1987) developed and validated equations that model the TLD as an equivalent linear TMD.
- b. Sun et al. (1995) conducted experiments to estimate the nonlinearities that are inherent in TLD behaviour. Contrary to the case in TMDs, critical values such as natural frequency, inherent damping, and sloshing mass are amplitude dependant in TLDs. As a result, empirical amplitude dependant parameters were added on well established TMD linear equations.
- c. Yu et al. (1999) was able to simplify the work of Sun et al. (1995) and empirically modified the model by considering the mass constant and developing an amplitude dependant equivalent stiffness and damping. This study focused on higher amplitudes (greater than 1% TLD length) where the nonlinear model would be necessary. It is not surprising that the mass could be considered constant and almost equal to the total mass of liquid in the TLD due to the nature of the TLD response under high amplitude excitation.
- d. Yalla (2001) introduced a sloshing-slamming model that took into consideration the effect of water slamming against tank walls in extreme amplitude cases.
- e. Tait et al. (2004) further developed an empirical obtained non linear TMD equivalent model, and coupled it with a SDOF structure. They assessed the accuracy of their model through comparing structure response obtained from their shake table experiments with that obtained from the developed TMD equivalent nonlinear model.

f. Tait (2008) modelled the effect of submerged screens as a linearized equivalent damping ratio and successfully integrated it with his previous equivalent non-linear TMD model

Like the potential flow theory, in all previous studies TLD characteristics under certain large amplitudes were not captured adequately. However, TLD-structure performance was predicted in a reasonable fashion that makes these models attractive for their simplified form.

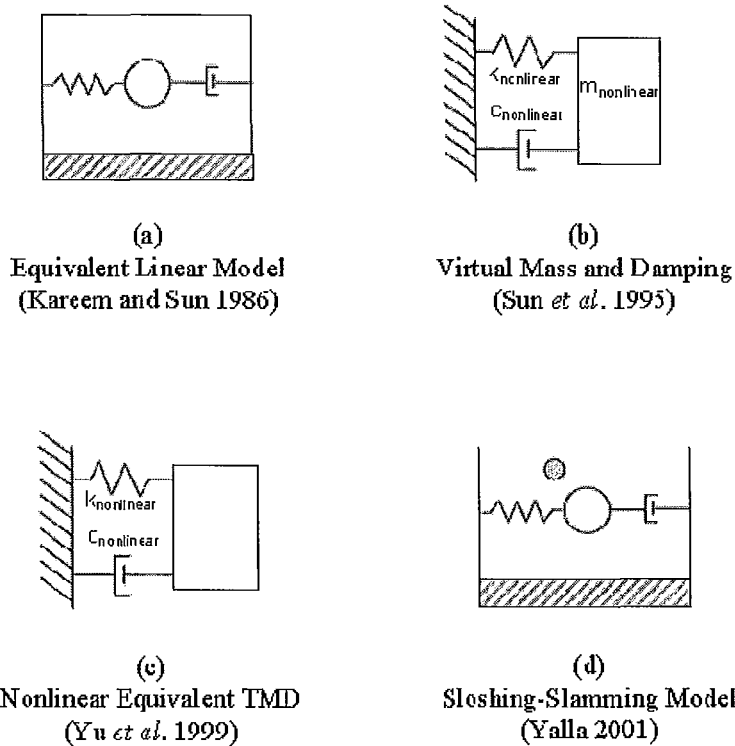


Figure 1.15 Schematic of the development of TMD equivalency method [Tait, 2004]

1.2.3.4 Non-linear Models

Siddique et al. (2004) developed a numerical model using stream-vorticity formulation and conformal mapping techniques to solve the full nonlinear moving boundary problem with wave heights reaching large values, without imposing any linearization. However they did not couple the TLD with a structure. Therefore, the effect of the TLD on structure sway was not investigated.

Marivani and Hamed (2009) developed and validated a numerical algorithm that solved the non-linear Navier Stokes equation incorporating the Volume of Fluid method to reconstruct the free surface. The model could handle a wide range of amplitudes of excitation and frequencies without any linearization assumptions. They also developed an integrated TLD-structure algorithm that was able to investigate the TLD effect on structure deflection and acceleration. Moreover, their algorithm fully resolved the flow through submerged screens, rather than model the screen as a point hydraulic resistance like past efforts [Kaneko and Ishikawa (1999), Tait (2004), and Hamelin (2007)]. This was done by modelling obstructions due to the screen using the Partial Cell Treatment method.

1.3 Research Scope and Objectives

This research is purely numerical in nature, and uses the algorithm developed by Marivani and Hamed (2009) for the TLD-structure coupling. The scope of this study has been determined by analysing previous research reported in literature and identifying points of interest that had not been studied before, or had not been modelled accurately due to limitations of the numerical models used. The following are the main objectives of this study:

- Investigate the best screen configuration that would yield minimum structure sway and acceleration under a non sinusoidal excitation.
- Study the effect of fluid height in TLDs on structure response under a wide range of excitation amplitudes (up to 3% of tank length). The results from this analysis would be compared with established findings reported numerously in literature stating that shallow water TLDs consistently yield better performance due to the added damping caused by wave breaking.
- Investigate the Partial Cell Treatment method to model the effect of a sloped bottom TLD. The objective is to validate with experimental data by Gardarsson et al. (2001) and compare with the only literature attempt to numerically model sloped bottom TLDs using the equivalent TMD method. When validated a number of test cases would be carried out to assess the following:
 - o Increased Effective mass participation. This directly leads to higher sloshing forces per unit water mass, and thus better vibration mitigation

- Higher inherent damping, leading to the decrease of the beating phenomenon experienced in rectangular TLDs with no added damping devices.
- Softening of the spring characteristics of a sloped bottom TLD. This ultimately means that upon sudden cessation of excitation, a sloped bottom TLD would tend not to transfer sloshing energy back to structure compared to a rectangular TLD.

1.4 Organization Of Thesis

Chapter two provides a brief description of the numerical model, including the fluid and structure algorithms and the way they are linked. Validation of the model is presented in chapter two. Chapter three presents the effect of the TLD and screen on structure response under harmonic excitation. Chapter four presents the investigation of best screen configuration under non-harmonic excitation considering the structure response as the deciding criterion. Chapter five presents the study of the effect of fluid height on TLD performance and structure response. Finally, chapter six discusses results of modeling the sloped bottom TLD using the algorithm developed by Marivani and Hamed (2009). It also includes the discussion of the difference in performance of sloped bottom TLDs and rectangular TLDs.

2 Chapter Two: Mathematical Formulation and Numerical Model

2.1 Introduction

This study utilizes the numerical model developed by Marivani (2009) which solves the two-dimensional, incompressible, free surface, fluid flow inside the rectangular TLD. The model incorporates an integrated TLD-Structure solver that couples the TLD with a SDOF structure exposed to external excitation, as shown in figure 2.1. The excitation considered in this study is unidirectional and can be harmonic or non-harmonic.

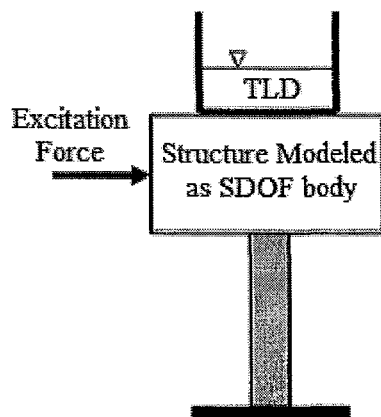


Figure 2.1 Schematic of TLD-Structure coupling used in this study

The tank geometry is defined by its Length (L), Height (d), and height of undisturbed water (h). Figure 2.2 shows a schematic of a rectangular TLD fitted with one screen. The two-dimensional algorithm determines the TLD behaviour in terms of the

sloshing force and energy dissipation per unit depth. When compared with experimental data obtained for a certain depth, the numerical results were normalized by multiplying sloshing force and energy dissipation by the depth considered in experiments. This is based on the fact that velocities, pressures, and free surface shape are independent of tank depth.

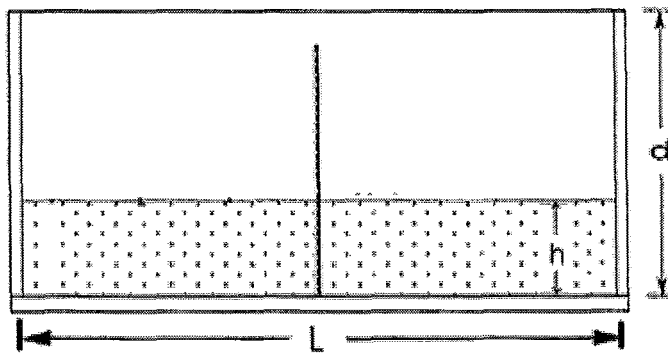


Figure 2.2 TLD fitted with one screen

2.2 Geometry of Submerged Slat Screens

A slat screen is made of a number of slats = n . Each slat has a height equal to D_s . Slats are uniformly arranged, see figure 2.3. The total solid area of the screen is $S_s = n.D_s$. The solidity ratio of the screen, S , equals S_s/h .

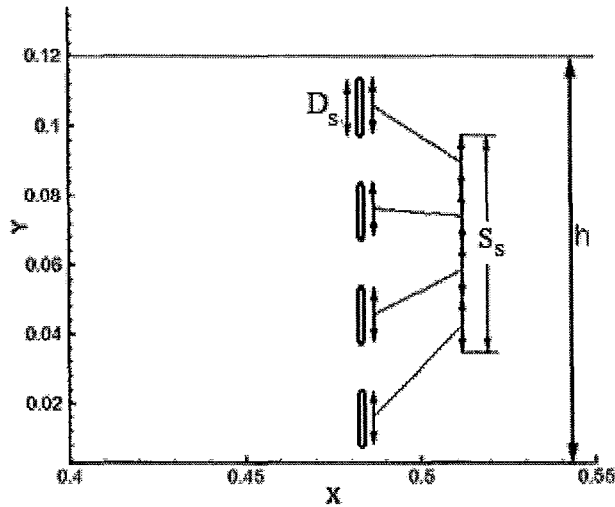


Figure 2.3 Screen Solidity [Marivani, 2009]

2.3 Flow Governing Equations and Boundary Conditions

The algorithm solves the full Navier-Stokes Equations for the liquid phase, despite the fact that upon discretization, the mesh cells along the free surface interface contain a gas phase. This is done by solving the momentum equations in the liquid phase, and the effect of the gas is taken into account through the stress boundary condition.

The two-dimensional, incompressible, free surface, fluid flow problem is modeled in an Eulerian frame. Fixed points \mathbf{x} in the domain ($\mathbf{x} = x\hat{i} + y\hat{j}$) are described using Cartesian coordinates. The velocity field \mathbf{V} depends upon space and time: $\mathbf{V} = u(x, y, t)\hat{i} + v(x, y, t)\hat{j}$

The governing equations of the incompressible, Newtonian, laminar flow in the Cartesian coordinate system are the following continuity and momentum equations:

$$\frac{\partial u}{\partial x} + \frac{\partial v}{\partial y} = 0 \quad (2.1)$$

$$\frac{\partial u}{\partial t} + u \frac{\partial u}{\partial x} + v \frac{\partial u}{\partial y} = -\frac{1}{\rho} \frac{\partial p}{\partial x} + g_x + \frac{1}{\rho} \frac{\partial \tau_{xx}}{\partial x} + \frac{1}{\rho} \frac{\partial \tau_{xy}}{\partial x} \quad (2.2)$$

$$\frac{\partial v}{\partial t} + u \frac{\partial v}{\partial x} + v \frac{\partial v}{\partial y} = -\frac{1}{\rho} \frac{\partial p}{\partial y} + g_y + \frac{1}{\rho} \frac{\partial \tau_{yy}}{\partial y} + \frac{1}{\rho} \frac{\partial \tau_{xy}}{\partial y} \quad (2.3)$$

Equations 2.1-2.3 are subject to the following set of boundary conditions.

-No-slip and no penetration velocity boundary condition at tank walls.

-On the free surface, the continuity of stress components which is referred to as dynamic boundary conditions must be satisfied.

$$(\sigma\kappa - p)\hat{n}_i = (\delta_{ik} - \hat{n}_i\hat{n}_k) \frac{\partial \sigma}{\partial x_k} - \tau_{ik}\hat{n}_k \quad (2.4)$$

where σ is fluid surface tension, \hat{n}_i is the unit normal vector, p is free surface pressure, and κ is local free surface curvature. For two-dimensional flows, projecting equation (2.4) along the unit normal \hat{n} and unit tangent \hat{t} results in an equivalent set of scalar boundary conditions. These are the normal stress boundary condition given by:

$$p - \sigma\kappa = 2\mu n_k \frac{\partial u_k}{\partial n} \quad (2.5)$$

and the tangential stress boundary condition given by:

$$\mu \left(t_i \frac{\partial u_i}{\partial n} + n_k \frac{\partial u_k}{\partial s} \right) = \frac{\partial \sigma}{\partial s} \quad (2.6)$$

where, $\frac{\partial}{\partial s} = \hat{t} \cdot \nabla$ is the derivative along the free surface and $\frac{\partial}{\partial n} = \hat{n} \cdot \nabla$ is the normal

derivative. Viscous effects are neglected at the free surface, so the continuity of tangential stress components are satisfied automatically. Also, since the surface tension, σ , is assumed to be constant, and the curvature radius of the free surface is expected to be large under conditions of interest in this study, the surface pressure ($\sigma\kappa$) effects has been ignored at the free surface. Thus the normal stress boundary condition becomes:

$$p = 0 \tag{2.7}$$

-The kinematic boundary condition must also be satisfied at the free surface. This boundary condition assumes the continuity of fluid velocity at the free surface in order to ensure conservation of mass.

2.4 Partial Cell Treatment Method

2.4.1 Screens

The algorithm used in the study employs the partial cell treatment method to fully resolve flow through the screen. In this method, internal obstacles are modeled as a special case of two phase flow in which the first phase is the liquid, with volume fraction $\theta = 1$, and the second phase is the obstacle with a fraction value of $\theta = 0$. The obstacle is characterized as a fluid of infinite density and zero velocity. The continuity and momentum equations thus are modified to be:

$$\nabla \cdot (\theta \vec{u}) = 0 \quad (2.8)$$

and

$$\frac{\partial(\theta \vec{u})}{\partial t} + \nabla \cdot (\theta \vec{u} \vec{u}) = \theta \left[\vec{g} - \frac{\vec{\nabla} p}{\rho} \right] + \nabla \cdot \left(\frac{\theta \vec{\sigma}}{\rho} \right) \quad (2.9)$$

When the two-phase flow equations of motion are specialized to these conditions, they yield:

$$\frac{\partial(\theta u_i)}{\partial x_i} = 0.0 \quad (2.10)$$

$$\frac{\partial(\theta u_i)}{\partial t} + \theta u_j \frac{\partial(\theta u_i)}{\partial x_j} = -\frac{\theta}{\rho} \frac{\partial p}{\partial x_i} + \theta g_i + \theta \frac{\partial}{\partial x_j} [2\nu \sigma_{ij}] \quad (2.11)$$

The cells that are partially occupied by the screen and the fluid will have θ values between 1 and 0. These values represent the degree of openness of the computational cell. In these “partial” cells and consequently all other computational cells, velocity and pressure are recalculated taking into account the partial obstruction from the screen

presence. In the case of screens the mesh is setup in such a way that cells have θ values of either 1 or zero, see figure 2.4.

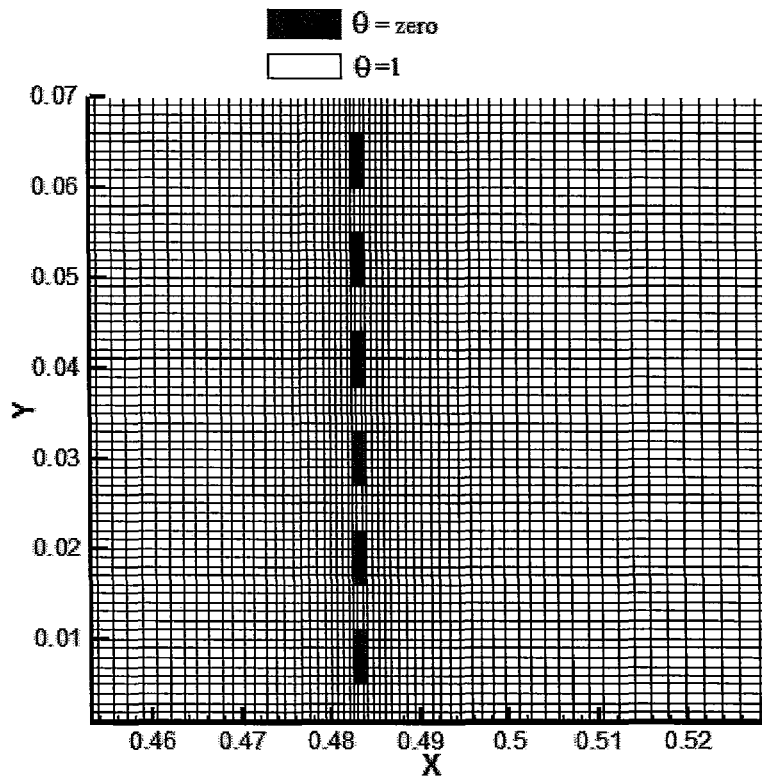


Figure 2.4 Contour plot of the θ value for cases of TLDs with screens [Marivani, 2009]

2.4.2 Sloped Bottom TLDs

In the same way as screens, the algorithm can be modified to account for the sloped bottoms through “obstructing” the flow in that region. θ values can be set to zero in the part of the tank that represents the slopes (see figure 2.5).

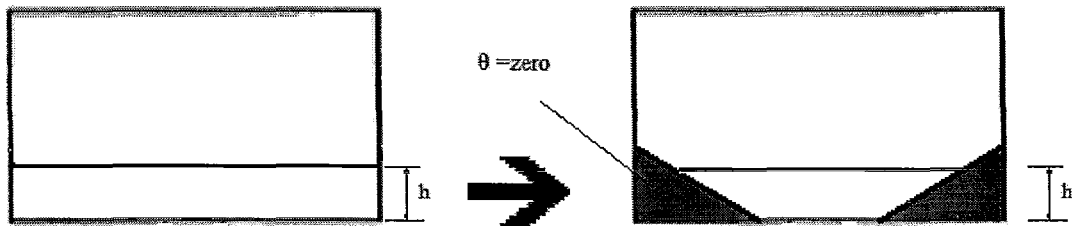


Figure 2.5 Setting obstruction ratio to zero in areas representing the sloped bottom

As with the screen's case, no additional boundary conditions are needed for this modification, regardless of the sloped bottom shape or angle. A significant drawback using this method is the necessity of decreasing grid size. Figure 2.6 shows a zoomed view of how the algorithm models the sloped bottom, and thus illustrating the negative effect of an increased grid size.

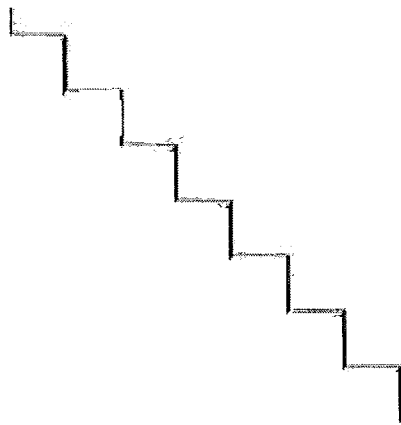


Figure 2.6 An upclose view of the modelled sloped bottom

2.5 Treatment of Free Surface

The free surface is reconstructed using the Volume of Fluid Method [Hirt and Nichols (1981); Pengzhi (2007)]. The time evolution of the liquid region is computed by solving the following equation,

$$\frac{\partial F}{\partial t} + u \frac{\partial F}{\partial x} + v \frac{\partial F}{\partial y} = 0 \quad (2.12)$$

where F is the local volume fraction of the liquid.

F is unity in computational cells occupied with liquid, and zero in cells occupied with gas. This means that the momentum and continuity equations will be solved normally where F=1, and will not be solved at all for F=0. Figure 2.7 shows a numerical example of F values in mesh cells in the liquid region, in the gas region, and along the free surface interface.

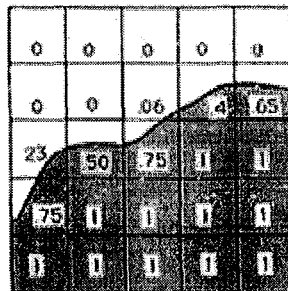


Figure 2.7 Volume fraction values around a free surface interface [Poo and Ashgriz (1990)]

For cells containing the interface between the liquid and gas phases, F lies between zero and unity. For these cells a donor-acceptor method is used, where at each boundary

of each computing cell, the two cells immediately adjacent to the interface are distinguished; one becoming a donor cell and the other an acceptor cell (see figure 2.8).

Cell velocity values are then given the subscripts D and A, respectively. The labelling is accomplished based on the algebraic sign of the fluid velocity normal to the boundary.

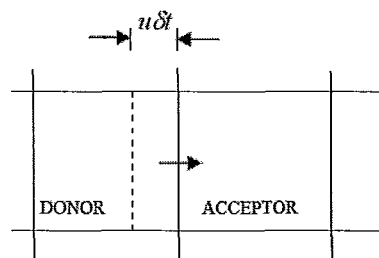


Figure 2.8 Donor acceptor diagram [Marivani, 2009]

Each cell will have four boundaries determined by the velocity u , and the time step δt (as seen in figure 2.8), and thus will have four different tags of A and D corresponding to the four cell surfaces. The volume of fluid flux is then calculated by a geometrical analysis using the free surface profile in the previous time step and the velocity field in the new time step. The new advanced F values are determined using the calculated volume of fluid flux at each cell face. The boundary slope and the side occupied by the liquid are determined using the gradient of F which represents the normal vector to the free surface.

Once the boundary slope and the side occupied by the liquid have been determined, a line can be constructed in the cell with the correct amount of F volume lying on the fluid side. This line is used as an approximation to the actual boundary and provides the information necessary to calculate the fluid height for the application of free surface pressure boundary conditions. Figure 2.9 shows a visual example of the free surface

reconstruction using the donor acceptor F method. It is evident that the shape of the surface will not be reproduced accurately, but with sufficient grid intensity the sloshing force due to free surface profile can be estimated effectively.

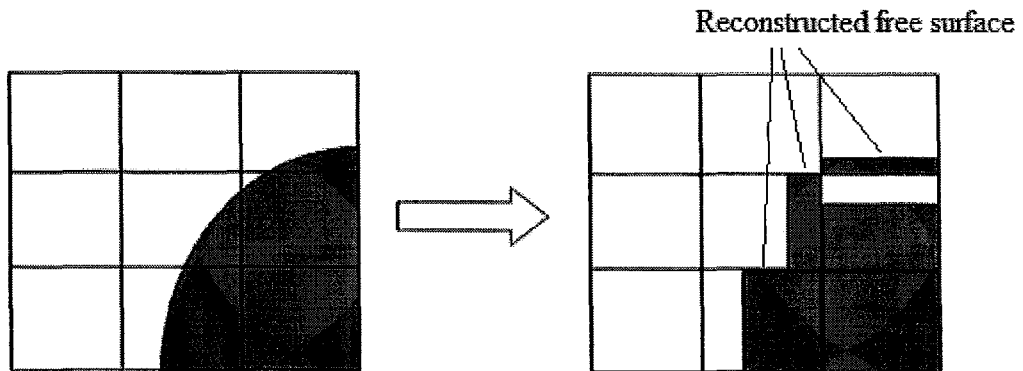


Figure 2.9 Free surface reconstruction [Marivani, 2009]

It is important to mention that due to numerical errors and round-offs, F is actually seldom exactly 1 or 0. A certain error threshold (0 ± 10^{-6} , 1.0 ± 10^{-6}) determined from previous numerical studies is used as a cutoff to round values that are very close to 1 or 0. Accompanying this error is also a probability of a computational cell having a value of more than 1 or less than 0. Similar precautions are taken to prevent this and ensure mass conservation.

2.6 Motion of Structure

The (SDOF) structure is defined in terms of its mass M_s , stiffness K_s , and damping coefficient C_s . Figure 2.10 shows the coupled system under external excitation F_e . The

TLD reacts with a sloshing force F_{TLD} supposedly anti-phase to the excitation force, and thus creates a damping effect that reduces the swaying motion of the structure. The equation of motion of the coupled system is expressed as:

$$M_S \ddot{X}_S + C_S \dot{X}_S + K_S X_S = F_e + F_{TLD} \quad (2.13)$$

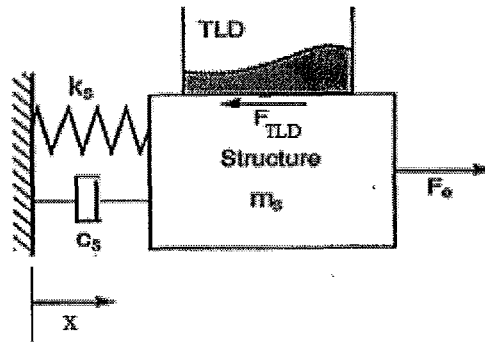


Figure 2.10 Free body diagram of structure properties shown with TLD

[www.eng.nus.edu.sg]

In each computational cell the mass and velocity are used to calculate the momentum (P). This value is summed up for all computational cells to arrive at an estimate of the total momentum of the sloshing fluid. The damping force F_{TLD} can then be determined by the following equation:

$$F_{TLD} = \frac{dP}{dt} \quad (2.14)$$

Duhamel integral method has been used to solve the equation of motion of the structure (see equation 2.15). The total displacement of the SDOF system exposed to an arbitrary external force $F(\tau)$ is given by:

$$X_s(t) = X_0 \cos \omega t + \frac{u_0}{\omega} \sin \omega t + \frac{1}{M\omega} \int_0^t F(\tau) \sin \omega(t - \tau) d\tau \quad (2.15)$$

Setting the initial displacement and velocity, X_0 and u_0 equal to zero results in:

$$X_s(t) = \frac{1}{M\omega_D} \int_0^t F(\tau) e^{-\xi\omega(t-\tau)} \sin \omega_D(t-\tau) d\tau \quad (2.16)$$

where F is the sum of the external excitation force and the TLD sloshing force.

2.7 Flow Chart of the Algorithm

Figure 2.11 presents the flow chart of the Fluid-Structure interaction model.

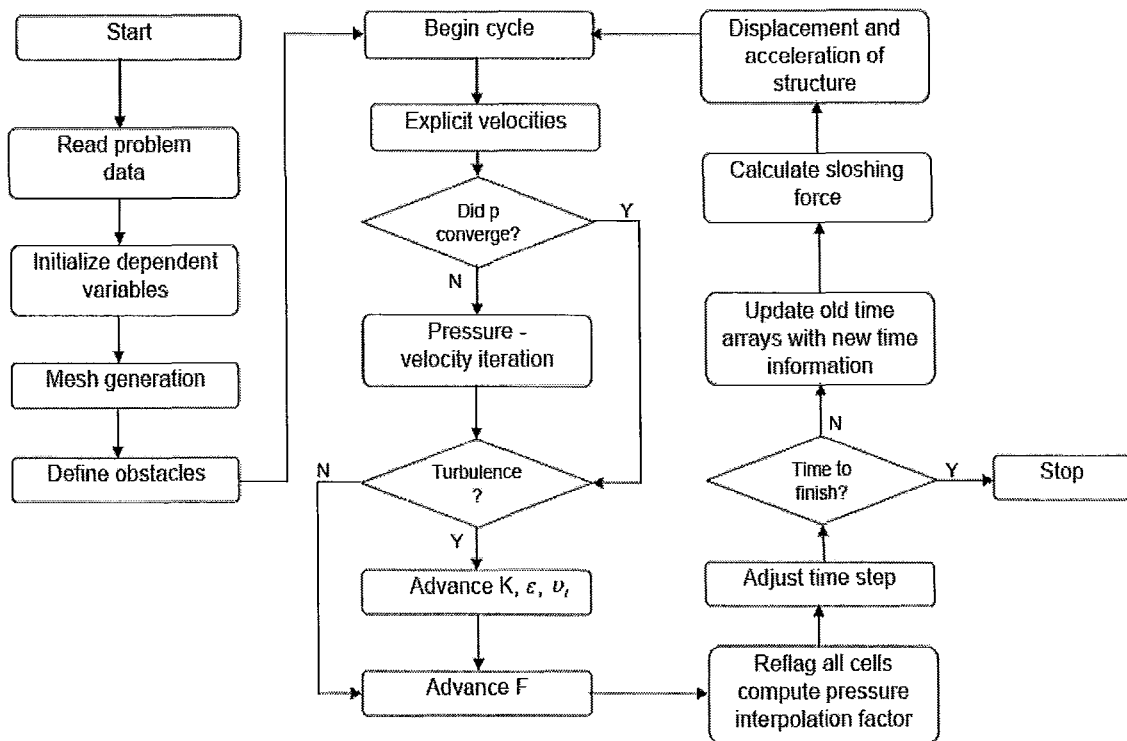


Figure 2.11 Flow Chart of Overall Solver [Marivani, 2009]

Marivani (2009) confirmed through experimentally validated results that the use of a turbulence model within the algorithm did not result in any appreciable differences. As a result, throughout this study the turbulence model will not be necessary.

First the TLD fluid field is discretized into a grid that had been previously tested for grid dependency. The screen (if existent) is defined in terms of position, slat height, solidity, and thickness. The initial excitation is then introduced, and the transport equations are solved in their discretized form to obtain velocities and pressures. To satisfy the continuity equation, pressures and velocities must be adjusted in each mesh cell. For cells that contain liquid only, the momentum equation is used to produce provisional velocity field. This is used with the continuity equation to obtain a pressure correction. This process is iterated until convergence, and the updated velocity and pressure fields are taken as the advanced time values. For cells that contain free surface, the cell pressure is obtained by interpolation between surface pressure and pressure for a neighbouring cell containing fluid only. The iteration process also occurs here using pressure correction values from the liquid occupied cells. After the velocity and pressure fields have been obtained for all the computational cells, F , which is the volume fluid fraction, is advanced in time using the donor and acceptor algorithm. The free surface shape is then determined using the F values, as this determines the sloshing force generated in the TLD at a certain time instant. This is then passed onto to the equation of motion of the SDOF structure to determine its response (displacement and acceleration). This marks the end of one time step, and the response together with the external excitation are then superimposed to determine the tank motion for the following time step. This procedure repeats until the desired timeline of excitation is reached

2.8 Grid Dependence

For rectangular TLDs without screens considered in chapters three, five, and six, numerical simulations were carried out using a 200 ×100 uniform grid. The dependence of numerical results on grid size was checked and the 200×100 grid gave acceptable results. Table 5 shows the maximum difference in free surface deflection predicted using two different grid sizes relative to 200x100 grid.

Table 2.1 Grid dependency analysis for TLD without screens

Mesh size	Maximum deviation
200x100	Selected mesh
160x80	1.8%
120x60	11%

For rectangular TLDs with screens considered in chapters three, four, five, and six, numerical simulations were carried out using a non-uniform grid in the x- direction and a uniform grid in y- direction. The non-uniform mesh in the x direction was designed such that higher mesh density is used at the screen location, with grid intensity expanding gradually away from the screen in both directions.

The dependence of numerical results on grid size was checked and a 260×200 grid gave acceptable results for the one screen case, and a 280×200 gave acceptable results for the 2 screen case. Table 2.2 shows maximum difference in the predicted free surface deflection using three different mesh sizes.

Table 2.2 Grid dependency analysis for TLD with one screen

Mesh size	Maximum deviation
260x200	Selected mesh
200x200	0.5%
150x200	2.0%

2.9 Model Validation

2.9.1 TLD-Structure System with One Screen and without Screens Exposed to Harmonic Excitation.

Since chapter three of this thesis considers a TLD with and without screens under harmonic excitation, a similar experimental test case carried out by Tait et al. (2005) was considered. In this experimental study the TLD was subjected to harmonic sinusoidal excitation. The tank was rectangular with length (L)= 0.966 m, and the initial depth of water (h) was 0.119 m. The tank shown in Figure 2.2 was forced to move horizontally under the harmonic excitation. The displacement of the container is given by:

$$D = A \sin(\omega t + \phi) \tag{2.17}$$

In this case the amplitude A , the period T , and the phase angle ϕ were 0.259 cm, 1.681s and 4.0, respectively. The screen was located in the middle of the tank and consisted of horizontal slats uniformly spaced apart. The solidity ratio S was set to 0.5, so the width of each slat (D_s) was 5 mm with 5 mm spacing between each slat, and the

thickness of each slat was 2.6 mm. Since the depth of fluid in the tank was 119 mm, the screen had twelve slats in total.

The test case dimensions and exact loading values were modeled using the present in-house numerical algorithm. In the experimental study, the free surface deflection was measured at a distance equal to 5% of tank length from the left side of the tank, and plotted against time. Figure 2.12 shows the variation of this parameter for both cases with and without screen. The qualitative trend of the numerical results are in good agreement with the experimental data. As expected, using the screen resulted in a linear and controllable sloshing motion. Figure 2.13 shows a direct comparison of values for the experimental and numerical studies. A slight phase shift appeared between the experimental and the numerical results, because of a slight phase shift between the actual excitation used in the experiment and the one used in the numerical computations.

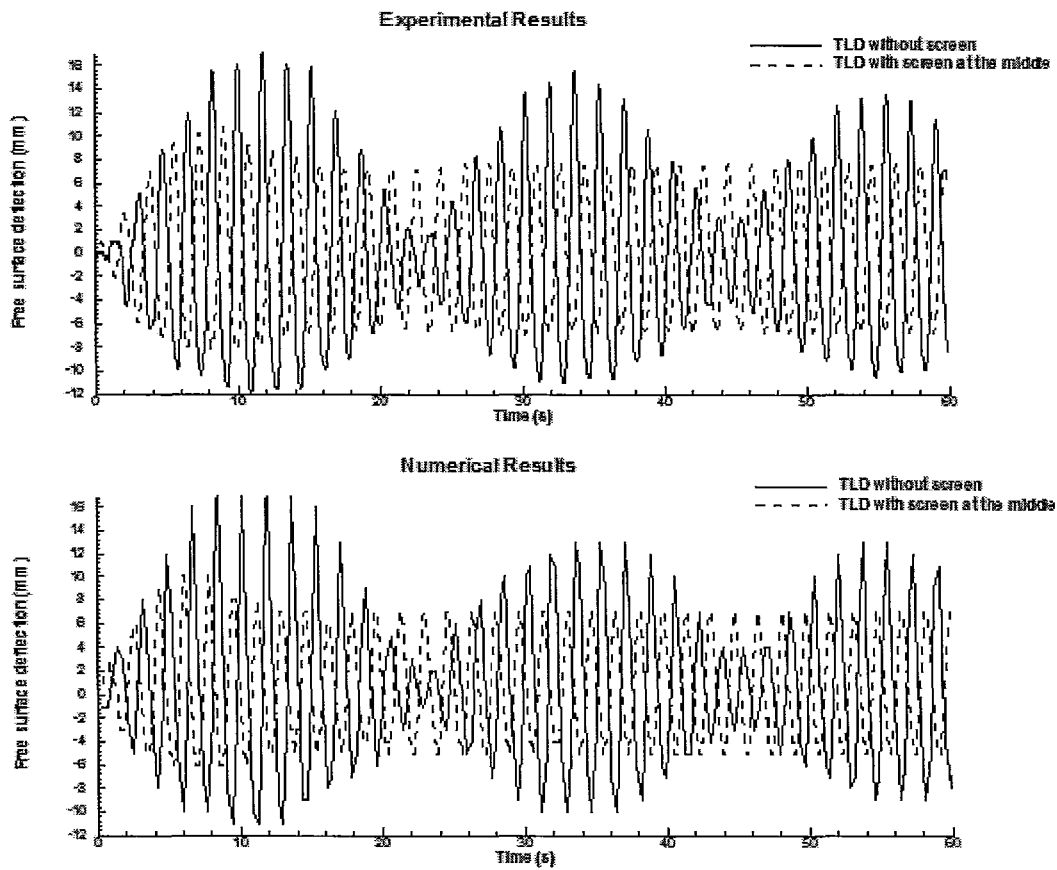


Figure 2.12 Comparison between numerical and experimental data of Free Surface Deflection [Marivani, 2009]

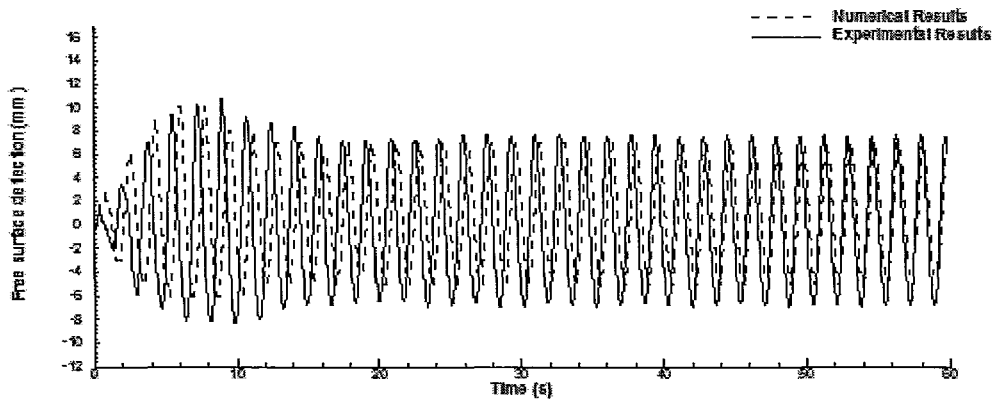


Figure 2.13 Comparison between numerical and experimental data of Free Surface Deflection [Marivani, 2009]

2.9.2 TLD-Structure System With Two Screens Exposed to Non-Harmonic Time Varying Excitation.

Since Chapter four and six of this thesis considers a TLD with and without screens under a non-harmonic excitation, a similar experimental test case carried out by Tait (2004) was considered. The TLD was rectangular with the same dimensions indicated in section 2.9.1. For that specific experimental run, two screens were located at 0.4 and 0.6 of the tank length. The solidity ratio was 0.42, so the width of each slat (D_s) was 5 mm with 7 mm spacing between each slat, and the thickness of each slat was 1 mm (see figure 2.14). The TLD was coupled to ballast mass representing a SDOF structure as shown in figure 2.15. Table 2.3 lists the structure properties. According to Lamb (1932), these tank dimensions would yield a TLD natural frequency equal to the natural frequency of the SDOF structure as required in TLDs.

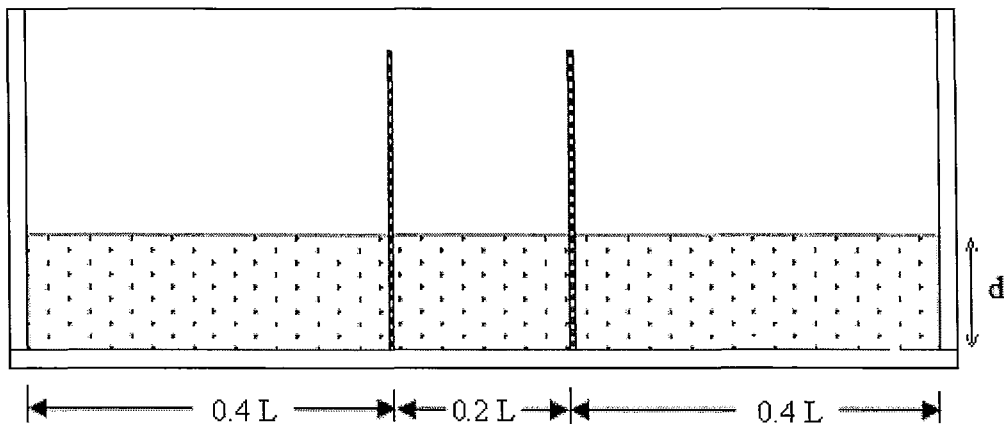


Figure 2.14 TLD fitted with 2 screens [Tait, 2004]

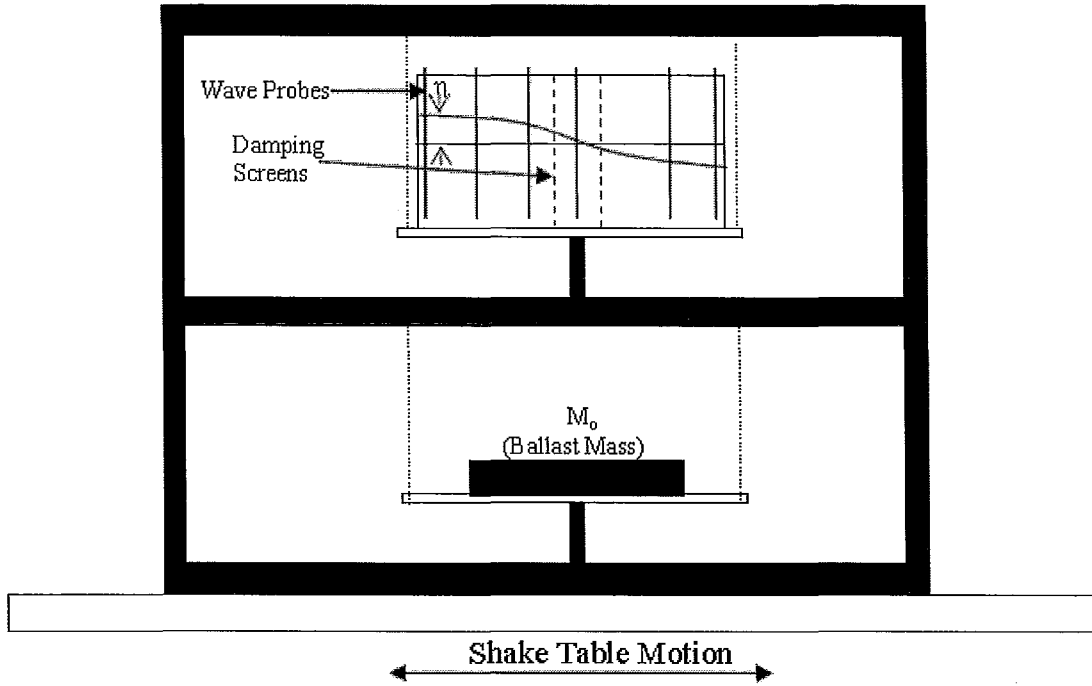


Figure 2.15 Schematic of the experimental test rig used by Tait (2005)

Table 2.3 SDOF structure properties

M_s	K_s	ξ	μ
(Kg)	(N/m)	(%)	(%)
4480	55100	0.1	2.5

The test case and exact loading conditions were modeled using the present in-house numerical algorithm. The grid throughout the TLD was checked for numerical dependency, and a final non-uniform grid of 280 x 200 grid points was used and gave acceptable results. The non-harmonic excitation force used in the experimental testing (figure 2.16) was used in the numerical simulation, and the measured output in both cases was the structure acceleration.

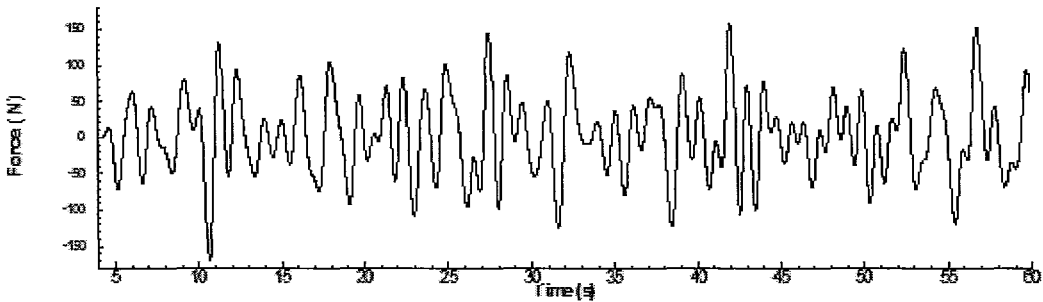


Figure 2.16 Non-harmonic excitation force used in both experimental and numerical runs

Figure 2.17 shows a comparison of the structural acceleration time history obtained from the numerical simulation and experimental results. The maximum discrepancy was within 3.4% of the full measured acceleration range. Overall the results showed an excellent agreement with experimental data.

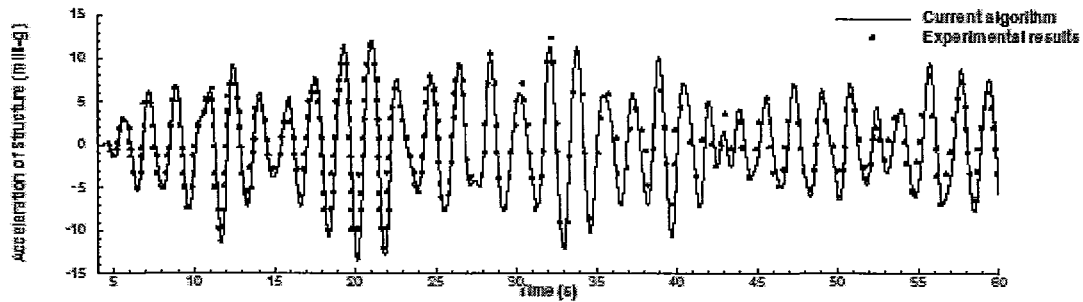


Figure 2.17 Comparison between experimental data and numerical results of structure acceleration [Marivani, 2009]

2.9.3 Frequency Domain Comparison with Equivalent TMD and Shallow Wave Numerical Methods

Figure 2.18 shows a comparison between the experimental data and numerical results based on the shallow wave theory of the normalized energy absorption reported by Tait et al. (2005) for a TLD with $h/L = 0.2$ and amplitude of excitation = 1 % of tank length. They showed that this h/L value and higher, the numerical model was unable to capture the non-linearities seen in the experimental data (figure 2.18) in the frequency sweep.

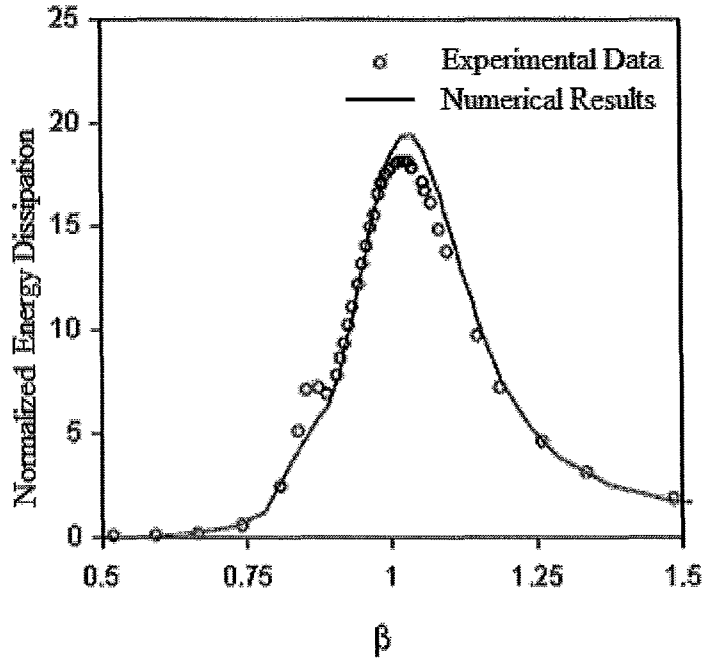


Figure 2.18 Energy absorption Vs normalized excitation frequency at $h/L= 0.2$ [Tait et al, 2005]

Figure 2.19 shows numerical results for the same conditions, using the current numerical algorithm compared with results obtained using the equivalent TMD numerical method, and the experimental data reported by Tait et al. (2005).

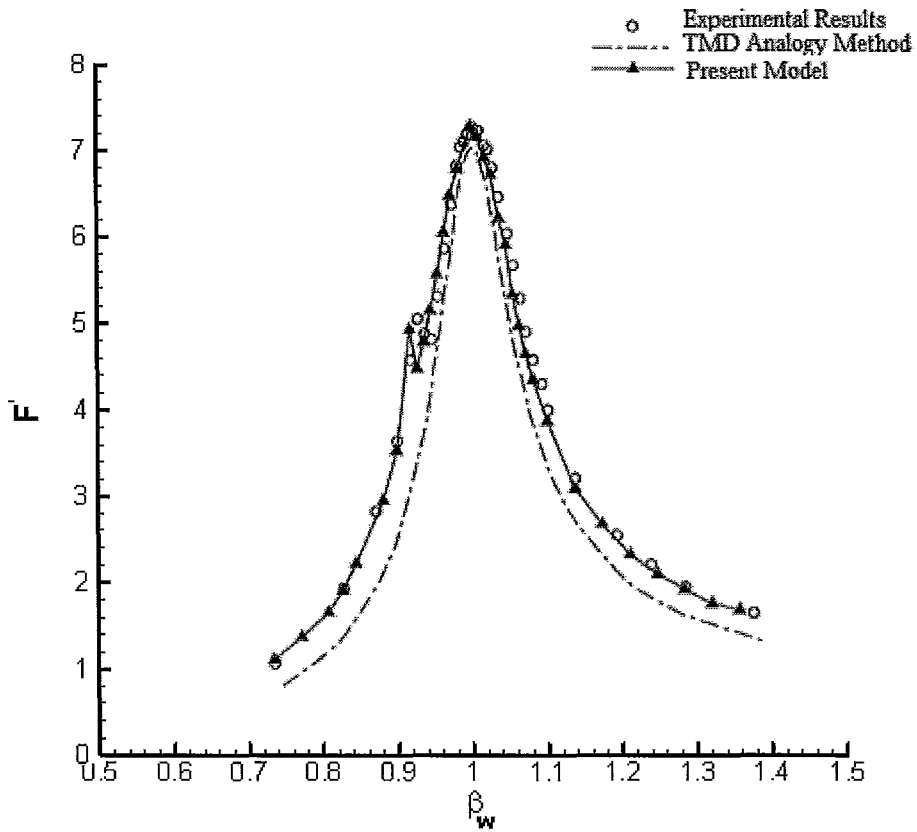


Figure 2.19 Normalized excitation force Vs excitation frequency [Marivani & Hamed, 2009]

Overall, numerical results obtained using the present model are in excellent agreement with the experimental data. The model is able to predict the non-linearities shown in figures 2.18 and 2.19.

2.9.4 Sloped Bottom TLD.

The experimental study conducted by Gardarsson et al. (2001) has been used as a reference to check results of various numerical models in the case of sloped-bottom TLD. Figure 2.20 shows the dimensions of the sloped bottom TLD used in the experimental study. L was set to 590 mm, with a tank depth (b) of 335mm. The undisturbed fluid height, h_o , was 10 cm, with an angle θ_t of 30° . The excitation amplitude was 2.5 mm. The same tank dimensions, water depth, and excitation amplitude were replicated in the present study.

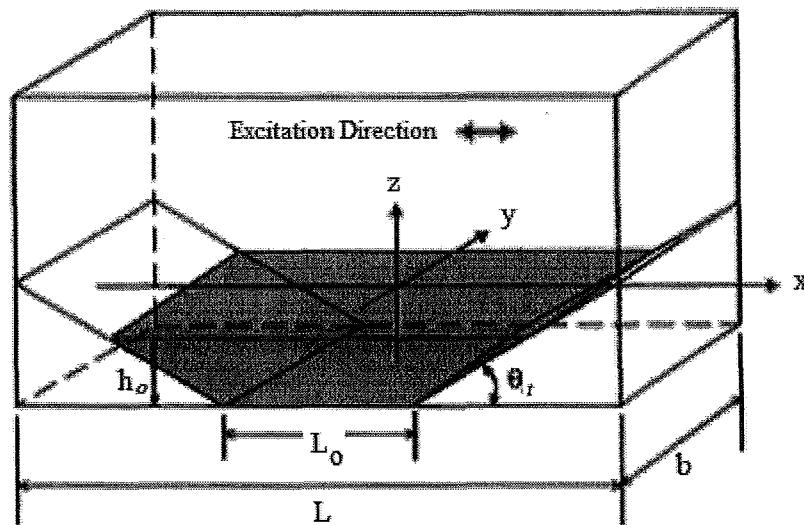


Figure 2.20 Schematic of the sloped bottom TLD [Olson and Reed, 2001]

There has been some numerical research effort to simulate sloshing in sloped bottom TLDs using equivalent TMD methods [Olson and Reed (2001)]. Figure 2.21 shows the difference in frequency response of experimental and previous numerical methods. At $\beta=0.925$ the maximum difference between numerical predictions and experimental data

was 49%. The numerical results also varied between over prediction and under prediction across the frequency bandwidth, which makes this numerical algorithm an unreliable design tool for sloped bottom TLDs.

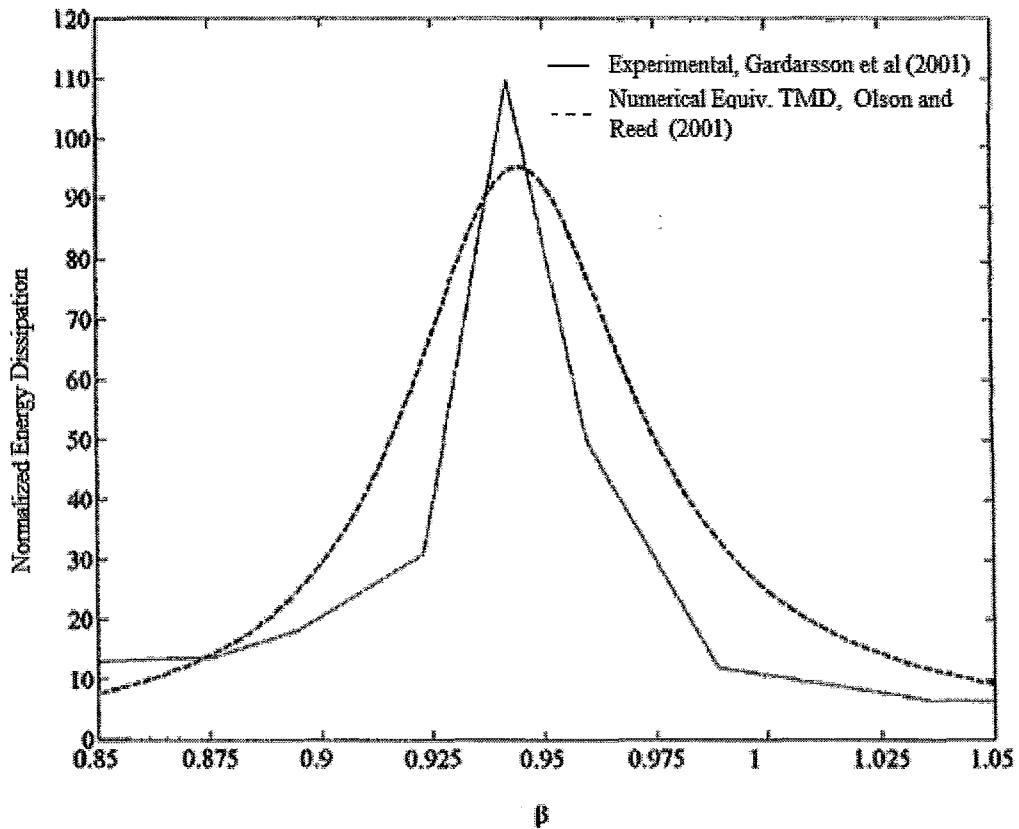


Figure 2.21 Comparison between numerical results, and experimental data of the frequency response of a sloped bottom TLD [Olson and Reed, 2001]

The existing numerical model is capable of capturing temporal variations of the sloshing fluid at any excitation frequency. To replicate the frequency sweep done experimentally, numerous numerical simulations were carried out at different excitation frequencies. In each run the maximum sloshing force was captured, and plotted against

the excitation frequency ratio. A grid of 140x200 was capable of accurately predicting the sloped bottom TLD characteristics outside the excitation frequency ratio between 0.94 and 0.98. Within this range a grid of 260x200 was needed to produce the most accurate attainable results.

Figure 2.22 shows very good agreement between numerical results of the present algorithm and experimental data reported by Gardarsson et al. (2001). The maximum difference is at β between 0.94 and 0.97, and is 14%. Compared to previous results from the equivalent TMD method, it is reasonable to say that the current algorithm produces more accurate qualitative trends and predictions.

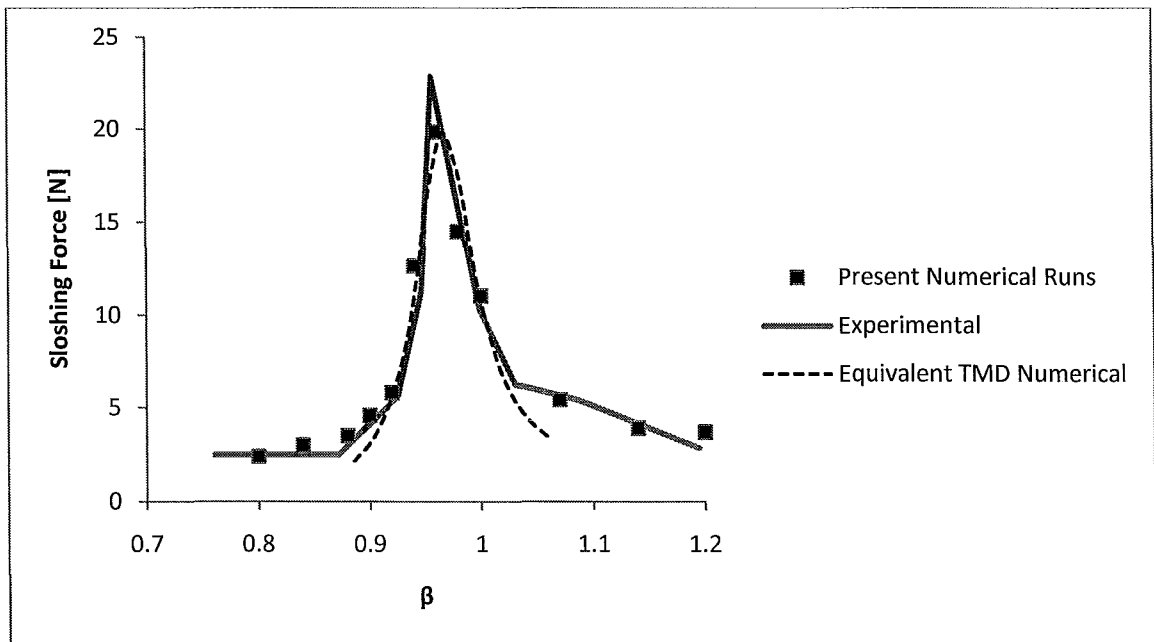


Figure 2.22 Comparison between experimental data [Gardarsson et al, 2001], equivalent TMD numerical data [Olson and Reed, 2001] and present numerical results of sloshing force Vs excitation frequency

3 Chapter Three: Investigation of the Effect of Screen Solidity on Structure Response under Harmonic Excitation

3.1 Introduction

In most of the experimental work carried out in literature, the shake table is excited by a harmonic excitation in the form of a sine function. Apart from the fact that harmonic excitations represent wind force, there are many other reasons why harmonic excitations were widely used in literature. First, numerous early studies assessed the performance of their TLD numerical models against well established TMD models, and the latter were valid under harmonic excitations and were function of the excitation frequency. Also, harmonic excitations made it possible to perform a frequency sweep of the energy dissipation and damping forces which in turn allows one to determine the accurate natural frequency of the TLD. Moreover, the use of harmonic excitations also helped in development of equivalent TMD method. Such development depends on empirical coefficients that were determined under harmonic excitation.

3.2 TLD and Structure Geometry

The TLD dimensions used in this chapter are the same dimensions listed in sections 2.9.1.

The TLD is coupled with a SDOF structure with properties listed in table 2.3.

3.3 Harmonic Excitation Used

In real life situations the excitation on any civil structure could be due to wind, where amplitudes involved are usually low in value. In high rise buildings, this kind of excitation force would cause structural deflection mostly sensed at the top floors. In minor cases, the occupants of these floors might feel nauseous due to the vibration. In major incidents, window panels were reported to fall off the building (John Hancock Tower, Boston, USA). The harmonic excitation chosen in all test cases has $A/L= 0.2 \%$. The excitation frequency was determined based on the natural frequency of the buildings (and TLD), which was 0.54 Hz. This was to ensure that TLD performance is examined at the worst loading conditions.

3.4 Structure Displacement and Acceleration

First, structure deflection in meters was captured as a function of time in three different cases:

- No TLD installed
- TLD without a screen installed
- TLD with a screen installed in the middle

These cases have been considered to confirm previous literature findings, that submerged screens have a positive effect on building response. In addition, the main objective was to investigate the effect of screen solidity ratio, S , on structure response. Three typical

solidity ratios of 0.4, 0.5, and 0.6 have been used, and the structure deflection was captured in each case.

Figure 3.1 shows variation of structure deflection with time. Results indicated up to 71 % reduction in structure displacement when using a TLD without a screen. Between time = 20 and 40 seconds, the structure experiences its worst deflection. In this region, installing a screen with $S = 0.4$ reduced structure deflection by an additional 21 % with respect to maximum deflection in the case of TLD without screen.

Figures 3.2, 3.3, and 3.4 show structure response for cases of screen solidity equals to 0.4, 0.5, and 0.6, respectively. To effectively compare on common grounds, the maximum deflection was captured in each case after the first 5 oscillation periods of transient response (see Table 3.1).

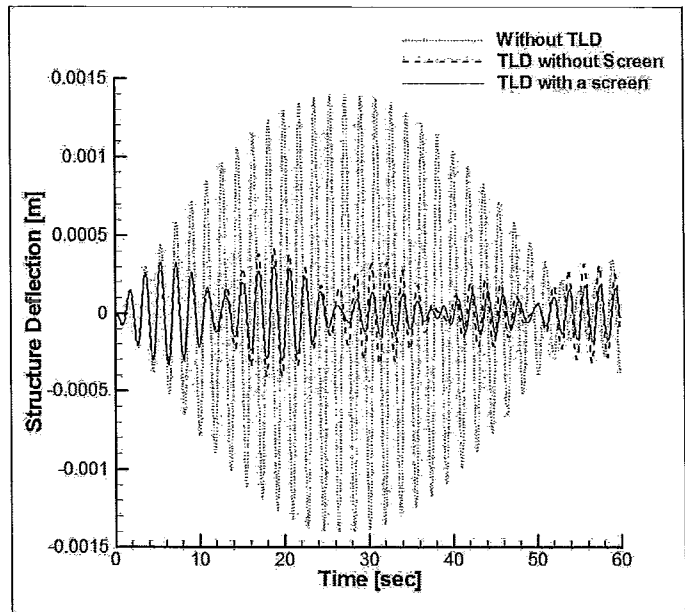


Figure 3.1 Temporal variation of structure deflection in cases without TLD, with TLD and no screen, and with TLD with one screen with $S=0.4$

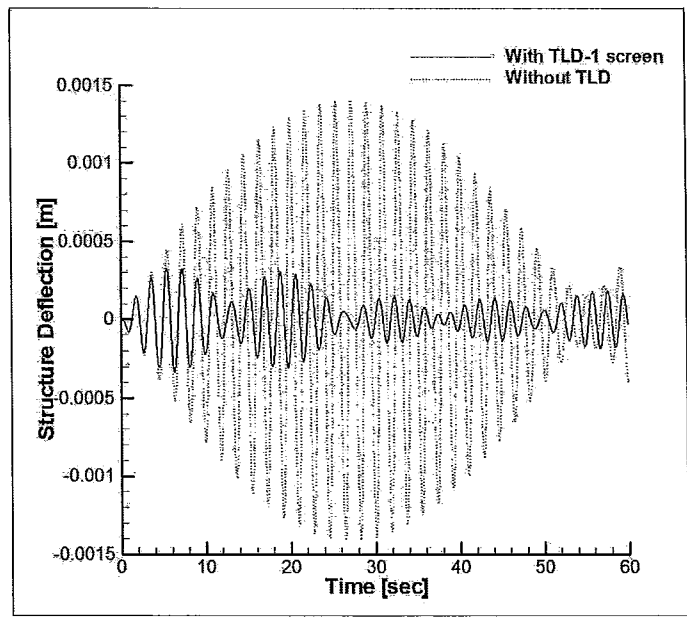


Figure 3.2 Temporal variation of structure deflection in cases without TLD and with TLD with one screen with $S=0.4$

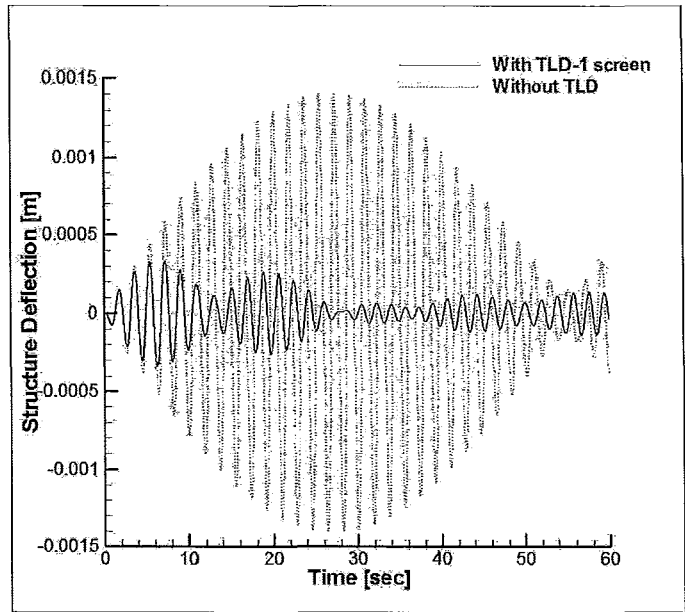


Figure 3.3 Temporal variation of structure deflection in cases without TLD and with TLD with one screen with $S=0.5$

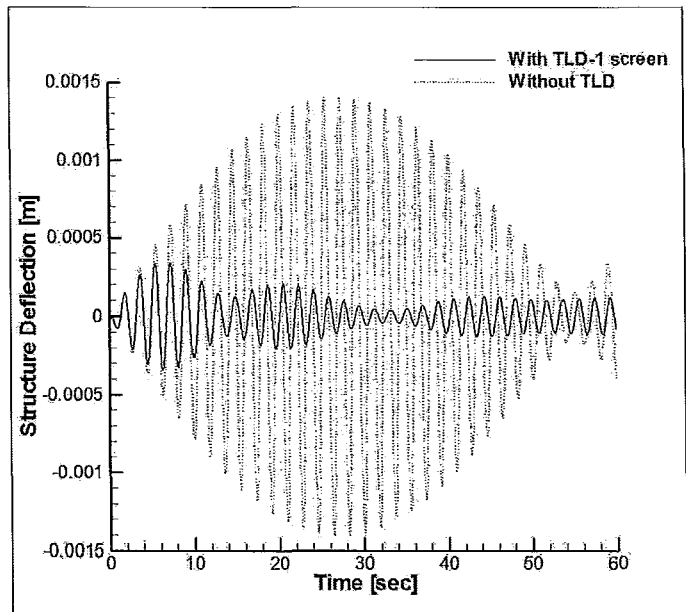


Figure 3.4 Temporal variation of structure deflection in cases without TLD and with TLD with one screen with $S=0.6$

Table 3.1 Results of maximum structure deflection at solidities 0.4, 0.5, and 0.6

Screen Solidity Ratio, S	Maximum deflection in mm after 10[sec]
0.4	0.31
0.5	0.26
0.6	0.21

3.5 Analysis of Results

TLDs that are properly tuned to the building natural frequency have an extreme effect on structure response under harmonic excitations. Structure deflection is decreased by up to 71 % even without using a screen. The introduction of a screen further increases TLD effectiveness through decreasing deflection by another 21%. The increase of the TLD screen solidity results in an expected increase in friction effect on the sloshing fluid through the screen, thus an increase in the damping ratio. If maximum structure deflection at $S=0.4$ is taken as a reference, then a change of solidity from 0.4 to 0.6 would lead to a 32.2 % further decrease in maximum structure deflection value. This increase in damping is also evident in the trend of the structure deflection plot in figures 3.1 through 3.4. Notice the beating phenomena is very obvious in figure 3.1 for the case of a TLD without a screen, and as the screen solidity is increased the beating phenomena fades away significantly due to the increase in damping.

4 Chapter Four: Investigation of The Effect of Screen Configuration on The Response of Structure under a Non-harmonic Time Varying Excitation

4.1 Introduction

The experimental and numerical research carried out by many researchers considered harmonic excitation for the reasons mentioned in chapter three. Kareem and Sun (1987), Sun et al. (1995), Reed et al. (1998), Yu et al. (1999), and Tait et al (2004, 2007,2008) are examples of the efforts that focused on TLD behaviour under harmonic excitation. Non-harmonic excitations represent other important dynamic excitations, hence it is important to investigate TLD performance under such excitations.

4.2 Non-harmonic Excitation Definition

In this part of the study, the TLD-structure coupling was chosen to have the same properties and dimensions as the one used for validation purposes. The excitation frequency was also chosen to be the exact same as the one shown in figure 2.16.

Since the objective was to determine the best screen configuration that would yield the best building response under non-harmonic excitations, there was no reason to change any of the validated model properties so as not to cast any shadow on the accuracy of the results. It was necessary to run a Fast Fourier Transform (FFT) on the Non-harmonic excitation to make sure that its imbedded frequencies had a wide range that included the critical natural frequency of the structure to be damped, 0.545 Hz in all the test cases.

Figure 4.1 shows the excitation force in the frequency domain. The frequencies range from 0.2 to 1.2 Hz, which confirms that the non-harmonic excitation frequency used in this study includes the required frequency bandwidth.

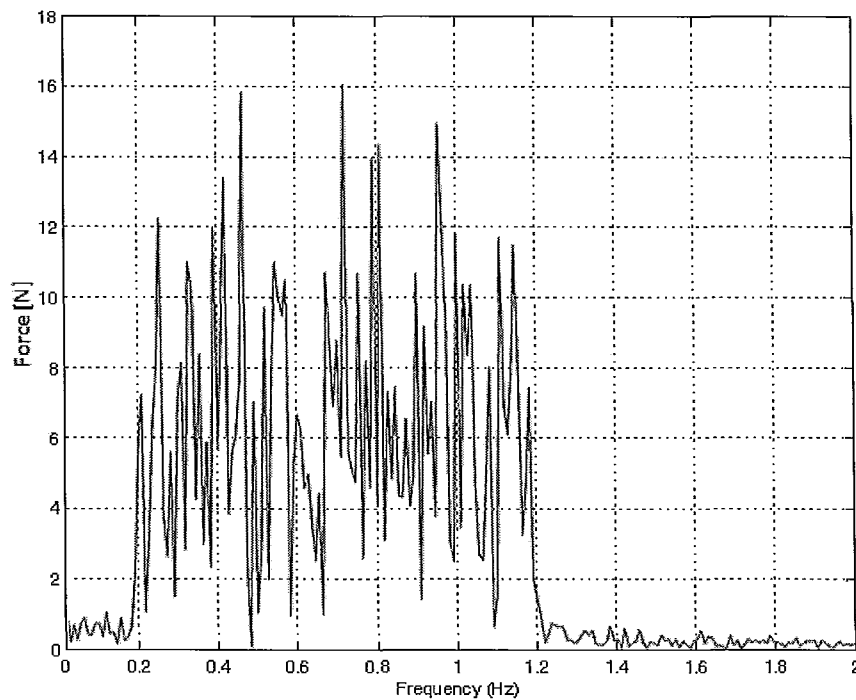


Figure 4.1 Fast Fourier Transformation on the excitation signal shown in figure 2.16

4.3 Different Screen Configurations Tested

The structure displacement and acceleration time histories were plotted for 19 different TLD screen configurations, including the no screen case. In the one screen case, three different solidities were considered. In the two screen case, three different solidities were considered for five screen positions.

Table 4.1 Test cases conducted under non-harmonic excitation

CASE		Location in Tank
no screen		
1 screen	S=0.4	0.5 Length
	S=0.5	0.5 Length
	S=0.6	0.5 Length
2 screen	S=0.4	0.1 L & 0.9L
		0.2 L & 0.8L
		0.25 L & 0.75L
		0.3 L & 0.7L
		0.4 L & 0.6L
	S=0.5	0.1 L & 0.9L
		0.2 L & 0.8L
		0.25 L & 0.75L
		0.3 L & 0.7L
		0.4 L & 0.6L
	S=0.6	0.1 L & 0.9L
		0.2 L & 0.8L
		0.25 L & 0.75L
		0.3 L & 0.7L
		0.4 L & 0.6L

4.4 Analysis and Selection Criteria

Figures 4.2-4.17 show structure displacement and acceleration measured in meters and milli-g respectively for samples of the cases considered in Table 4.1.

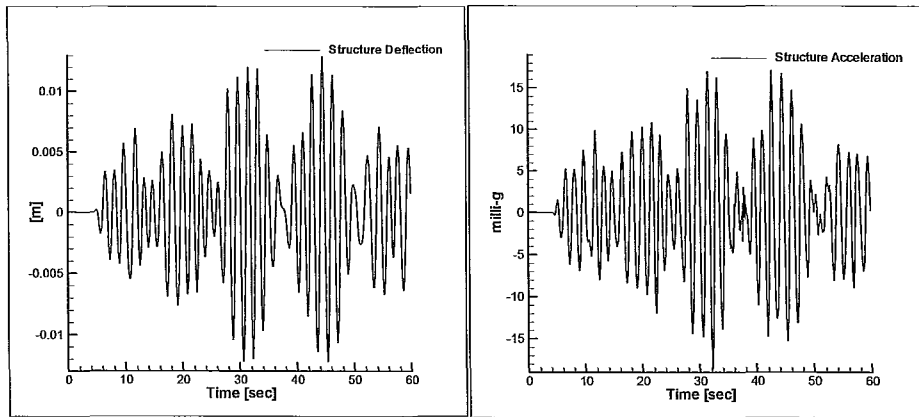


Figure 4.2, 4.3 Structure deflection and acceleration, case without screen

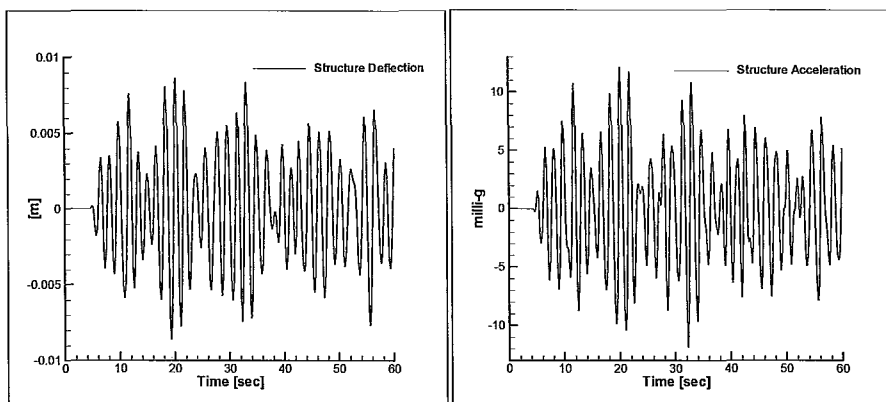


Figure 4.4, 4.5 Structure deflection and acceleration, case of one screen with $S=0.4$

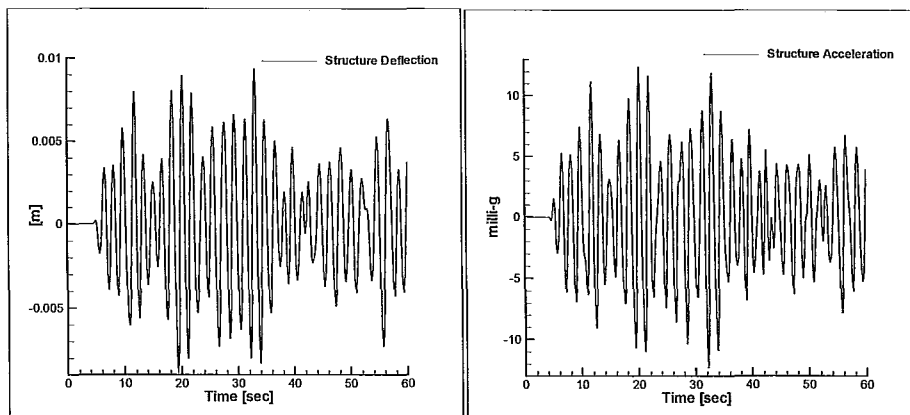


Figure 4.6, 4.7 Structure deflection and acceleration, case of one screen with $S=0.5$

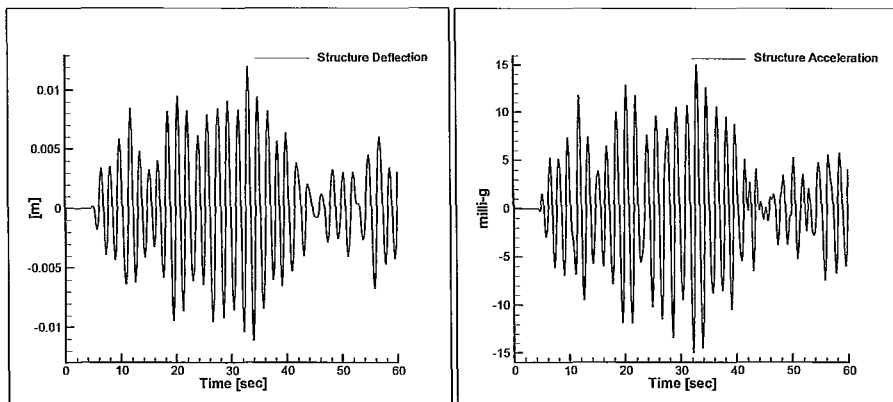


Figure 4.8, 4.9 Structure deflection and acceleration, case of one screen with $S=0.6$

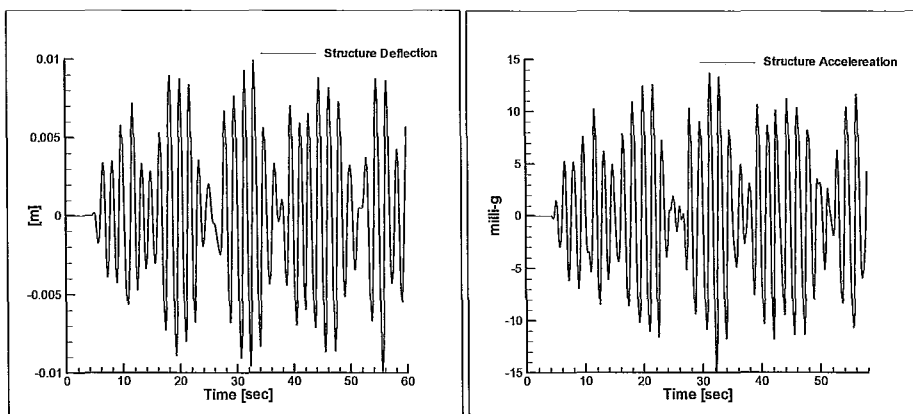


Figure 4.10, 4.11 Structure deflection and acceleration at $x=0.1L$ and $0.9L$, case of two screens with $S=0.4$

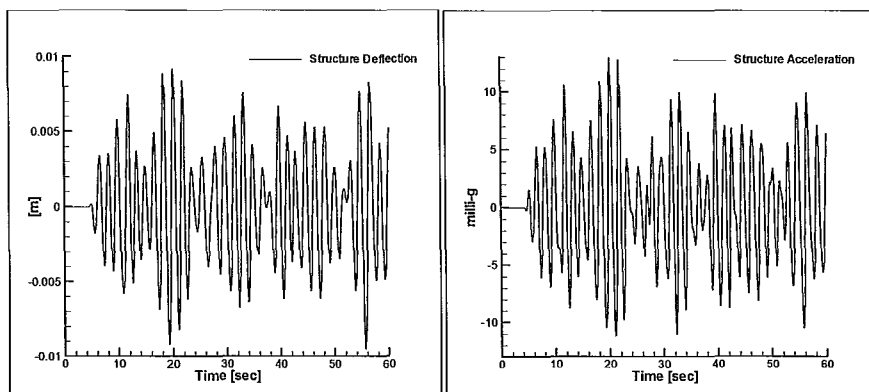


Figure 4.12, 4.13 Structure deflection and acceleration at $x=0.2L$ and $0.8L$, case of two screens with $S=0.4$

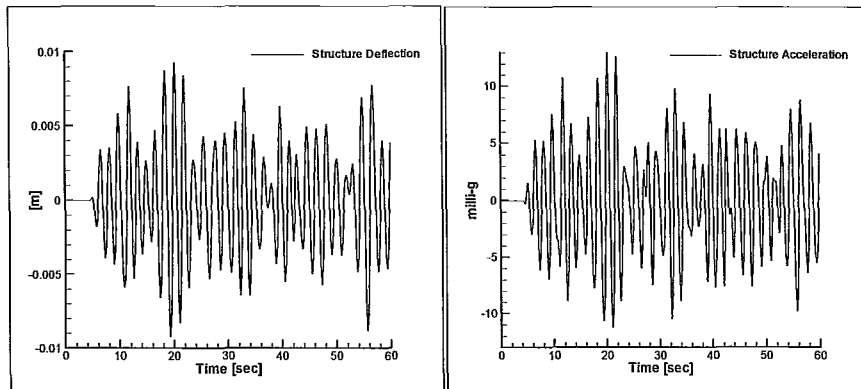


Figure 4.14, 4.15 Structure deflection and acceleration at $x=0.25L$ and $0.75L$, case of two screens with $S=0.4$

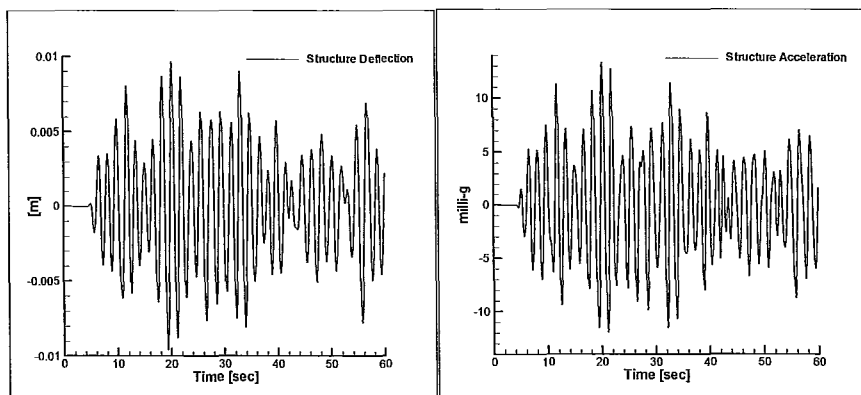


Figure 4.16, 4.17 Structure deflection and acceleration at $x=0.4L$ and $0.6L$, case of two screens with $S=0.4$

Table 4.2 shows maximum building acceleration and building displacement values that were captured from the previous time plots. Figures 4.18 to 4.21 show the structure response plotted and illustrate the response trend with different screen configuration.

Table 4.2 Results of structure response under non-harmonic excitation

CASE		Location in Tank	Max. acceleration [milli-g]	Max. deflection [mm]
no screen			18.5	12.92
1 screen	Solidity=0.4	0.5 Length	12.14	8.66
	Solidity=0.5	0.5 Length	12.37	9.35
	Solidity=0.6	0.5 Length	15.11	12.04
2 screen	Solidity=0.4	0.1 L & 0.9L	14.98	9.96
		0.2 L & 0.8L	12.96	9.51
		0.25 L & 0.85L	12.98	9.26
		0.3 L & 0.7L	13.14	9.43
		0.4 L & 0.6L	13.35	9.68
	Solidity=0.5	0.1 L & 0.9L	13.59	10.2
		0.2 L & 0.8L	13.04	9.31
		0.25 L & 0.85L	13.05	9.41
		0.3 L & 0.7L	13.28	9.8
		0.4 L & 0.6L	14.85	11.79
	Solidity=0.6	0.1 L & 0.9L	12.81	10.03
		0.2 L & 0.8L	13.21	9.56
		0.25 L & 0.85L	14.01	11.08
		0.3 L & 0.7L	16.32	12.94
		0.4 L & 0.6L	19.11	15.26

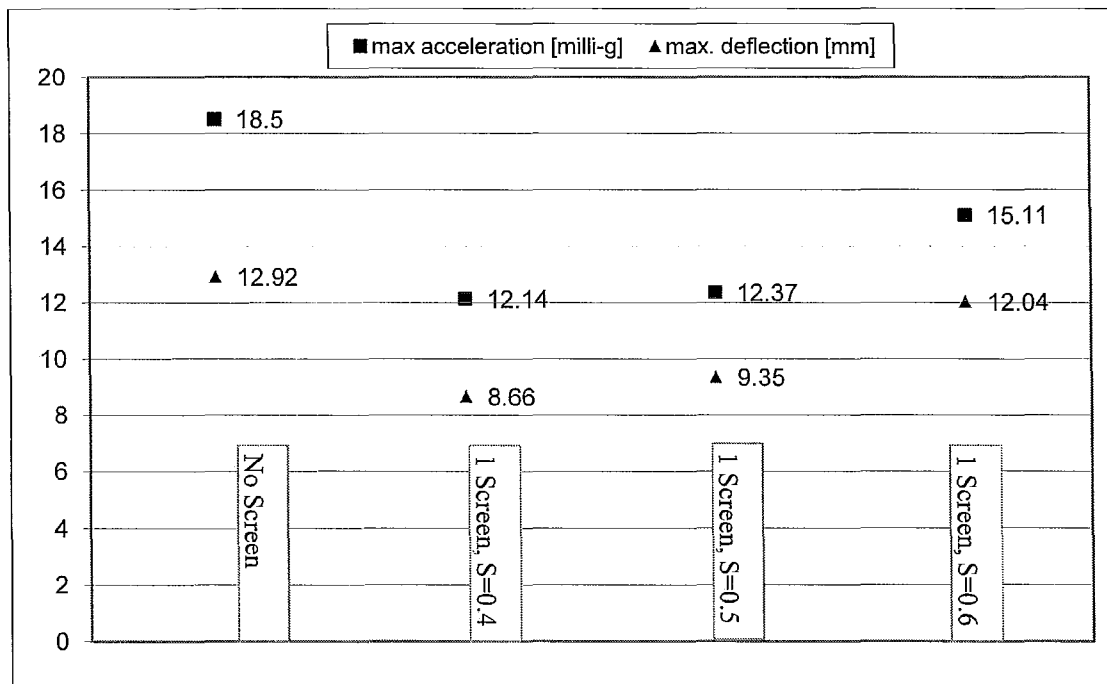


Figure 4.18 Maximum structure acceleration and deflection for the case of no screen and one screen with different solidities

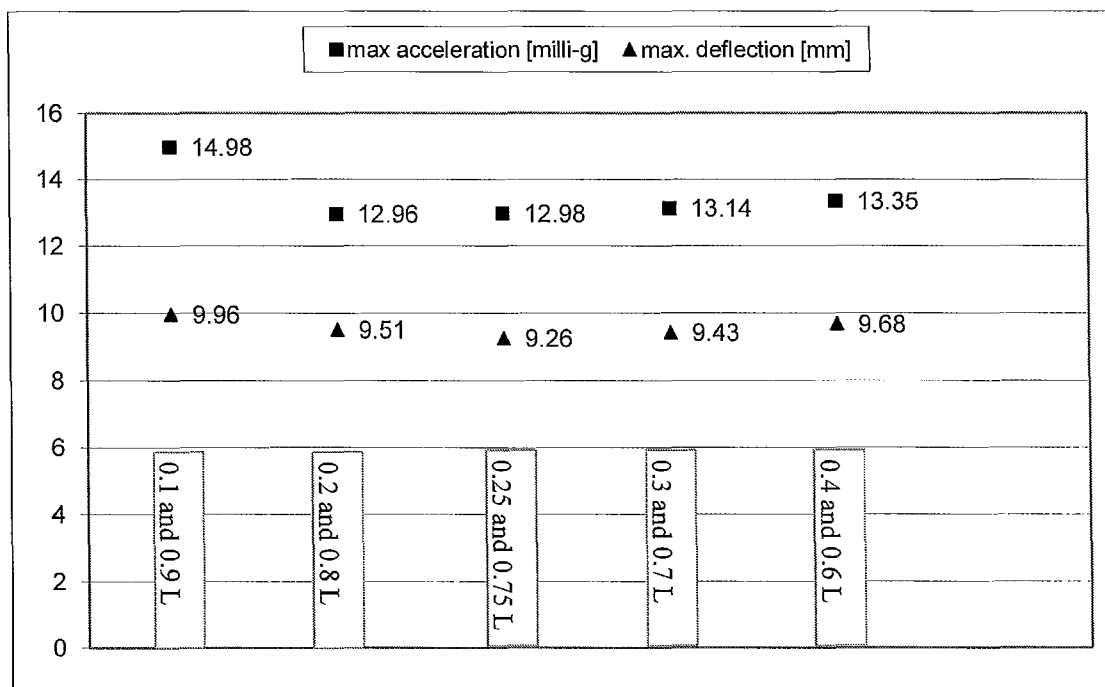


Figure 4.19 Maximum structure acceleration and deflection for the case of two screens at solidity 0.4 and different locations

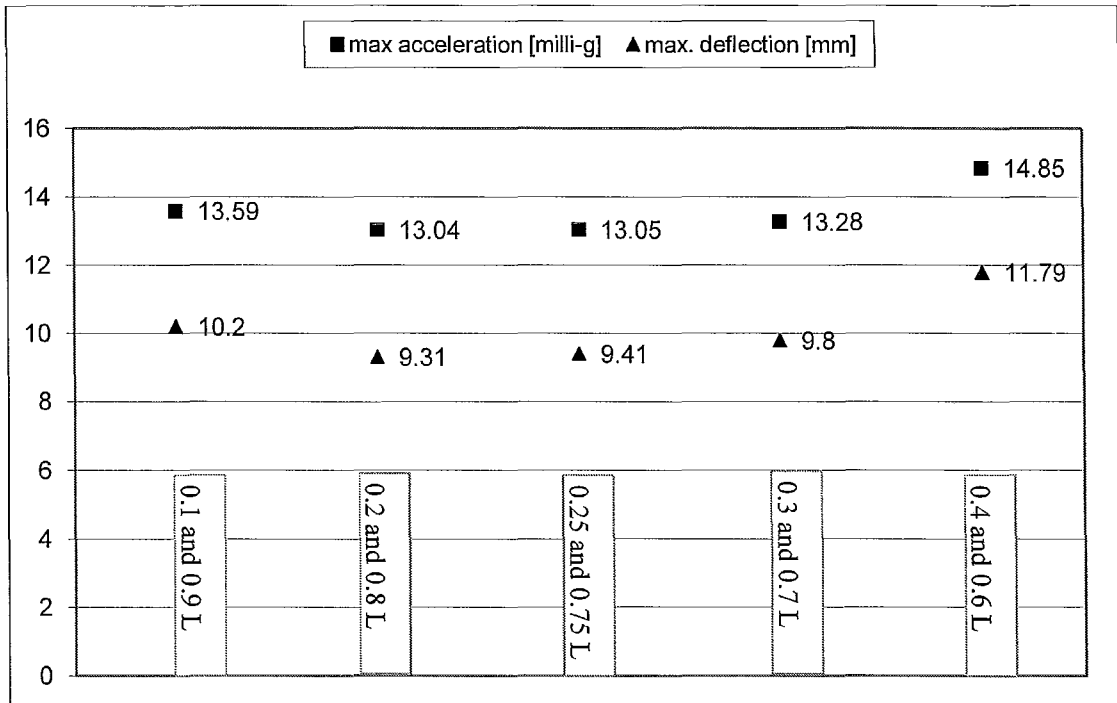


Figure 4.20 Maximum structure acceleration and deflection for the case of two screens at solidity 0.5 and different locations

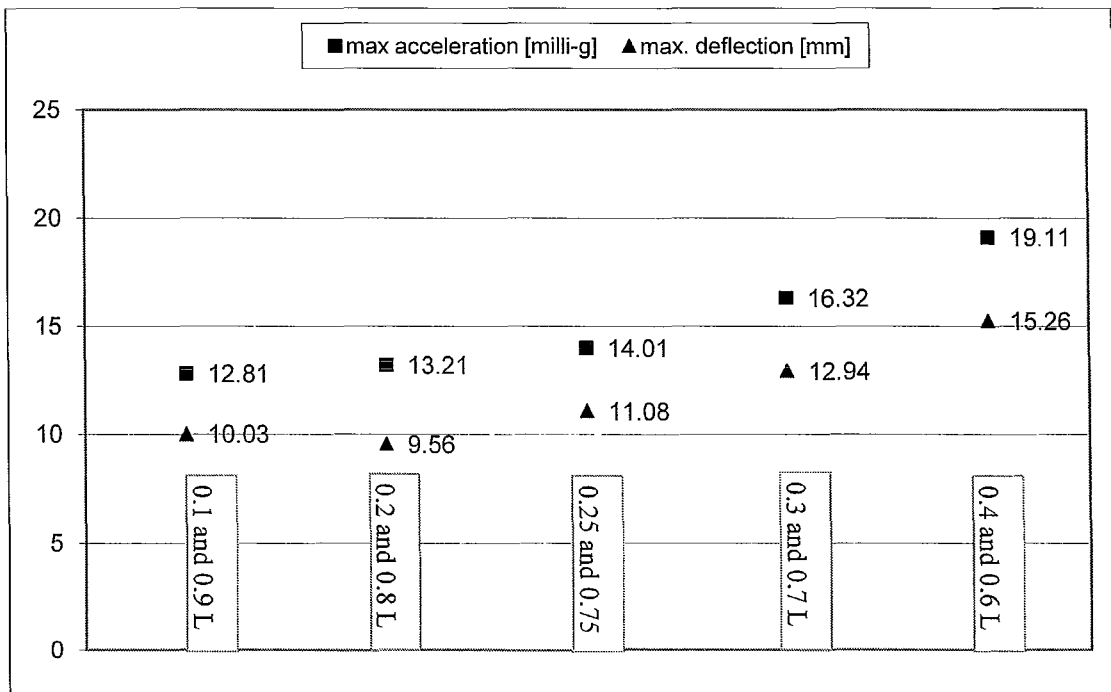


Figure 4.21 Maximum structure acceleration and deflection for the case of two screens at solidity 0.6 and different locations

The one screen case with $S = 0.4$ proved to be the best configuration for both minimum building acceleration and displacement. It is important here to discuss the reason behind the one screen case being the best case. In the cases of harmonic excitation discussed in the previous chapter, it was found that an increase in the number of screens or solidity ratio would yield the best energy dissipation by the TLD, and thus the best building response. According to Warburton (1982), tank dimensions used and SDOF structure properties considered in this study would result in an optimal damping ratio of around 5.7%. The actual damping ratio of the TLD without the screen could be estimated using the linear wave theory relations Sun (1991), equation 1.5.

Without screens the damping ratio would be approximately 0.45% (an order of magnitude less than the needed optimal damping). The addition of screens and increase of solidity ratios would increase that value more and more towards the optimal value. An increase in the solidity ratio suppressed the beating phenomenon experienced in low damping ratio cases in Chapter 3. Accordingly, the case that resulted in minimum structure displacement was the one with increased solidity.

However from a different perspective, an equally important parameter to consider is the sloshing force created inside the TLD (F_{TLD}). As mentioned in chapter 1, this force would supposedly be anti-phase with the exciting force, and would result in building deflection suppression. The uniform to and fro motion of the structure and tank that is caused by harmonic excitation is almost non-existent under non-harmonic excitation. The abrupt changes of direction would not permit the sloshing mass of water to gain enough momentum. This would directly lead to decreased values of F_{TLD} . More resistance in the

water represented by additional screens or increased solidity would contribute more to this decrease in F_{TLD} . The effect of this decrease on the overall structure deflection suppression would be very significant and could outweigh any increase in the damping ratio. To prove this reasoning, the liquid velocities at the screen locations were examined at each time step.

An average value over the time steps was then calculated along the screen, and the maximum average velocity was recorded. A higher average velocity would mean an increased momentum and thus higher sloshing force values. Table 4.3 shows the chosen cases and the velocity findings.

Table 4.3 Maximum velocity at the screen for different test cases

Case		Location	Max. Velocity [m/s]
1 Screen	Solidity=0.4	0.5 Length	0.193
	Solidity=0.5	0.5 Length	0.167
	Solidity=0.6	0.5 Length	0.132
2 Screen	Solidity=0.4	0.25 L & 0.75L	0.191
		0.3 L & 0.7L	0.177
		0.4 L & 0.6L	0.166
	Solidity=0.5	0.25 L & 0.75L	0.153
		0.3 L & 0.7L	0.141
		0.4 L & 0.6L	0.142

A number of points can be drawn from the results shown in table 4.3:

- In the one screen case, the decrease in solidity was accompanied with an increase in the maximum velocity as expected in the previous reasoning.
- Moreover, the trend of decrease in structure displacement and acceleration is in agreement with the trend of increase in maximum velocities. At solidity ratio of 0.4 the maximum average velocity was recorded.
- Three other cases with solidity ratios of 0.4 and 0.5 showed the same trend. An increased average velocity yielded better building response.
- In the two screen case, the velocity value for a fixed location with two different solidities was indicative of which case yielded the better building response.

4.5 Conclusions

After a series of runs with different screen configurations was performed, the best configuration was identified. It was found that the criterion used previously to reach a conclusion of best screen configuration was only applied in cases where harmonic excitation was considered. In cases where the TLD-structure coupling is subjected to non-harmonic excitation different criteria have to be set, due to the nature of the excitation; namely structure displacement and acceleration.

It was interesting to notice that depending on the criterion chosen (minimum structure acceleration or minimum displacement), the best configuration for a certain number of

screens could be different. In the two screen case at solidity of 0.4 the location of 0.2L and 0.8L resulted in better acceleration, whereas the location of 0.25L and 0.75L resulted in better structure deflection. This, however, wasn't the case for the one screen case, as the minimum acceleration and displacement occurred using the same best configuration.

In real life applications, a practitioner would have to determine the criterion that mattered most for the specific application. For example, if structure integrity is not at stake, then the TLD would serve more as a habitability facilitating tool. In this case, the designer would focus on the minimum acceleration criterion. The designer would also have to determine the nature of excitation and structure sway for the application at hand to correctly identify the dominant nature of the excitation, whether it is more harmonic or non-harmonic. Accordingly, the best screen configuration could be very much different.

5 Chapter Five: TLD Fluid height effect on Structure Response

5.1 Introduction

Several studies have considered the effect of fluid height on the inherent damping ratio of the TLD. Some of those studies used numerical models based on the shallow wave theory, and verified the fluid height effect experimentally on the damping ratio. The most recent of these studies is the one carried out by Tait et al. (2005), which considered fluid height values (h/L) between 0.062 and 0.2. This study confirmed previous literature findings; that lower h/L values yielded higher damping ratios associated with wave breaking. At $h/L \geq 0.2$, the model could not accurately predict TLD characteristics due to limitations of the shallow wave theory. Other studies adopted the equivalent TMD method in simulating the TLD. Most recently these studies [Tait (2008) & Deng (2007)] reported results confirming the same finding that the shallow water wave theory studies found. However, limitations in the equivalent TMD model meant that the maximum amplitudes used had to be between 0.5% and 1% of tank Length, L , which are considered low to moderate excitation amplitudes.

In this chapter, a set of numerical simulations were carried out to examine the effect of fluid height on TLD performance using different amplitudes ranging from low to high, and a range of fluid height values h/L up to 0.4. A TLD was coupled to a SDOF structure, and harmonically excited. This study chose to depart from the conventional

literature choice of damping ratio as the monitored output because ultimately a practitioner in the field would require a TLD that yields minimum structure sway, and the utilized numerical algorithm can calculate this parameter accurately under any required conditions and dimensions. In all test cases, the best structural response was the deciding factor of fluid height effect on TLD effectiveness. It was anticipated that higher damping ratios would yield better structure response in all test cases, based on literature.

5.2 Description of Parameters Involved

In all test cases the model was a TLD coupled to a SDOF structure as shown in figure 2.1. The structure ξ and μ values are the same as the experimental validation (table 2.3). The TLD dimensions were chosen to be similar to the dimensions shown in the experimental validation. A 3D schematic is shown in figure 5.1..

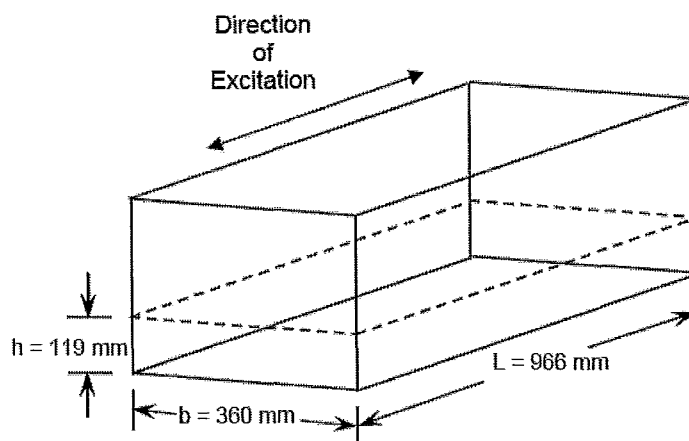


Figure 5.1 TLD dimensions

The test cases were designed such that each case would test structure response under harmonic excitation under a different fluid height. The range of non-dimensional fluid heights (h/L) was chosen to be from 0.09 to 0.4, based on practical current applications of TLDs. In order to isolate the effect of fluid height, it was important to keep all other parameters constant. This is where an accurate numerical approach is advantageous, because in contrast to experiments, parameters can be adjusted very easily.

These parameters include:

- The tuning frequency, which is the ratio of the natural frequency of the TLD to the natural frequency of the SDOF structure to be damped. Any substantial deviation from a value of unity would cause the damping forces not to be anti-phase to the excitation forces. This would cause the TLD to deteriorate the structure response instead of damp it at certain time instances. It is important to note that the TLD natural frequency was calculated according to the linear theory, but a series of tests were conducted to assess the error associated with this linearization assumption. A numerical frequency sweep was carried out on two fluid heights ($h/L=0.1$ and 0.2) at the three excitation amplitudes to be used in this section of the study to determine the actual natural frequency (See figures 5.2 and 5.3). The maximum error was 1% at the lower fluid height and much less with the higher fluid height.

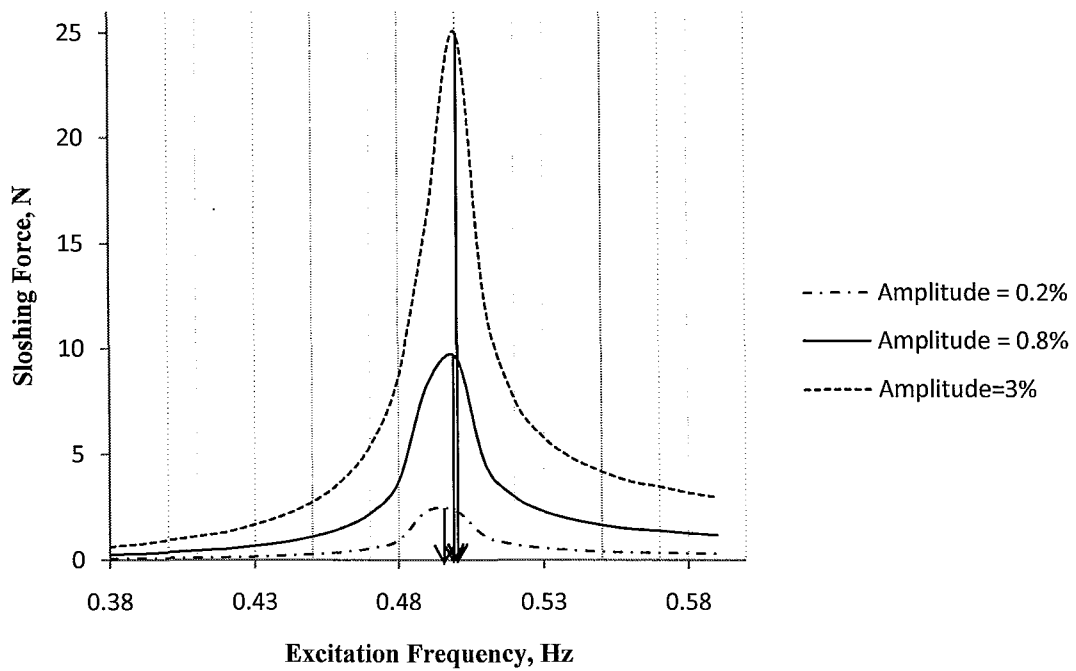


Figure 5.2 Frequency sweep (sloshing force vs excitation frequency) for $h/L = 0.1$

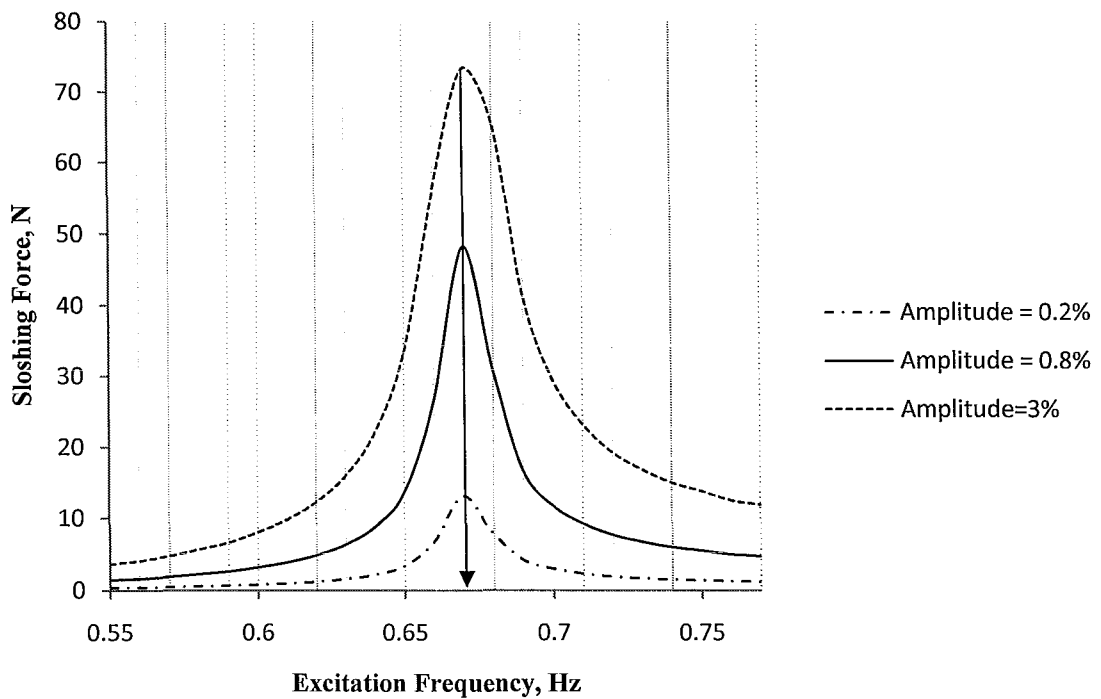


Figure 5.3 Frequency sweep (sloshing force vs excitation frequency) for $h/L = 0.2$

- The mass ratio. Any change in this ratio would change the structure response.

To achieve these two conditions, the following mathematical procedure was followed:

- A h/L value was specified
- A corresponding h value was calculated with $L=0.996$ [m]
- The resulting natural frequency of the TLD was calculated using equation 1.8
- The mass ratio was made constant at 2.5%. The resulting mass of the SDOF structure was calculated.

$$M_s = m_{TLD} / 0.025$$

- The K_s of the SDOF structure is then selected to keep the tuning frequency at unity.

The next section presents the test cases, and the calculated parameters based on the previous procedure.

5.3 Test Cases

Table 5.1 shows all test cases conducted in this study. Because each test run had different structure mass and stiffness, it was important to establish a non-dimensional parameter for the structure response. In each run, the structure response at resonance after six oscillation periods without the TLD was selected to be the denominator of this non-dimensional term. The structure response under the same resonant condition but with the TLD outfitted was selected to be the numerator for this term in each case.

Table 5.1 Test cases of different fluid height and corresponding natural frequency and structure properties

h/L value	h value	L value	natural frequency	M_s	K_s
0.09	0.08694	0.966	0.472	3273.035	28786.866
0.1	0.0966	0.966	0.496	3636.706	35320.861
0.11	0.10626	0.966	0.518	4000.376	42376.011
0.12	0.11592	0.966	0.539	4364.047	50052.605
0.13	0.12558	0.966	0.559	4727.718	58322.337
0.14	0.13524	0.966	0.578	5091.388	67150.865
0.15	0.1449	0.966	0.596	5455.059	76498.287
0.16	0.15456	0.966	0.612	5818.729	86038.08
0.17	0.16422	0.966	0.628	6182.4	96257.843
0.18	0.17388	0.966	0.643	6546.071	106847.015
0.19	0.18354	0.966	0.657	6909.741	117747.649
0.2	0.1932	0.966	0.671	7273.412	129283.46
0.21	0.20286	0.966	0.684	7637.082	141058.543
0.22	0.21252	0.966	0.696	8000.753	153006.217
0.23	0.22218	0.966	0.707	8364.424	165057.249
0.24	0.23184	0.966	0.718	8728.094	177634.795
0.25	0.2415	0.966	0.728	9091.765	190226.36
0.3	0.2898	0.966	0.771	10910.118	256034.177
0.35	0.3381	0.966	0.804	12728.471	324823.971
0.4	0.3864	0.966	0.829	14546.824	394672.605

5.4 Results and Analysis

Three amplitudes of excitation ($A/L = 0.2, 0.8$ and 3%) were used in this study ranging from low to moderately high, to very high. Because previous literature considered the low to moderate range of excitation, it was important to study the effect of fluid height in that range. This was necessary to confirm the validity of using this non-dimensional structure response term as a judging criterion instead of the inherent damping ratio. Figures 5.4 and 5.5 show the percentage decrease in structure response based on the non-dimensional parameter mentioned before, with the fluid height variation at low and moderate excitation amplitudes. This is actually in agreement with literature,

as results indicate that increased fluid heights result in no wave breaking. This is accompanied by a drop in the inherent damping ratio, and subsequently a lower TLD performance. Figure 5.6 shows the same variation but under very high excitation amplitude. It is surprising to see that an opposite trend in structure response is experienced with increased fluid height.

In figure 5.4 one can notice a sharp drop in structure response in the height interval between 0.1 and 0.12 h/L. This drop was more pronounced in the case of no screen than in the case of a screen. This drop was expected due to the existence of wave breaking at very low heights. At higher fluid heights wave breaking disappeared because the excitation amplitude was low. The existence of wave breaking was confirmed by time captures of the fluid sloshing shown in figure 5.7. The change in structure response was not as pronounced in higher amplitudes, because the wave breaking does not drop abruptly with increasing fluid height.

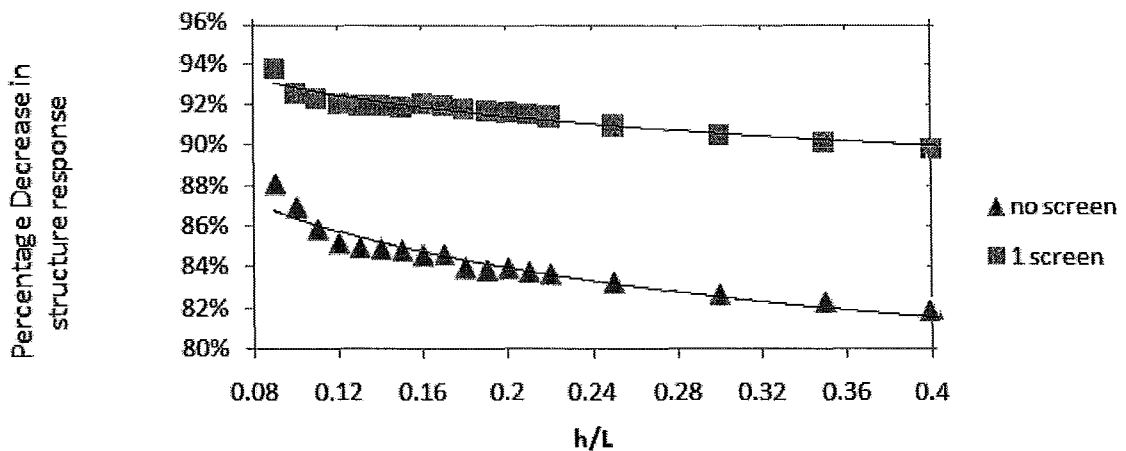


Figure 5.4 Structure response Vs fluid height at A/L=0.2%

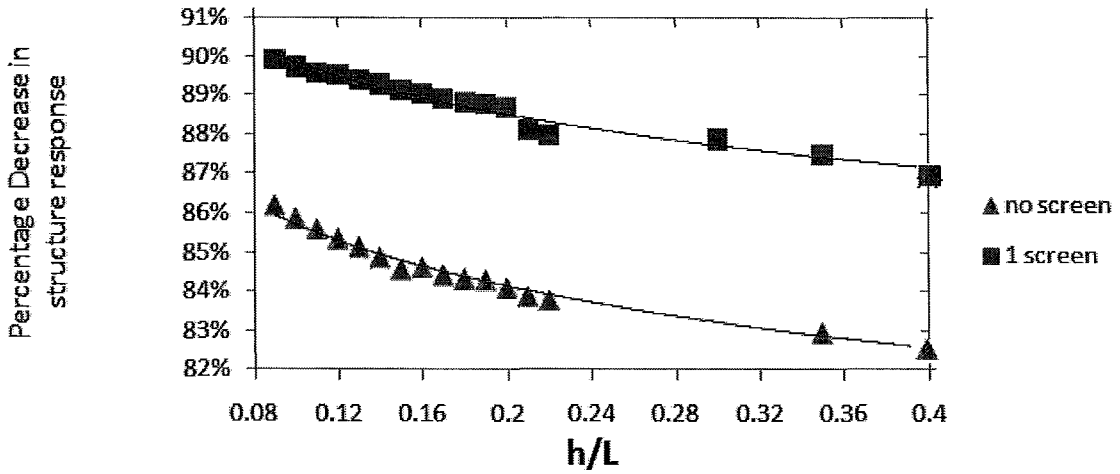


Figure 5.5 Structure response Vs fluid height at A/L=0.8%

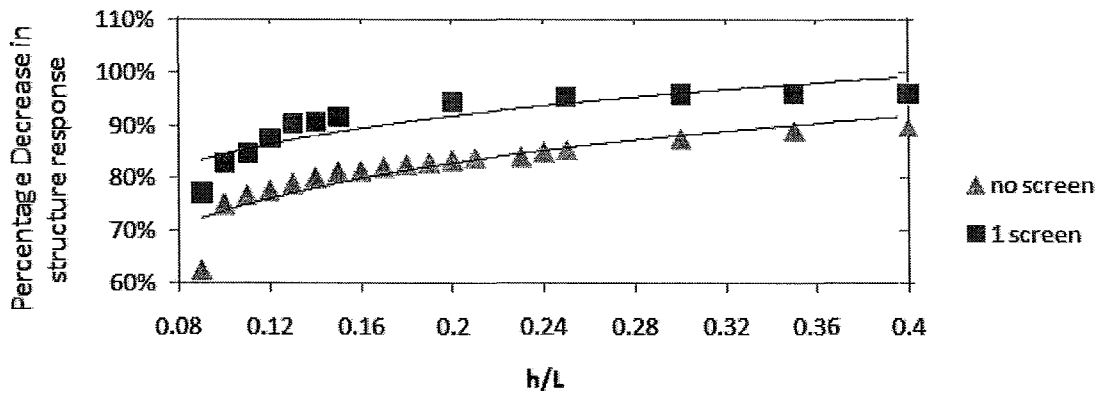


Figure 5.6 Structure response Vs fluid height at A/L=3%

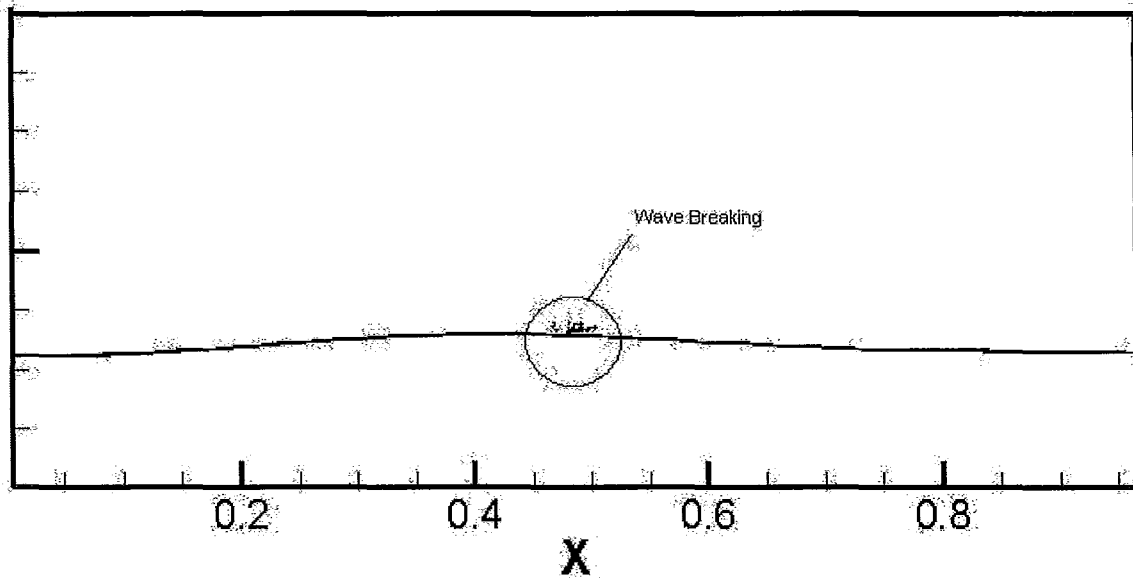


Figure 5.7 Time Capture of Sloshing under $A/L = 0.2\%$ showing wave breaking

5.5 Analysis

It is important to point out that the most recent experimental and numerical investigations regarding fluid height effect have all confirmed that increased fluid height yields lower damping thus lower TLD performance. Figure 5.8 shows results obtained by Deng (2007), where the normalized energy dissipation by the TLD was captured against the fluid height (h/L) at different amplitudes. Amplitude values however were measured with q_0/L , which represents the ratio between wave height and tank length. It is important to point out that results of the present numerical investigation indicate that all three q_0/L ranges quoted are within the low and moderate amplitude ranges shown in figures 5.4 and 5.5. This is in agreement with present findings for that range, as increased TLD energy dissipation should yield less structure sway. In the extremely high amplitude, due to extreme non-linearities experienced in the TLD, the contributing mass and damping

values were completely changed. In figure 5.9, Tait (2004) indicated that the contributing mass changes about 20% than predicted using linear numerical models within amplitude range from 0 to 3%. His results also show that damping ratios increase to around 10 to 15% if excitation amplitude increases to 3%.

Warburton (1982) performed rigorous experimental studies to come up with the optimal damping ratio for a certain TLD dimension and mass ratio. All present test runs would have optimal damping ratios around 5%. At the very high excitation amplitude, increasing the fluid height would in fact decrease the damping ratio, as mentioned in literature, but due to the fact that it is already at the 10 to 15% mark, the decrease would bring the TLD closer to the optimal ratio, thus having an overall positive effect on the TLD performance.

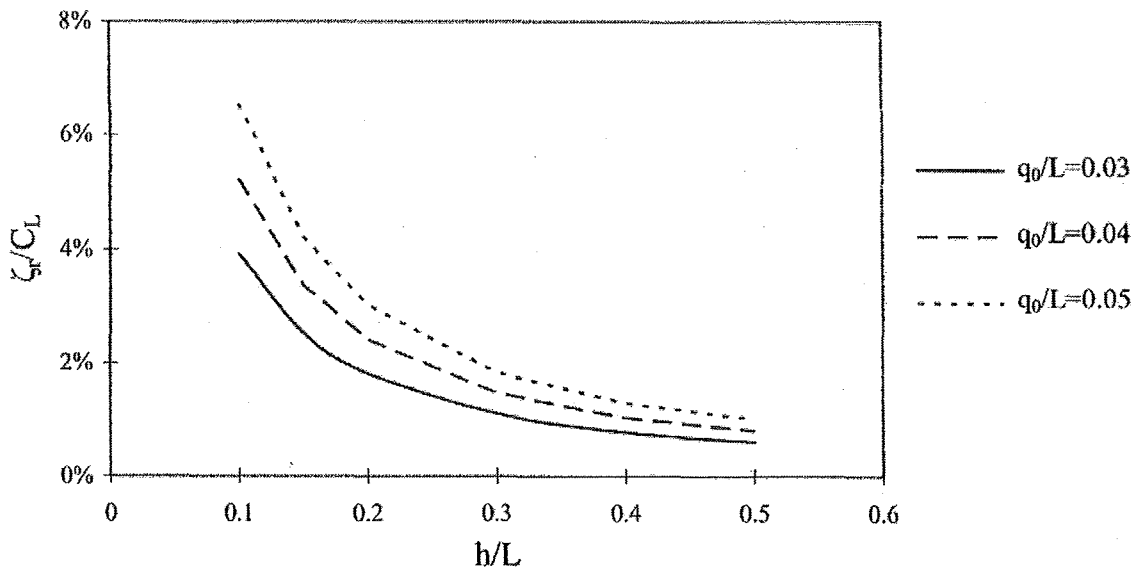


Figure 5.8 Generalized damping ratio Vs fluid height [Deng, 2007]

It can be concluded that damping ratios are not the most accurate measure of TLD performance, as amplitude changes causes the range of damping ratios to be either above or below the optimal damping mark. This would ultimately mean that different amplitudes would yield different favourable trends of damping ratios depending on whether the range is above or below the optimal damping ratio. It is therefore more accurate to assess TLD performance based on the end result of better or worse structure response.

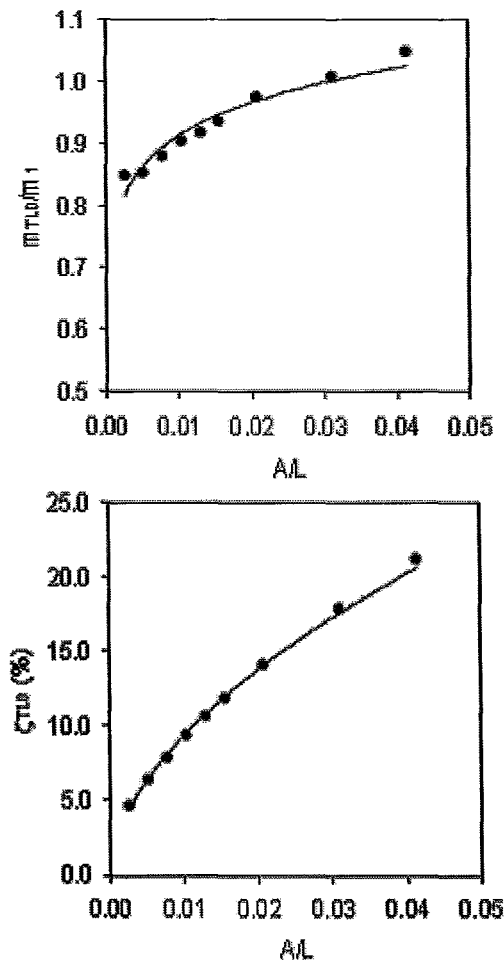


Figure 5.9 Actual sloshing mass and damping ratio Vs excitation amplitude [Tait, 2004]

6 Chapter Six: Sloped Bottom TLD

6.1 Introduction

As mentioned in Chapter 1, simple TLDs do not have enough inherent damping. That is the reason behind the numerous studies analyzing the effect of using additional damping devices in TLDs, including sloped bottoms. Gardarsson et al. (2001) experimentally studied the effect of a 30° sloped bottom at the 2 corners of the TLD, as shown in figure 6.1.

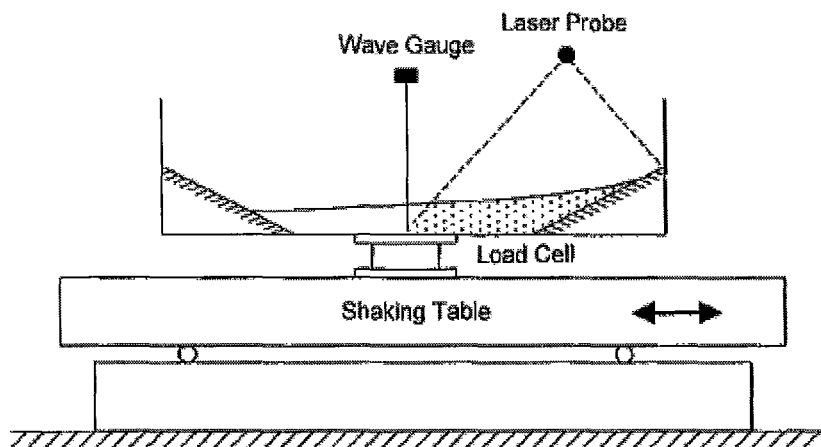


Figure 6.1 Experimental apparatus used for sloped bottom TLD [Gardarsson et al, 2001]

A number of observations were made regarding their experiments:

- The linear equation that predicts the natural frequency of the TLD (equation 1.8), had to be modified. The value of L in the equation was empirically determined as:

$$L = L_0 + \frac{2h_0}{\sin \theta_t} \tag{6.1}$$

Where L_0 , h_0 and θ_t are shown in figure 6.2

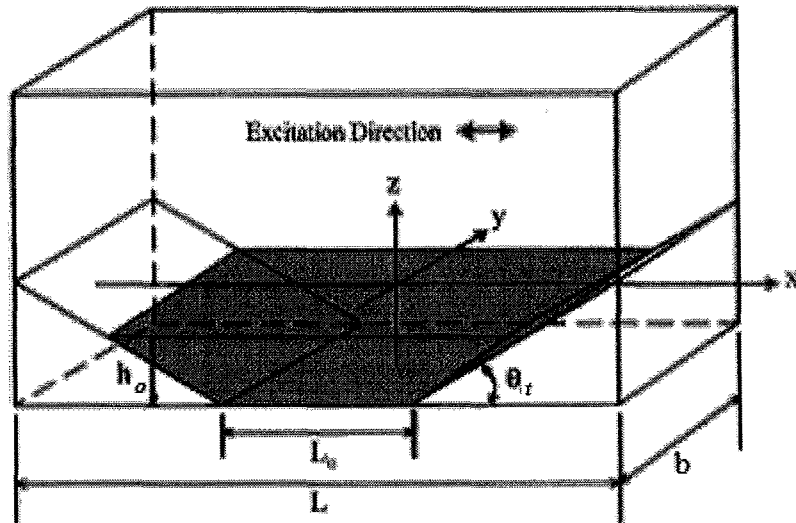


Figure 6.2 Schematic of the sloped bottom TLD [Olson and Reed, 2001]

- The sloped bottom TLD acts more like a softening spring, contrary to rectangular TLDs that behave like a hardening spring. This gives an indication that the wave run up onto the sloped surface gives the expected dampening outcome analogous to the natural phenomenon oceans and seas.
- During shake table testing, the sloshing force generated at a certain sloped bottom TLD was almost equal to a box-shaped TLD, although the water mass in the latter TLD was almost 2.5 times the mass in the sloped-bottom one. This meant that the effective liquid mass, m_{eff} , for a rectangular TLD is much higher than for a sloped bottom TLD. From a fluid dynamics perspective, this was again expected,

as a relatively large portion of the liquid mass does not contribute to the sloshing force due to recirculation in tank corners, see figure 6.3. Figure 6.4 shows 3 time captures of the streamlines inside a rectangular TLD subjected to a non-harmonic excitation, and the recirculation zones appear clearly in each time capture. Figure 6.5 shows 3 time captures at the same intervals for a sloped bottom TLD subjected to the same non-harmonic excitation. It is immediately evident how the sloped bottom geometry almost eliminates the recirculation zones and results in a higher contributing sloshing mass.

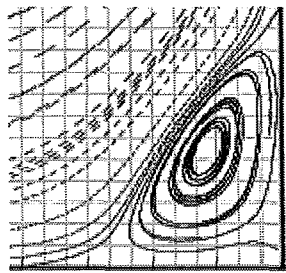


Figure 6.3 . Recirculation Zone forming at a rectangular TLD corner

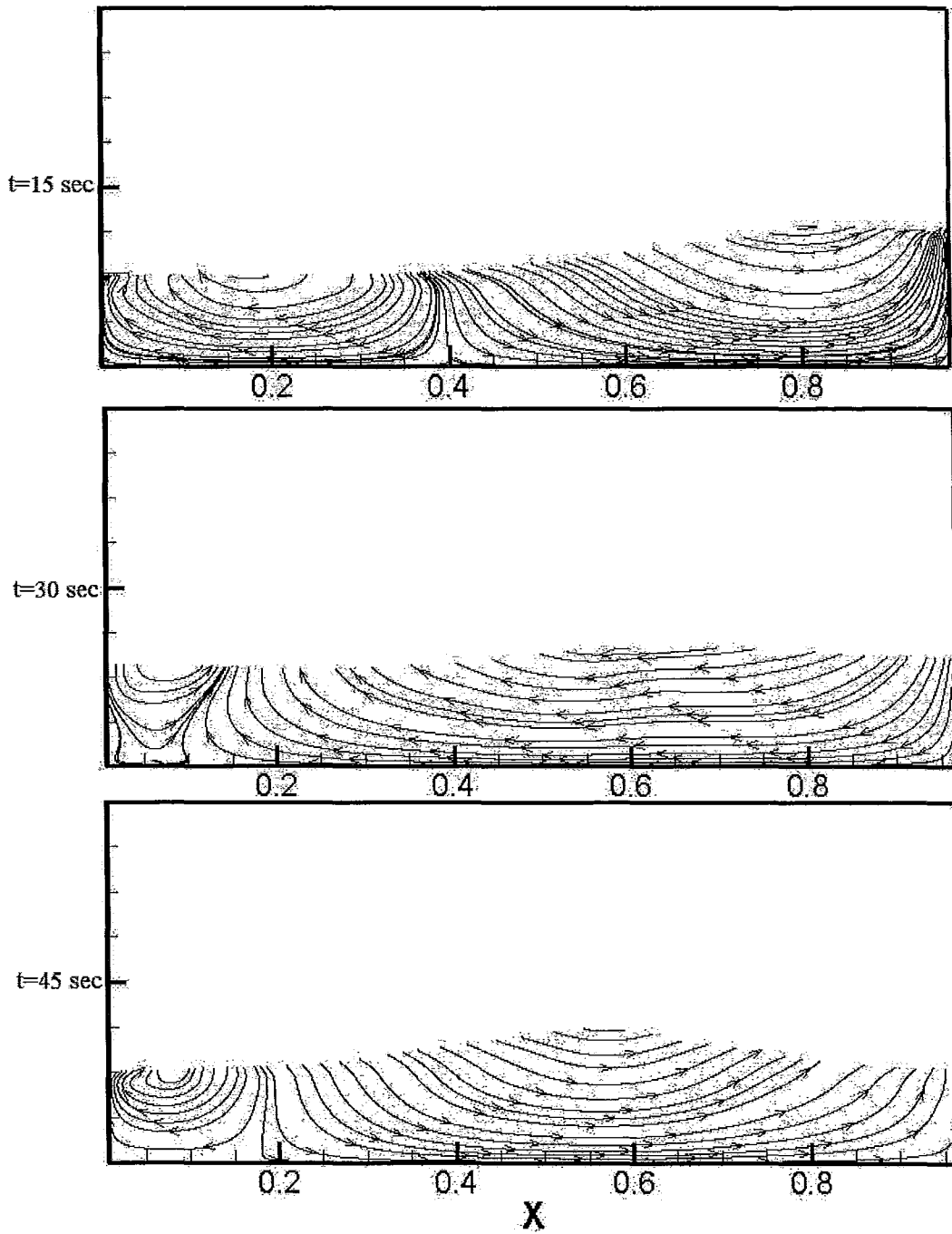


Figure 6.4 Streamlines in the rectangular TLD at 3 time captures showing the recirculation zone

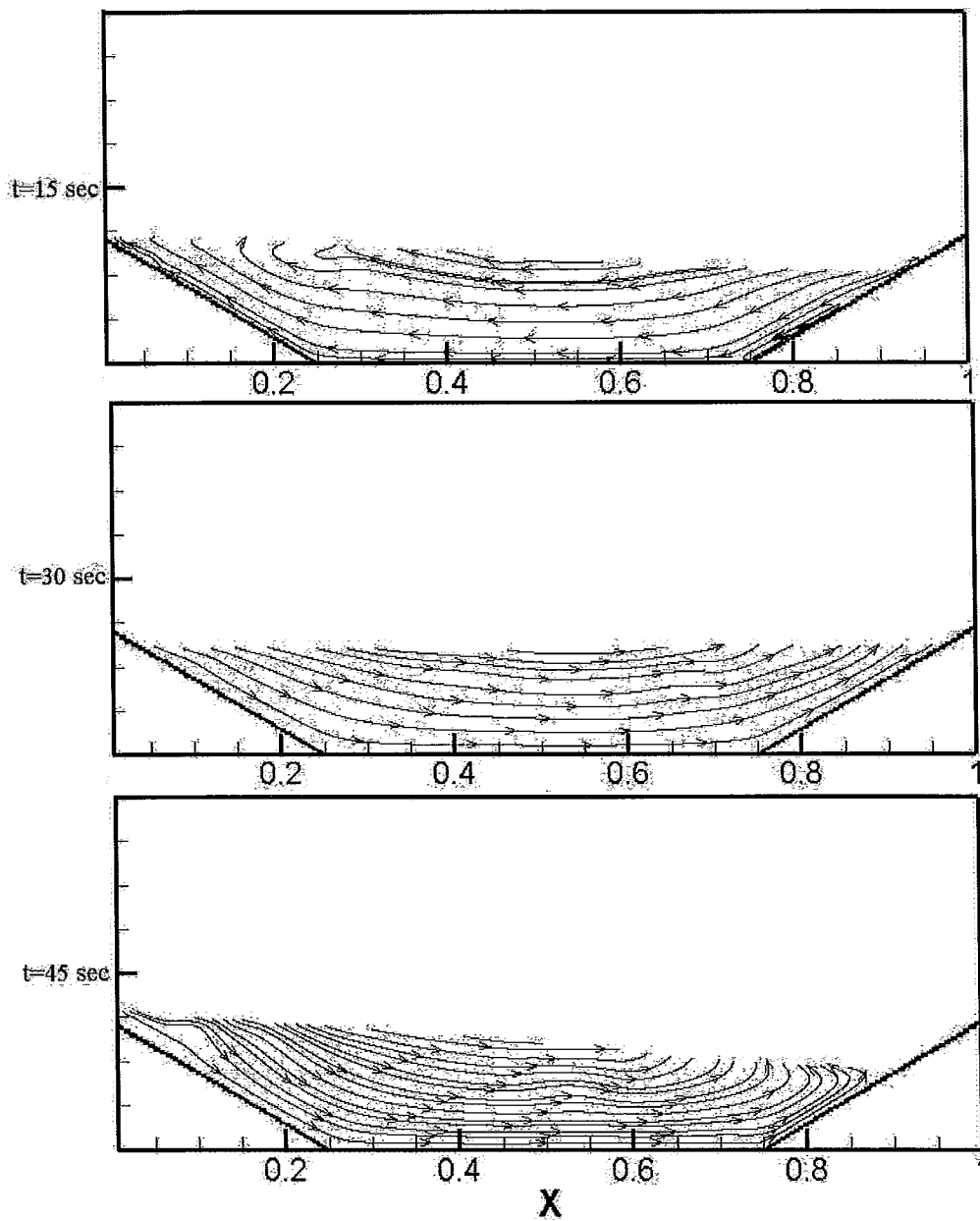


Figure 6.5 Streamlines in the sloped bottom TLD at 3 time captures showing no recirculation zone

6.2 Performance and Significance of Sloped Bottom TLDs

The objective of this part of the present study is to assess the benefits of the sloped bottom TLD using the present numerical algorithm. Structure response has been captured under several excitation amplitudes and types, to verify and analyze a number of critical issues:

- Whether or not the structure response experiences the beating phenomenon. Sloped bottom TLDs should possess higher inherent damping to effectively decrease the beating.
- The difference in structure sway when coupled to a sloped bottom TLD compared to a rectangular TLD. The sloped bottom TLD should give better results because of the higher effective sloshing mass.
- When there is a sudden cessation of the excitation force, does the structure take less time to damp out its vibration when coupled to a sloped bottom TLD? Literature findings have mentioned that the softening spring characteristics of this type of TLD means that the sloshing wave diminishes quickly, preventing the energy absorbed by the TLD from transferring back to the structure [Fujino et al. (1988)].
- Recently, it has been partially agreed upon that TLDs might not be the first method of choice when safeguarding civil structures against earthquake excitations. That is because it has been observed that the response of a structure outfitted with a TLD is no different than without a TLD during the first 2 to 4 periods of oscillation, until the sloshing force inside the TLD builds up. In 2009 a 60 storey condo tower in San

Francisco under the name One Rincon Hill, had been outfitted with a TLD (see figure 6.6). However, the TLD was utilized to stabilize top floors against wind excitation for human comfort reasons. For earthquake response, the tower was fitted with steel braces as shown in figure 6.6. The question is, would the use of a sloped bottom TLD result in decreased structure response during the first few periods of oscillations?

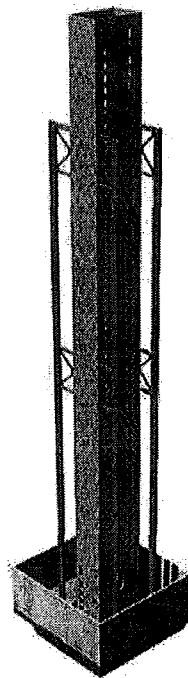


Figure 6.6 Schematic of the braces fitted on the One Rincon Hill,
[www.structuremag.com/images]

A sloped bottom TLD has been coupled to the model SDOF structure used in chapters 3 and 4, and previously used in the experimental study carried out by Tait (2004). The structure was set to be lightly damped to better represent actual civil applications. The specific structure properties are listed in Table 2.3. The sloped bottom TLD's natural frequency was tuned slightly higher than the SDOF structure to achieve optimal response as advised by previous experimental and numerical runs [Olson and Reed (2001)]. To get this natural frequency setting, eqns. 1.8 and 6.1 were used to obtain the length L and fluid height h . It was found that $L=1$ [m], and $h=0.12$ [m].

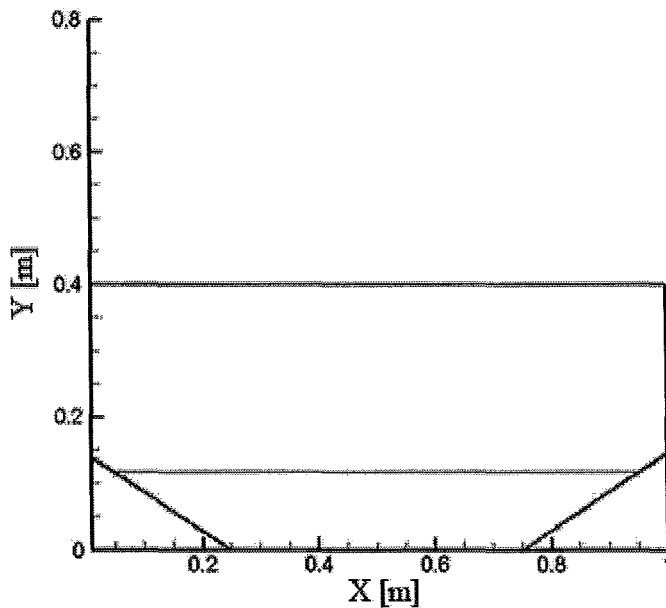
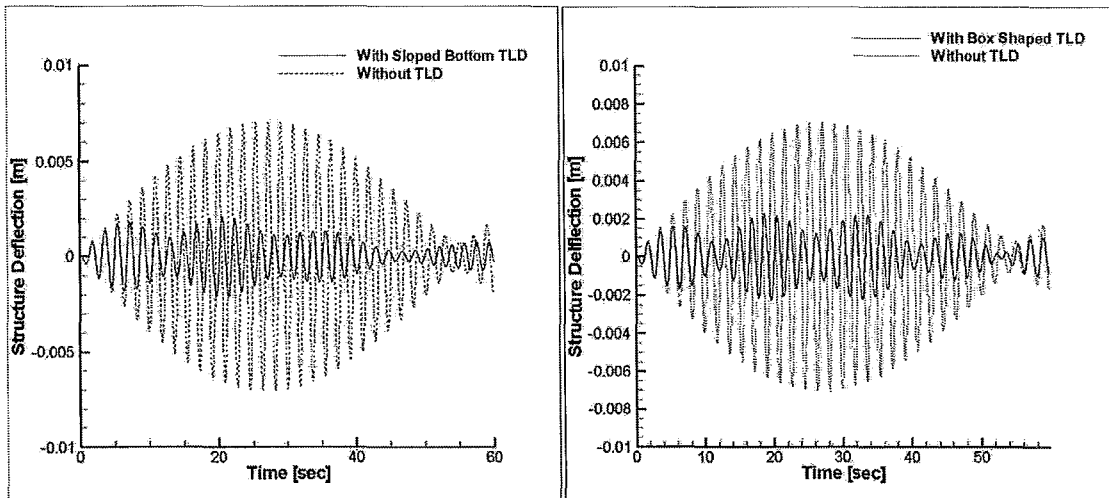


Figure 6.7 Sloped bottom TLD Geometry

Consequently the mass of water inside would be 84.94 [kg]. The box-shaped TLD that will be compared to the sloped bottom TLD, in terms of the performance criteria mentioned earlier, has the same dimensions as the one used in chapters 3 and 4. This

means that water mass is equal 119.52 [kg], which is approximately 41% more water mass than in the sloped bottom TLD.

Figure 6.8 shows the structure deflection with and without a TLD in case of a sloped bottom TLD, and a box shaped TLD with no screens, under harmonic excitation with an amplitude of 2.5 mm. One can easily observe the obvious dampening of the beating phenomenon. With the help of Figure 6.9 showing structure deflection with a TLD in both cases, the second observation is that the structure deflection is decreased by 36%.



(a)

(b)

Figure 6.8 a) Structure deflection with sloped bottom TLD b) Structure deflection with rectangular TLD without screen

To ensure a consistent conclusion, both TLDs were excited again but this time using a non-harmonic excitation, and the structure response was once more observed. Figure 6.10 shows a 30% decrease in structure response with the sloped bottom TLD.

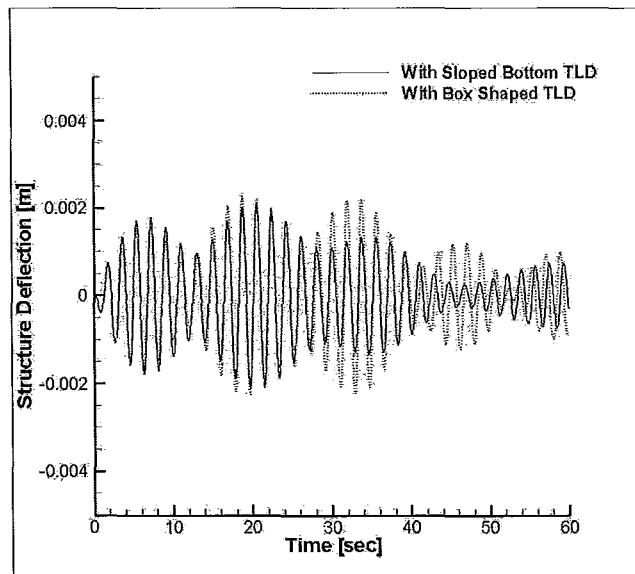


Figure 6.9 Comparison of structure response in cases of sloped and rectangular TLD

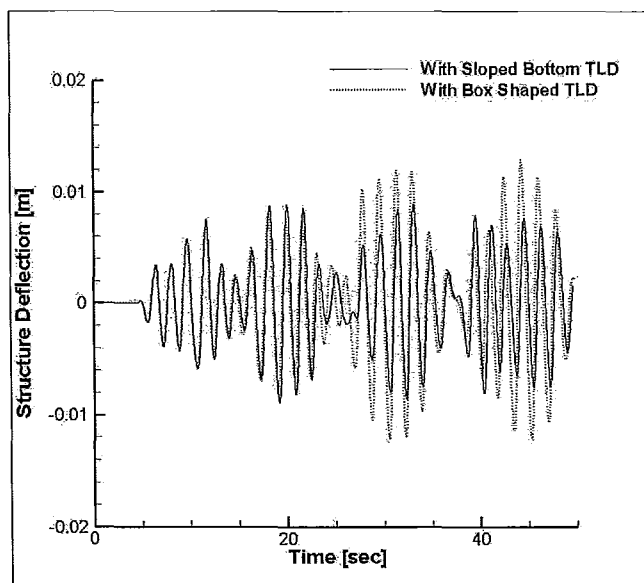


Figure 6.10 Comparison of structure response in cases of sloped and rectangular TLD in case of non-harmonic excitation

Despite better structure performance, the sloped bottom TLD did not show any signs of lower response time. The structure sway was almost unchanged during the first 4.5 seconds with or without a TLD in both TLD types. That translates approximately to 2 periods of oscillation without any significant improvement in structure response.

The next set of simulations was done to investigate the softening spring characteristics of the sloped bottom TLD. To do that, a special non-harmonic excitation was generated such that it would come to a sudden stop after a certain period. The objective was to see how the structure sway faded down with the sloped bottom TLD compared to the rectangular TLD. Figure 6.11 shows the excitation force signal used, with the cessation starting after 30 seconds of excitation.

Figure 6.12 shows a 63% improvement in structure response after excitation cessation. The logarithmic decrement, δ , was used to calculate the difference in damping between the rectangular and sloped TLD.

$$\delta = \frac{1}{n} \ln \frac{x_0}{x_n} \quad (6.2)$$

where x_0 is the greater amplitude and x_n is an amplitude n periods away. The estimated damping ratio was 0.44% in the rectangular TLD versus 0.96% in the sloped bottom TLD. This does confirm that rectangular TLDs without screens transfer back the sloshing energy to the structure after excitation cessation due to insufficient inherent damping. However, Figure 6.13 shows that rectangular TLDs with two screens possess far superior performance in that area compared to the performance of a sloped bottom TLD with an inherent damping calculated to be 5.9 %.

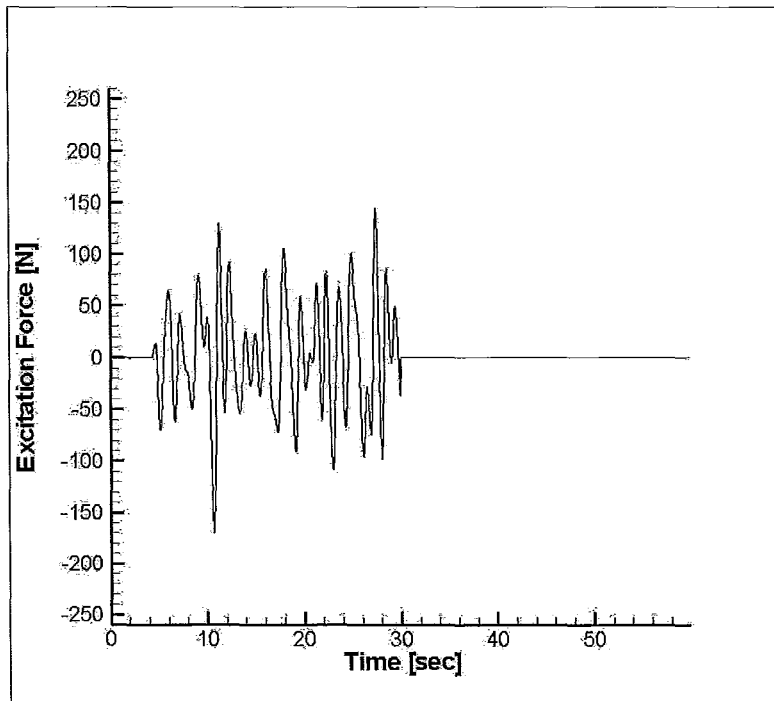


Figure 6.11 Non-harmonic excitation generated to test TLD dampening behaviour

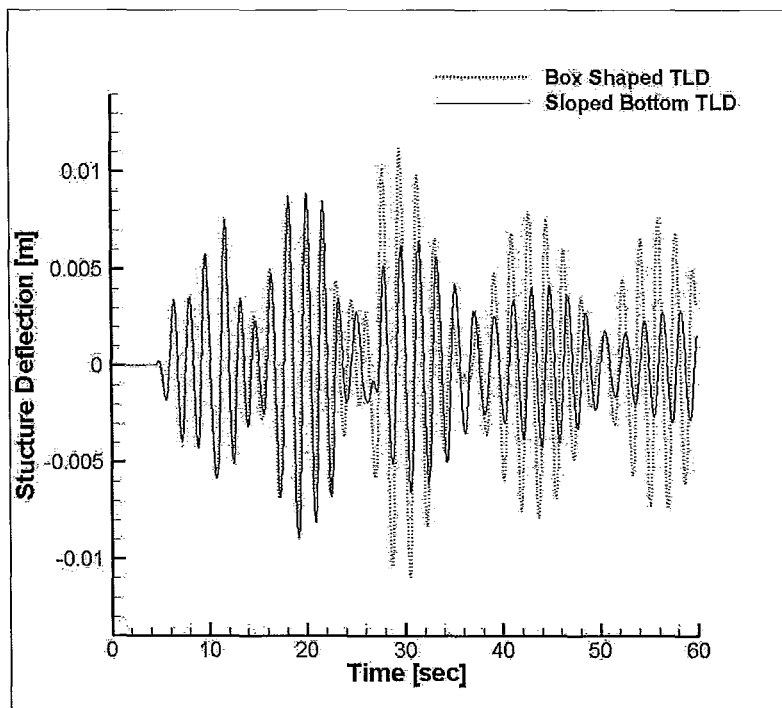


Figure 6.12 Dampening behaviour in terms of structure response in cases of sloped and rectangular TLDs

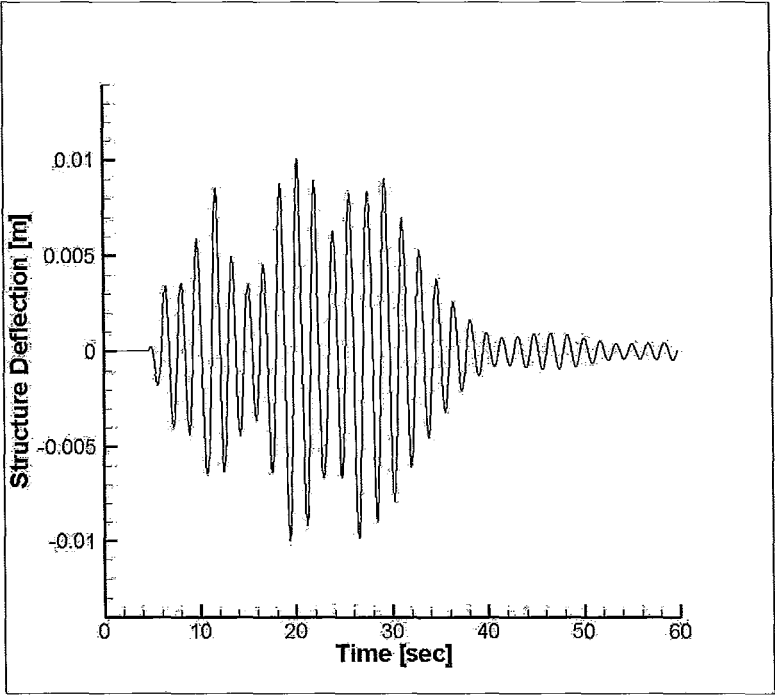


Figure 6.13 Dampening behaviour in terms of structure response in case of rectangular TLD with two screens

7 Chapter Seven: Comments on TLD Performance Criteria

This study confirmed that the most suitable criterion upon which TLD design and screen configuration are chosen should be based on structure response. Other criteria based on optimal damping ratios (ζ_{opt}) and sloshing force values could be sometimes misleading. For example increasing the number of screens has always been regarded as a method to increase the inherent damping to a value closer to the optimal damping, resulting in an increase in the energy dissipation over a wide range of excitation frequencies. However, in the case of non-harmonic excitation, increased damping might lead to worsening structure response, simply due to prevention of momentum build up inside the TLD, which directly leads to the decrease of the sloshing force generated, and consequently increasing structure sway. It was concluded that in the case of non-harmonic excitation, one screen could be the best needed configuration.

Moreover, the values of the inherent damping and the optimal damping are both highly nonlinear, so no unique inherent damping value or a unique natural frequency can be defined for a certain TLD configuration [Tait (2004)].

It is also important to note the sloshing force magnitude also is not recommended as a criterion for TLD effectiveness. In some cases, a generated sloshing force does not yield better structure response. That is because in real life applications the TLD and structure are never perfectly tuned. This is due to difficulties in assessing structure exact natural frequency beforehand, and because TLD natural frequency is amplitude dependant. And that is why when designing TLDs, their natural frequencies are

calculated using the simple linear equations, as deviations from structure natural frequency are bound to happen anyway.

Figures 7.1 and 7.2 show the comparison between the structure response and the sloshing force between a case where 1 screen was used, and another where 2 screens were used. In both cases the TLD was coupled to the structure with properties listed in Table 2.3, and the same amplitude excitation was used. In both cases also, tuning was done using the linear equation. It is clear that between time intervals 14 and 26 [sec], the 1 screen case gave higher sloshing force, but resulted in worsened structure response. Although after that increased sloshing force did vary proportionally with better structure response, it cannot be a general consensus.

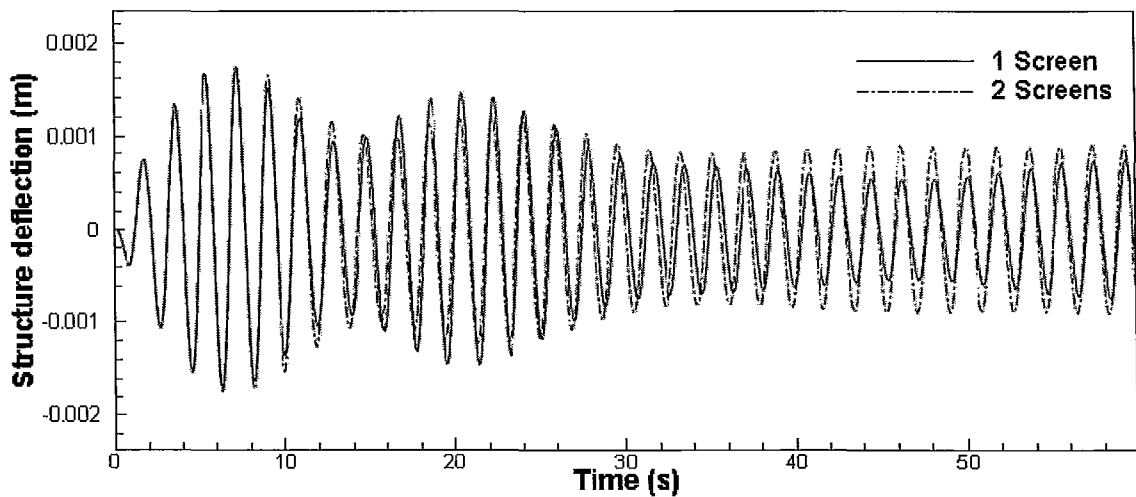


Figure 7.1 Comparison between structure responses in the case of one screen and two screens [Morteza, 2009]

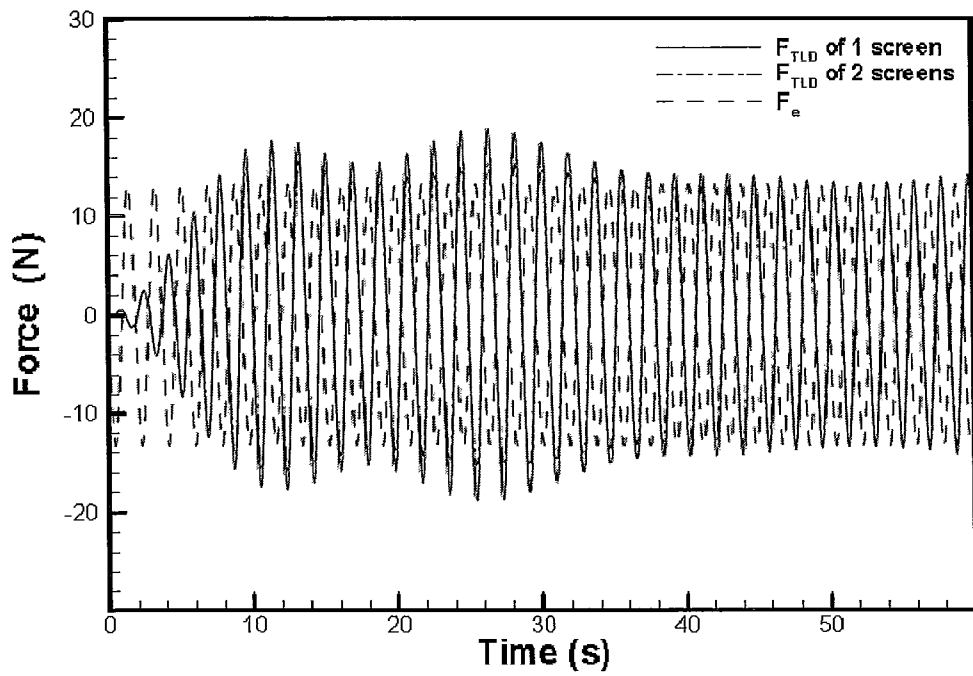


Figure 7.2 Comparison between sloshing forces in the case of one screen and two screens

[Morteza, 2009]

8 Chapter Eight: Summary and Conclusions

8.1 Summary of Rectangular TLD Investigation

In the case of a TLD-structure coupling subjected to harmonic excitation, the effect of the screen solidity was investigated. Results showed that structure deflection was decreased by up to 71 % upon using a TLD without screens. The installation of a screen in the middle of the TLD with solidity of 0.4 further decreased the structure sway by another 21%. If maximum structure deflection at $S=0.4$ is taken as a reference, then a change of solidity from 0.4 to 0.6 would lead to a 32.2 % further decrease in maximum structure deflection value. The added inherent damping from the increased solidity was evident from the significant reduction of the beating phenomenon as the solidity ratio was increased from 0.4 to 0.6.

In the case of a TLD-structure coupling subjected to non-harmonic excitation, the best screen number, location and solidity was identified based on minimal structure response. The 1 screen case placed in the middle of the TLD with solidity of 0.4 gave both the best structure displacement and acceleration. In the remaining screen configurations, minimal structure response did not consistently yield minimal structure acceleration. In the two screen case at solidity of 0.4 the location of 0.2L and 0.8L resulted in better acceleration, whereas the location of 0.25L and 0.75L resulted in better structure deflection.

The isolated effect of the fluid height on structure response was also investigated. The excitation amplitude used varied from low to moderate to high (0.2 to 3% of TLD length), with the fluid height varying from 0.09 to 0.4 of TLD length. Although the most recent experimental and numerical investigations regarding fluid height effect have all confirmed that increased fluid height yields lower damping thus lower TLD performance, results for the high excitation amplitude showed an opposite trend. At the high excitation amplitude, increasing the fluid height would in fact decrease the damping ratio, as mentioned in literature, but due to the fact that it is already at the 10 to 15% mark, the decrease would bring the TLD closer to the optimal ratio, 5%, thus having an overall positive effect on the TLD performance.

It can be concluded that damping ratios are not the most accurate measure of TLD performance, as amplitude changes causes the range of damping ratios to be either above or below the optimal damping mark. This would ultimately mean that different amplitudes would yield different favourable trends of damping ratios depending on whether the range is above or below the optimal damping ratio. It is therefore more accurate to assess TLD performance based on the end result of better or worse structure response.

8.2 Sloped Bottom TLD Importance

The present study successfully utilised and validated the algorithm developed by Marivani and Hamed (2009) to model the sloped bottom TLD adequately. Sloped bottom TLDs consistently proved that they can perform much better than rectangular TLDs in terms of structure response with much less mass ratio. The increased inherent damping was obvious in the structure response, and in the structure damping upon sudden excitation cessation. Under harmonic and non-harmonic excitations, the use of the sloped bottom TLD resulted in decreased structure response by 36% and 30% respectively, compared to the rectangular TLD, even with 41% less liquid mass.

It was also concluded however that no improvement in response time is evident in the sloped bottom TLD. The higher effective mass and higher inherent damping both have no relation observed to better initial structure performance under vibration. This does actually confirm the recent consensus of TLD ineffectiveness with earthquake vibration.

8.3 Recommendations and Future Work

Although probably the most accurate numerical model to date – to the author's best knowledge- this algorithm is essentially 2 dimensional. Many recent experimental publications have studied the benefits of using cylindrical TLDs [Deng (2007)]: no need for orientation positioning study, as there is no primary direction for certain natural

frequencies as in the case with rectangular TLDs. Some also have utilized the sloped bottom concept and studied conical TLDs [Casciati et al. (2003)]. To extend this work to include this type of TLD, a 3D model has to be developed.

As for sloped bottom TLDs, an optimal angle for minimal structure response should be investigated. With lower sloped angles, the contributing mass is predicted to increase, which should in turn decrease structure response. This effect however, is accompanied by a decrease in the liquid run-up and thus decreased damping.

It's also worth mentioning that upon discussions with Rowan Williams Davies & Irwin (RWDI), the leading structure damping company in North America, an important observation came up: In most cases of practical TLD installations, the spaces available are extremely limited. That prevents the TLD designer from installing a fully rectangle or cylindrical TLD. Sometimes very irregular volume spaces are the only ones available for TLD installation, and there is no literature experimental or numerical to guide the design process, starting from the very basic tuning. A 3D model that would employ the partial cell treatment used in this code could potentially simulate any shape of TLD required.

References

- Abramson, H., (1967). "*The dynamic behaviour of liquid in moving containers*", NASA SP-106: Washigton, D.C.
- Banerji, P., Murudi, M., Shah, A.H., and Popplewell, N. (2000). "Tuned Liquid Dampers for Controlling Earthquake Response of Structures," *Earthquake Engineering & Structure Dynamics*, Vol. 29, pp. 587 - 602.
- Bauer, H.F. (1964). "Nonlinear Propellant Sloshing in a Rectangular Container of Infinite Length," *Developments in Theoretical and Applied Mechanics*, Vol. 3, pp. 725 - 759.
- Bauer, H.F. (1984). "New Proposed Dynamic Vibration Absorbers for Excited Structures," *Vibration Damping Workshop Proceedings*, pp. 1 - 27.
- Bhuta, P.G. and Koval, L.R. (1966). "A Viscous Ring Damper for a Freely Precessing Satellite," *International Journal of Mechanical Science, ASC*, Vol. 8, pp. 383 - 395.
- Carrier, G.F. and Miles, J.W. (1960). "On the Annular Damper for a Freely Precessing Gyroscope," *Journal of Applied Mechanics*, Vol. 27, pp. 237 - 240.
- Casciati, F., De Stefano, A., and Matta, E. (2003). "Simulating a Conical Tuned Liquid Damper," *Simulation Modelling Practice and Theory*, Vol. 11, pp. 353 - 370.
- Cassolato, M., (2007). "*The Performance of a TLD With Inclined and Oscillating Screens*", M.A.Sc. Thesis, McMaster University, Hamilton, Canada.
- Chopra, A. K., (2000). "*Dynamics of Structures: Theory & Applications to Earthquake Engineering*", 2nd Edition, Prentice-Hall Inc.: Upper Saddle River, NJ.
- Dean, R. G. and Dalrymple, A. D, (1984). "*Water Wave Mechanics for Engineers and Scientists*", 1st Edition, Prentice-Hall Inc: Englewood Cliffs, NJ.
- Den Hartog, J. P., (1956). "*Mechanical Vibrations*", 4th Edition, McGraw-Hill: New York, New York.
- Deng, X., (2007). "*The Performance of Tuned Liquid Dampers With Different Tank Geometries*", M.A.Sc., McMaster University, Canada,

Dutta, S. and Laha, M.K. (2000). "Analysis of the Small Amplitude Sloshing of a Liquid in a Rigid Container of Arbitrary Shape Using a Low-Order Boundary Element Method," *Journal for Numerical Methods in Engineering*, Vol. 47, pp. 1633 - 1648.

Fediw, A.A., Isyumov, N., and Vickery, B.J. (1995). "Performance of A Tuned Sloshing Water Damper," *Journal of Wind Engineering and Industrial Aerodynamics*, Vol. 57, no.2-3, pp. 237 - 247.

Frandsen, J.B. (2005). "Numerical Predictions of Tuned Liquid Tank Structural Systems," *Journal of Fluids and Structures*, Vol. 20, pp. 309 - 329.

Fujino, Y., Pacheco B.M., Chaiseri, P., and Sun, L.M. (1988). "Parametric Studies on Tuned Liquid Damper (TLD) Using Circular Containers by Free-Oscillation Experiments," *Journal of Engineering Mechanics, ASCE*, Vol. 5, pp. 381 - 391

Gardarsson, S., Yeh, H., and Reed, D. (2001). "Behavior of Sloped-Bottom Tuned Liquid Damper," *Journal of Engineering Mechanics, ASCE*, pp. 266 - 271.

Graham, E.W. and Rodriguez, A.M. (1952). "The Characteristics of Fuel Motion Which Affect Airplane Dynamics," *Journal of Applied Mechanics*, Vol. 19, pp. 381 - 388.

Hamelin, J., (2007). "*The Effect of Screen Geometry on the Performance of a Tuned Liquid Damper*", M.A.Sc., McMaster University,

Hanson, R. D. and Soong, T. T., (2001). "*Seismic Design With Supplemental Energy Dissipation Devices*", Earthquake Engineering Research Institute: Buffalo, New York.

Hirt, C.W. and Nichols, B.D. (1981). "Volume of Fluid (VOF) Method for the Dynamics of Free Boundaries", *Journal of Computational Physics*, Vol. 39, pp. 201 - 215

Ju, Y.K., Yoon, S.W., and Kim, S.D. (2004). "Experimental Evaluation of a Tuned Liquid Damper System," *Structures and Buildings*, Vol. 157, pp. 251 - 262.

Kaneko, S. and Ishikawa, M. (1999). "Modelling of Tuned Liquid Damper With Submerged Nets," *Journal of Pressure Vessel Technology*, Vol. 121, pp. 334 - 341.

Kareem, A. and Sun, W.J. (1987). "Stochastic Response of Structures With Fluid-Containing Appendages," *Journal of Sound & Vibration*, Vol. 119, pp. 389 - 408.

Lamb, H., (1932). "*Hydrodynamics*", The University Press: Cambridge, England.

Marivani, M., (2009). "*Numerical Investigation of Sloshing Motion Inside Tuned Liquid Dampers With & Without Submerged Nets*", Ph.D., McMaster University, Canada,

Marivani, M. and Hamed, M.S. (2009). "Numerical Simulation of Structure Response Outfitted With a Tuned Liquid Damper," *Computers & Structures*, Submitted.

Mei, C. C., (1983). "*The applied dynamics of ocean surface waves*", Wiley: New York, New York.

Miles, J.W. (1967). "Surface Wave Damping in Closed Basins," *Proceedings of Royal Society of London*, Vol. A297, pp. 459 - 475.

Olson, D.E. and Reed, D. (2001). "A Nonlinear Numerical Model for Sloped-Bottom Tuned Liquid Dampers," *Earthquake Engineering & Structure Dynamics*, Vol. 30, pp. 731 - 743.

Pengzhi, L. (2007). "A Fixed Grid Model for Simulation of Moving Body in Free Surface Flows," *Computers & Fluids*, Vol. 36, pp. 549 - 561.

Poo, J.Y. and Ashgriz, N. (1990). "FLAIR - Flux Line Segment Model for Advection and Interface Reconstruction," *Journal of Computational Physics*, Vol. 93, no.2, pp. 449 - 468.

Reed, D., Yu, J., Yeh, H., and Gardarsson, S. (1998). "Investigation of Tuned Liquid Dampers Under Large Amplitude Excitation," *Journal of Engineering Mechanics, ASCE*, Vol. 124, pp. 405 - 413.

Shimizu, T. and Hayama, S. (1987). "Nonlinear Responses of Sloshing Based on Shallow Water Wave Theory," *JSME International Journal*, Vol. 30, no.263,

Siddique, M.R., Hamed, M.S., and El Damatty, A.A. (2004). "A Nonlinear Model for Sloshing Motion in Tuned Liquid Dampers," *International Journal for Numerical Methods in Heat & Fluid Flow*, Vol. 15, no.3, pp. 306 - 324.

Soong, T. T. and Dargush, G. F., (1997). "*Passive Energy Dissipation Systems in Structural Engineering*", John Wiley & Sons: West Sussex, England.

Sun, L.M., (1991). "*Semi-Analytical Modelling of TLD With Emphasis on Damping of Liquid Sloshing*", Ph.D., University of Tokyo, Japan,

Sun, L.M. and Fujino, Y. (1994). "A Semi-Analytical Model for Tuned Liquid Damper (TLD) With Wave Breaking," *Journal of Fluids and Structures*, Vol. 8, pp. 471 - 488.

Sun, L.M., Fujino, Y., and Koga, K. (1995). "A Model of Tuned Liquid Damper for Suppressing Pitching Motions of Structure," *Earthquake Engineering & Structure Dynamics*, Vol. 24, pp. 625 - 636.

Tait, M., (2004). "*The Performance of 1-D and 2-D Tuned Liquid Dampers*", Ph.D., University of Western Ontario, Canada,

Tait, M., El Damatty, A.A., and Isyumov, N. (2004). "Testing of Tuned Liquid Damper With Screens and Development of Equivalent TMD Model," *Wind and Structures*, Vol. 7, no.4, pp. 215 - 234.

Tait, M.J. (2008). "Modelling and Preliminary Design of a Structure-TLD System," *Engineering Structures*, Vol. 30, pp. 2644 - 2655.

Tait, M.J., El Damatty, A.A., Isyumov, and Siddique, M.R. (2005). "Numerical Flow Models to Simulate TLDs With Slat Screens," *Journal of Fluids and Structures*, Vol. 20, pp. 1007 - 1023.

Warburton, G.B. (1982). "Optimum Absorber Parameters for Various Combinations of Response & Excitation Parameters," *Earthquake Engineering & Structure Dynamics*, Vol. 10, pp. 381 - 401.

XiaoHua, D., Meziane, I., MengLin, L., and GenDa, C. (2009). "Experimental Study on the Seismic Performance of a Large-Scale TLD Model With Sloped Bottoms," *Proceeding of the 2009 Structure Congress*,

Yalla, S., (2001). "*Liquid Dampers for Mitigation of Structural Response: Theoretical Development & Experimental Validation*", Ph.D., University of Notre Dame, Indiana,

Yalla, S. and Kareem, A. (2002). "Discussion of Paper: Tuned Liquid Dampers for Controlling Earthquake Response of Structures by P.Banerji Et Al., *Earthquake Engng Struct. Dyn.* 2000; 29 (5):587-602," *Earthquake Engineering & Structure Dynamics*, Vol. 31, pp. 1037 - 1039.

Yu, J., (1997). "*Nonlinear Characteristics of Tuned Liquid Dampers*", Univeristy of Washington, Dept. of Civil Engineering, Seattle, WA,

Yu, J., Wakahara, T., and Reed, D. (1999). "A Non-Linear Numerical Model of the Tuned Liquid Damper," *Earthquake Engineering & Structure Dynamics*, Vol. 28, pp. 671 - 686.